FUNCTIONAL ROLE OF LOW DENSITY LIPOPROTEIN RECEPTOR-RELATED PROTEIN 5 AND 6 IN ALZHEIMER'S DISEASE

ZHANG LUQI

(B.Sc. (Hons.), Xiamen University)

A THESIS SUBMITTED

FOR THE DEGREE OF DOCTOR OF PHILOSOPHY

DEPARTMENT OF PHARMACY

NATIONAL UNIVERSITY OF SINGAPORE

2014

DECLARATION

I hereby declare that the thesis is my original work and it has been written by me in its entirety. I have duly acknowledged all the sources of information which have been used in the thesis.

This thesis has also not been submitted for any degree in any university previously.

Zhang Luqi

15 August 2014

ACKNOWLEDGEMENTS

I want to express my deepest gratitude to my supervisor Assistant Professor Ee Pui Lai Rachel for her guidance and support in both my research and personal growth. She taught me how to conceptualize research projects, carry out experiments systemically and troubleshoot problems. She also helped me improve my scientific communication skills. Especially, she is a great teacher who cares about students' opinion and helps students in putting the ideas into action.

I would also like to thank my laboratory members for their scientific support and friendship: Priti Bahety, Wang Ying, Li Yan, Jasmeet Singh Khara, Ashita Nair and final year students who worked in our laboratory. They gave me many helpful scientific suggestions and cheered me on when I met with difficulties in my research. I am also thankful to Ms. Ng Sek Eng and Wong Winnie for their technical assistance. A special appreciation is due to National University of Singapore for giving me the NUS Research Scholarship which allowed me to carry out the scientific pursuit.

Lastly, I would like to thank my family and friends for their support and encouragement.

LIST OF PUBLICATIONS AND PRESENTATIONS

Publications and manuscripts in preparation:

1. **Zhang L**, Ong WQ, Ee PL. Apolipoprotein E4 disrupts normal mitochondrial dynamics through binding to low-density lipoprotein receptor-related protein 5/6 in SH-SY5Y cells. Manuscript in preparation.

2. **Zhang L**, Bahety P, Ee PL. Protective role of Wnt signaling co-receptors LRP5/6 against hydrogen peroxide-induced neurotoxicity and tau phosphorylation in SH-SY5Y neuroblastoma cells. Manuscript in preparation.

3. Bahety P, **Zhang L** and Ee PL. Dihydrofolate reductase enzyme inhibition synergizes with a glycogen synthase kinase-3β inhibitor for enhanced neuroprotective effect in SH-SY5Y neuroblastoma cells. Manuscript in preparation.

4. Bahety P, Tan YM, Hong Y, **Zhang L**, Chan CY, Ee PL. Metabotyping of Docosahexaenoic Acid - Treated Alzheimer's Disease Cell Model. PLoS One. 2014 Feb 27;9(2):e90123.

Conference Abstracts:

1. **Zhang L**, Ong WQ, Ee PL. Apolipoprotein E4 binds to low-density lipoprotein receptor-related protein 5/6 and disrupts normal mitochondrial dynamics in SH-SY5Y cells. 13th International Geneva/Springfield Symposium on Advances in Alzheimer Therapy, Switzerland. 26 – 29 March 2014. Poster presentation.

2. **Zhang L**, Ee PL. Overexpression of LRP5 and LRP6 reduces tau phosphorylation and overcomes neurotoxicity induced by hydrogen peroxide through modulating Wnt signaling in SH-SY5Y. 18th Biological Sciences Graduate Congress, Malaysia. 6 – 8 January 2014. Oral presentation.

3. **Zhang L**, Ee PL. Overexpression of LRP5/6 reduces tau phosphorylation and improves neuronal cell survival in Alzheimer's disease cell model. Annual Pharmacy Research Symposium 2013, Singapore. 03 April 2013. Poster and Oral presentation. First Prize in Abstract Presentation Contest.

4. **Zhang L**, Ee PL. The missing link between LRP5 and ApoEs in the pathogenesis of Alzheimer's Disease. Globalization of Pharmaceutics Education Network Meeting 2012, Melbourne, Australia. 28 November to 01 December 2012. Abstract and Poster presentation.

5. **Zhang L**, Ee PL. The role of LRP5 in Alzheimer's Disease. 7th PharmSci@Asia Symposium "Exploring Pharmaceutical Sciences: New Challenges and Opportunities". Kent Ridge Guild House, National University of Singapore, Singapore. 06-07 June 2012. Abstract and Poster Presentation.

TABLE OF CONTENTS

SUMMARY

Alzheimer's disease (AD) is the most common type of dementia for the elderly and is the sixth-leading cause of death in the U. S.. The complete mechanism of AD still remains unclear and currently there is no effective disease-modifying drug to delay or cure this disease. Although aberrant Wnt inhibition has been implicated in AD pathogenesis, the role of Wnt co-receptors low density lipoprotein receptor-related protein (LRP) 5 and LRP6 has yet to be established. Thus, the overall goal of this study is to explore the functional role of LRP5 and LRP6 in AD. Herein we explored two different objectives:

(1) To assess the protective role of LRP5 and LRP6 against hydrogen peroxide-induced neurotoxicity and tau phosphorylation.
(2) To investigate the effect of LRP5 and LRP6 on apolipoprotein (apo) E4-induced abnormalities in mitochondrial dynamics.

In the first part, we showed that the overexpression of LRP5 and LRP6 activated Wnt signaling in SH-SY5Y cells which was evidenced by elevated T-cell specific transcription factor/lymphoid enhancer factor 1 (TCF/LEF) reporter activities and increased β-catenin protein levels. The transcription of downstream survival

genes Axin2 and Cyclin D1 is consequently increased. On the other hand, knockdown of LRP5 and LRP6 in SH-SY5Y cells resulted in a decrease in Wnt/β-catenin activity and a reduction in survival gene expression. We further demonstrated that overexpression of LRP5 and LRP6 protected SH-SY5Y cells from cell death caused by hydrogen peroxide-induced oxidative stress. In addition, this overexpression significantly suppressed the activity of GSK3β and resulted in the reduction of tau phosphorylation. In the second part, we established the direct interaction between apoE isoforms and LRP5/6. We observed that the interaction between apoE isoforms and LRP5 disrupted the activation ability of LRP5 and exerted isoform-specific effects on GSK3β activity. Furthermore, we demonstrated the detrimental effect of apoE4 in causing mitochondrial dynamics disruption with the aberrantly increased expression of mitochondrial fission proteins, dynamin-related protein 1 (Drp1) and mitochondrial fission 1 (Fis1), and decreased expression of mitochondrial fusion protein mitofusin (Mfn) 2. Subsequently, the changes in mitochondrial morphology towards fission were observed. In addition, we identified dickkopf (DKK) 1 as the inhibitor to disrupt the interaction between apoE4 and LRP5/6. Subsequent disruption of apoE4 and LRP5/6 interaction by DKK1 resulted in a reduction of the elevated mitochondrial fission proteins and an increase of the repressed mitochondrial fusion protein, followed by the restoration of normal mitochondrial dynamics. In conclusion, our data not only indicated the functional role of LRP5 and LRP6 in AD, but also

provided a better understanding in the mechanisms underlying apoE4-induced AD pathology. With further characterization and studies, LRP5 and LRP6 may potentially be explored as the novel therapeutic targets for treating AD.

LIST OF TABLES

LIST OF FIGURES

LIST OF ABBREVIATIONS

AD	Alzheimer's disease
APC	adenomatous polyposis coli
apoE	apolipoprotein E
apoER2	apolipoprotein E receptor 2
APP	amyloid precursor protein
AR	Aspect Ratio
Arg	Arginine
Aβ	β-amyloid
BLAST	Basic Local Alignment Search Tool
BSA	bovine serum albumin
C83	C-terminal fragment 83
C99	C-terminal fragment 99
CIP	Calf Intestinal Alkaline Phosphatase
CK1	casein kinase 1
CNS	central nervous system
Cys	cysteine
ddH_2O	double-distilled H_2O
DKK	dickkopf
DMEM	Dulbecco's modified Eagle medium
Drp1	dynamin-related protein 1
Dvl	dishevelled
EGF	epidermal growth factor
EOAD	early-onset Alzheimer's disease
FBS	fetal bovine serum

FF	Form Factor
Fis1	mitochondrial fission 1
fz	frizzled
GBP	glycogen synthase kinase 3 binding protein
GSK	glycogen synthase kinase
GWAS	genome-wide association study
HDAC	histone deacetylase
IB	immunoblotting
IP	immunoprecipitation
LCM	control L-cell conditioned medium
LDL	low density lipoprotein
LOAD	late-onset Alzheimer's disease
LRP	low density lipoprotein receptor-related protein
L-Wnt-3a cells	L-cells stably transfected with a Wnt-3a expression factor
Mff	mitochondrial fission factor
Mfn	mitofusin
miniprep	minipreparation
mtDNA	mitochondrial DNA
MTT	3-(4,5-dimethylthiazol-2-yl)-2,5-diphenyltetrazolium bromide
NCBI	National Center for Biotechnology Information
NFT	neurofibrillary tangle
OPA1	optic atrophy 1
PBS	phosphate buffer saline
PCC	Pearson’s correlation coefficient
PCR	Polymerase Chain Reaction
PI	propidium iodide

PSEN	presenilin
ROS	reactive oxygen species
S.E.M.	standard error of the mean
sAPPα	soluble APP fragment α
sAPPβ	soluble APP fragment β
Ser	Serine
siRNA	double stranded short interfering RNA
SNP	single nucleotide polymorphism
SorLA/LR11	sorting protein-related receptor/lipoprotein receptor 11
STS	staurosporine
TAE	Tris-Acetate-EDTA
TBST	Tris Buffer Saline with 0.1% Tween 20
TCF/LEF	T-cell specific transcription factor/lymphoid enhancer-binding factor 1
WCM	Wnt3a-conditioned medium
ΔΨm	mitochondrial transmembrane potential

CHAPTER 1. INTRODUCTION

1.1 Alzheimer's disease and current therapeutic approaches

Alzheimer's disease (AD) is a progressive age-associated neurodegenerative disorder and is the most common type of dementia among the elderly. It was first discovered by a German psychiatrist named Alois Alzheimer in 1906 [1] and manifests as a progressive decline in memory and cognitive functions followed by changes in behavior. AD is pathologically characterized by senile plaques formed by abnormal assemblies of β-amyloid (Aβ) and neurofibrillary tangles (NFTs) composed of hyperphosphorylated forms of microtubule-associated tau protein, as well as the loss of neurons and synaptic connections [2-5]. In the U.S. alone, it was estimated that 5.2 million people suffered from AD in 2013, out of which approximately 200,000 people are younger than 65 years while the other 5 million makes up the late-onset AD population. [6]. The AD population is projected to affect 13.8 million people in the U.S. by 2050 [6].

Despite intensive scientific research, there are currently no effective pharmacotherapeutic options that can slow down or stop AD progression. To date, only symptomatic treatment aimed at counterbalancing the disturbance in neurotransmitter levels is available for the treatment of AD. These drugs are designed based on the cholinergic hypothesis which states that changes in the

cholinergic system such as loss of acetylcholine neurons, reduced choline uptake and acetylcholine release are responsible for the deterioration in cognitive functions observed in AD [7-9]. Thus, cholinesterase inhibitors, blocking the degradation of acetylcholine between the synapses, are developed and used as the standard first-line treatment for AD. These drugs mainly include donepezil, rivastigmine and galantamine, approved for the treatment of mild to moderate AD [10]. Another agent currently approved for the treatment of moderate to severe AD is memantine [11], an N-methyl-D-aspartate receptor antagonist. Memantine selectively blocks abnormal transmission of the excitotoxic neurotransmitter, glutamate, that was released at high levels in transgenic mice as well as AD patients [12].

Despite the effectiveness in treating behavioral symptoms, the major drawback of these symptomatic agents is the lack of improvement in cognitive functions in AD patients. Thus, novel treatment approaches or 'disease-modifying' drugs, aimed at reversing the pathogenic steps in AD have been under extensive development [13,14]. Based on the amyloid hypothesis that overproduction and aggregation of Aβ is the main driver of AD pathogenesis, a large group of disease-modifying drugs has been developed to counteract the increase in Aβ production and plaque deposition. However, results from human clinical trials with these amyloid-targeting drugs have largely been disappointing (Table 1-1). A second group of compounds targeting the underlying mechanism of NFT formation has been

Table 1-1. Disease-modifying treatments targeting Aβ.

Drug name	Mechanism	Results	Phases	Ref.
Tramiprosate	Interfere with the binding of glycosaminoglycanes and Aβ, resulting in inhibiting Aβ aggregation	(-) The overall changes in psychometric scores and hippocampus volume were not significant	III	[15]
Colostrinin	Inhibit Aβ aggregation and neurotoxicity	(±) The beneficial effects on cognition function (p=0.02) and daily activities (p=0.03) were moderate.	II	[16]
Scyllo-inositol	Stabilize oligomeric aggregates of Aβ and inhibit Aβ toxicity	(-) The changes in neuropsychological test and daily activities were not significant.	II	[17]
PBT2	Affect the Cu^{2+}-mediated and Zn^{2+}-mediated toxic oligomerization of Aβ	(±) The improvement in ADAS-cog score was near-significant.	IIa	[18]
Semagacestat	Inhibit γ-secretase	(-) Detrimental effects on cognition and functionality were observed.	III	[19, 20]
Tarenflurbil	Inhibit γ-secretase	(-) No improvement was observed in ADAS-cog score and ADCS-ADL scale.	III	[20]
Avagacestat	Inhibit γ-secretase	Ongoing	II	[21]
Etazolate	Stimulate α-secretase non-amyloidogenic pathway	(+) Etazolate was shown to be clinically safe.	IIa	[22]

Table 1-1. Disease-modifying treatments targeting Aβ. (continued)

Drug name	Mechanism	Results	Phases	Ref.
AN-1792	Human Aβ1-42 to initiate active immunization	(-) No significant increase in ADAS-cog scores was seen.	II	[23]
CAD-106, V950, ACC-001	Human Aβ residues (4-10) to initiate active immunization	Ongoing	II	[24]
Bapineuzumab	Aβ N-terminal directed, humanized monoclonal antibody	(-) No improvement in ADAS-cog and DAD scores was shown.	III	[25]
Solanezumab	Aβ central domain directed, humanized monoclonal antibody	(-) Solanezumab failed to improve cognition or functional ability.	III	[24]
IVIg	Natural anti-amyloid antibodies found in human intravenous immunoglobulins	(-) No significant differences in cognitive and functional abilities were observed.	III	[26]

Results for clinical trials: +, encouraging results; -, disappointing results; ±, doubtful results.

Abbreviations: ADAS-cog, AD Assessment Scale-cognitive; ADCS-ADL, AD Cooperative Studies–activities of daily living; DAD, Disability Assessment for Dementia.

developed and is currently in early stages of clinical trials or pre-clinical trials. These agents mainly include methylene blue for interfering with tau deposition [27], lithium for disrupting tau phosphorylation [28] and tau targeting vaccines [13]. Treatments targeting a number of other pathogenic mechanisms have also been considered, including inflammation [29], oxidative stress [30], iron deregulation [31] and cholesterol metabolism [32]. Despite promising premises associated with different pathogenic pathways, phase III clinical trials of many potentially disease-modifying drugs failed to demonstrate any improvement on cognition. Hence, the mechanisms of AD pathogenesis still need to be thoroughly understood and investigated before large efforts are put into drug development and clinical trials.

1.2 AD classification

1.2.1 Early-onset AD

The pathogenesis of AD involves an interplay of complex interactions between multiple genetic and environmental factors. Early-onset AD (EOAD) or familial AD develops before the age of 65 and only accounts for less than 1% of AD population [33,34]. The primary cause for EOAD has been attributed to the overproduction and aggregation of Aβ, owing to mutations in either the amyloid precursor protein (*APP*) gene or presenilin (*PSEN*) 1 or 2 genes which are the essential components in the γ-secretase complex. Figure 1-1 shows the amyloidogenic and non-amyloidogenic processing of APP by three different

enzymes, α-, β- and γ-secretases [3,35]. α- secretase cleaves APP within Aβ sequence and generate soluble APP fragment α (sAPPα) and C-terminal fragment 83 (C83). C83 is further cleaved by γ-secretase into non-amyloidogenic peptide p3 [36]. In this non-amyloidogenic pathway, the production of Aβ is precluded and none of these products are toxic. On the other hand, in the amyloidogenic pathway, β-secretase cleavage of APP creates soluble APP fragment β (sAPPβ) and C-terminal fragment 99 (C99), the latter of which is subsequently processed by γ-secretase to release Aβ. Genetic mutations in *APP* and *PSEN1&2* accelerate the generation of Aβ which was proposed as the prime pathogenic driver for AD by the amyloid hypothesis [37]. Elevation and aggregation of Aβ subsequently leads to tau phosphorylation, cell death and other histological features in AD.

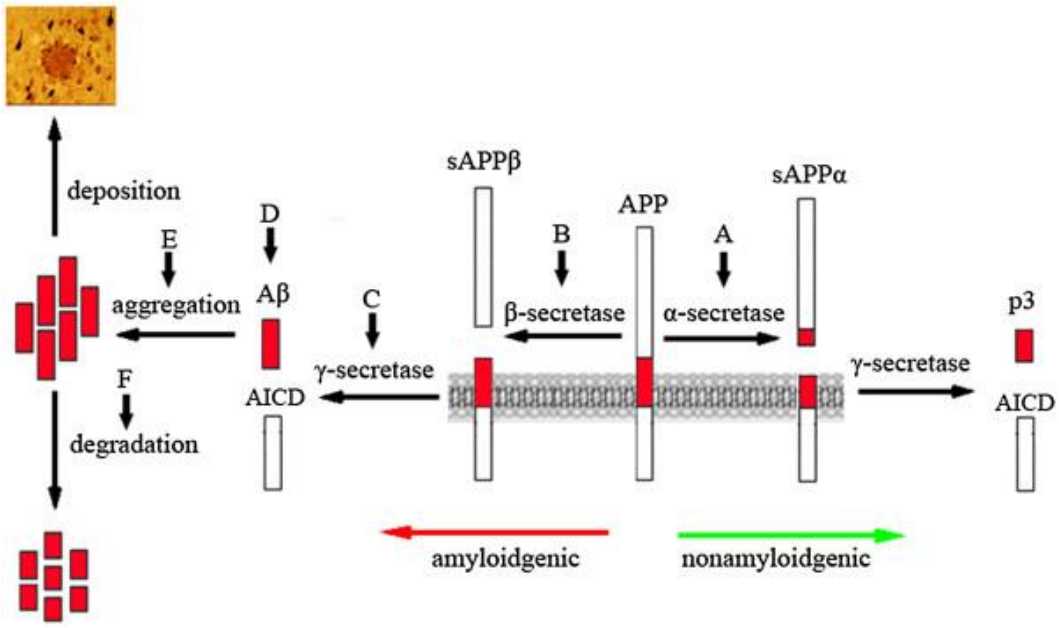

Figure 1-1. Amyloidogenic and non-amyloidogenic processing of APP. sAPPα, soluble APP fragment α; sAPPβ, soluble APP fragmentβ; AICD, amyloid precursor protein intracellular domain. The image was taken from Ref [38].

1.2.2 Late-onset AD

Over 99% of AD cases occur late in life (>65 years) and are referred as late-onset AD (LOAD). Genome-wide association studies (GWAS) have shown that the ε4 allele of the apolipoprotein E (*APOE4*) gene is the main genetic risk factor for LOAD [33,34,39]. Human *APOE* gene exists as three polymorphic alleles ε2, ε3, and ε4 which have a frequency of 8.4%, 77.9% and 13.7% respectively in the general population, but a frequency of 3.9%, 59.4% and 36.7% respectively in the AD population (Figure 1-2) [40]. Aging is the most important known non-genetic risk factor for LOAD. Other potential environmental risk factors include brain trauma, diabetes mellitus, hypertension, obesity, smoking, depression, cognitive inactivity or low educational attainment, and physical inactivity [41-44].

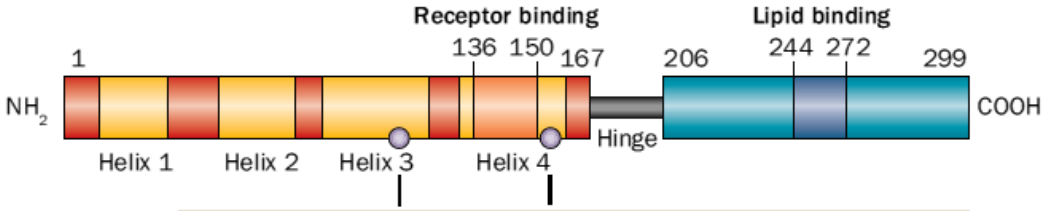

	Isoform-specific amino acid difference		Allele frequency (%)	
	112	158	General	AD
Apo-E2	Cys	Cys	8.4	3.9
Apo-E3	Cys	Arg	77.9	59.4
Apo-E4	Arg	Arg	13.7	36.7

Figure 1-2. The structure of apoE and the meta-analysis on the populations of people with apoE isoforms. This image was taken from Ref [45].

1.3 Apolipoprotein E4

1.3.1 Structure and function

The human apoE protein is a 299-amino acid glycoprotein with a molecular weight of 34 kDa [46,47]. ApoE is synthesized by various organs with the highest expression in liver and central nervous system (CNS). In brain cells, apoE is primarily expressed by astrocytes and microglia [48,49]. Neurons are also able to express apoE in response to pathological stimulation such as excitotoxic injury [50,51]. The human *APOE* gene has multiple single nucleotide polymorphisms (SNPs) across the whole gene [52]. The three most common SNPs result in common isoforms of apoE with different amino acid residues in 112 and 158, where either cysteine (Cys) or arginine (Arg) is present: apoE2 (Cys112, Cys158), apoE3 (Cys112, Arg158), and apoE4 (Arg112, Arg158) [53]. ApoE has two structural domains: a 22-kDa N-terminal domain (residues 1-191) containing the low-density lipoprotein (LDL) receptor binding region (residues 136-150), a 10-kDa C-terminal domain (residues 216-299) containing the lipid binding region (residues 244-272) and a hinge region to join the two domains (Figure 1-2) [45,47]. Cys158 in apoE2 disrupts the receptor binding ability in N-terminal domain [54], while Arg158 in apoE4 mediates N-terminal and C-terminal domain interaction which leads to reduced protein stability and formation of molten globule [55,56].

ApoE plays important roles in regulating lipid homeostasis via lipid transportation among cells in CNS [46,57,58]. ApoE-containing lipoproteins redistribute lipids such as cholesterol to repair the injured neurons. However, apoE4 does not seem to be as efficient as apoE3 in protecting neurons. Expression of apoE3, not apoE4, protects against excitotoxin-induced neuronal damage in mice and age-dependent neurodegeneration in *APOE*$^{-/-}$ mice [59]. ApoE3 and 4 also have opposite effects on neurite extension with apoE3 stimulating and apoE4 inhibiting neurite outgrowth [60-62]. Blocking apoE3 by specific antibody completely abolishes the neurite-promoting effect [62].

1.3.2 ApoE4 neuropathology in AD

1.3.2.1 Effect of apoE4 on Aβ production and clearance

Studies with transgenic mice and humans indicated that apoE4 induces Aβ accumulation and deposition in the brain [63-66]. Although the underlying molecular basis is still largely unknown, *in vitro* and *in vivo* studies suggested that apoE isoforms may have differential effects on Aβ production as well as soluble Aβ clearance. In rat neuroblastoma B103 cells overexpressed with human wild-type APP, apoE4 increased Aβ production to a greater extent than apoE3 (60% vs 30%) [67]. In addition to the effect on stimulating Aβ production, apoE4 disrupts the clearance of soluble Aβ in the brain. Sadowski et al. reported a reduced Aβ pathology by antagonizing the apoE/Aβ interaction [68], suggesting this process may be mediated by the interaction between apoE and Aβ. Indeed, Castellano et

al. demonstrated that greater binding affinity of apoE2 and apoE3 to Aβ corresponded to greater Aβ clearance in mice [65]. Studies with microglial cells indicated that the endolytic degradation of Aβ was dramatically enhanced by apoE3 rather than apoE4 [69]. Moreover, apoE4 potentiated Aβ-induced lysosomal leakage and apoptosis, leading to neuronal degeneration [70].

1.3.2.2 Effect of apoE4 on tau phosphorylation

Other than inducing pathological effects through Aβ, apoE4 also contributes to AD by inducing tau hyperphosphorylation and aggregation. Increased tau phosphorylation was observed in neurons expressing apoE4 [71-74]. Unlike apoE3, recombinant apoE4 did not interact with tau to form a bimolecular complex *in vitro*. Binding assays showed that apoE3 bound to the microtubule-binding repeat region of unphosphorylated tau, suggesting the interaction may inhibit tau self-assembly into higher helical structure [75]. Thus, apoE4 may not be as efficient as apoE3 in inhibiting tau aggregation.

1.3.2.3 Effect of apoE4 on mitochondrial dysfunction

Mitochondrial dysfunction has been described as one of the pathological hallmarks of AD and has been reported to be exacerbated by apoE4 presence [76-78]. In an early study, apoE was shown to interact with mitochondrial F1-ATPase with high affinity [79], suggesting that apoE might play a role in mediating

mitochondrial function. More recently, study with Neuro-2a cells indicated that truncated apoE fragment translocated to mitochondria and caused mitochondrial dysfunction via an unknown mechanism that was mediated by the lipid binding region on apoE [80]. Nakamura et al. later reported that apoE fragment bound to UQCRC2 and cytochrome c, which are the components of mitochondrial respiratory complex III, and COX IV 1, the component of complex IV [81]. The steady-levels of mitochondrial respiratory complexes have been shown to be significantly lower in apoE4-expressing neurons compared with apoE3-expressing neurons, but this effect was not observed in astrocytes, indicating a neuron-specific effect [82]. Subsequently, the reduced enzymatic activity of mitochondrial complex IV from mouse primary neurons indicated that apoE4 lowered mitochondrial respiratory capacity [82]. Similar pattern was also observed in mitochondria isolated from peripheral tissues of AD patients [83].

In addition to its effects on mitochondrial respiratory capacity, apoE4 has been reported to dysregulate other mitochondrial functions. Proteomic analysis showed that mitochondria isolated from hippocampal tissues in apoE3 and apoE4 transgenic mice presented differential protein levels of several molecules that are involved in the processes of energy production, metabolism, oxidative stress and organelle transportation [84]. Post-mortem brain tissue analysis identified 30 transcripts of differential expression proteins related to mitochondrial oxidative function in apoE ε4 carriers compared to non-carriers [85]. Consistent with this

observation, i*n vitro* studies with B12 cells revealed that apoE isoforms possessed different antioxidant abilities in a manner correlated with AD risk (E2> E3> E4) [86]. It is possible that the beneficial or detrimental effects of different apoE isoforms are carried out through regulating the levels of reactive oxygen species (ROS), of which mitochondria is the major endogenous source [87]. In addition, low rates of glucose metabolism have been repeatedly associated with apoE4 in both normal and AD subjects [88-91]. Taken together, dysregulated mitochondrial function plays an important role in apoE4-induced AD pathogenesis. Other than disrupted mitochondrial functions, perturbance in mitochondrial dynamics has also been implicated in AD [78,92,93].

1.3.3 Mitochondrial dynamics

Mitochondria are highly dynamic organelles that constantly move and undergo structural transitions. Moving along cytoskeletal tracks, individual mitochondria encounter each other and undergo fusion with the merging of double membranes. Conversely, an individual mitochondrion can divide by fission process to yield two or more shorter mitochondria. In addition to controlling mitochondrial shape and distribution, these two processes also facilitate the mixing of outer membranes, inner membranes and matrix contents to maintain genetic and biochemical uniformity within mitochondrial population. Balanced mitochondrial dynamics play a protective role in mitochondria with fission facilitating mitophagy of defective mitochondria and fusion contributing to retention of

critical material [94]. Mixing of mitochondrial proteins and DNA contents by mitochondrial fusion process is also critical in maintaining mitochondrial DNA (mtDNA) stability and mitochondrial respiratory function. Loss of mitochondrial fusion reduces mtDNA dramatically and causes severe mitochondrial dysfunction and compensatory mitochondrial proliferation [95]. Several cell lines including mouse embryonic fibroblasts [96], cerebellar Purkinje cells [97], skeletal myocytes [95], and cardiac myocytes [98] lacking mitochondrial fusion proteins mitofusins (Mfns) displayed declined respiratory capacity. Moreover, mitochondrial fission has been implicated in the process of apoptosis. Inhibiting mitochondrial fission protein dynamin-related protein 1 (Drp1) activity by knockdown approach or overexpressing a dominant-negative mutant of Drp1, delayed the release of apoptotic effector cytochrome c [99-101]. Apoptosis is also alleviated when mitochondrial fission factor (Mff) or mitochondrial fission 1 (Fis1) is reduced [102,103]. Disturbance in mitochondrial dynamics have been implicated in many diseases with AD being one of them [104,105].

1.3.4 Disrupted mitochondrial dynamics in AD

Multiple lines of evidence support that mitochondrial fusion and fission processes are perturbed in AD. Morphometric analysis revealed that mitochondria in AD neurons not only decreased in number but also enlarge in size [78]. The finding of enlarged and swollen mitochondria was also reported in AD cybrid cells [92] and fibroblasts from LOAD patients [106]. The elongated mitochondria in LOAD

fibroblasts were found to accumulate in perinuclear area with significantly decreased level of Drp1. Overexpression of wild-type Drp1 in these fibroblasts rescued mitochondrial abnormalities [106]. A more detailed immunoblot analysis indicated that the levels of Drp1, optic atrophy 1 (OPA1), Mfn 1 and 2 were significantly decreased whereas the level of Fis1 was increased in AD brain. Contrary to the above reported studies, Manczak et al. showed an increased expression of Drp1 and a reduction in those of Mfn1 and Mfn2 in AD patients [107]. Despite several studies indicating altered mitochondrial dynamics to be involved in AD pathogenesis, the upstream drivers of this pathological effect have yet to be established. Moreover, the role and mechanism of apoE4 in altering these mitochondrial dynamics remains unknown. It is likely that apoE4 carries out the detrimental effects through its receptors. Among all the apoE4 receptors, LRP5 and LRP6 are of particular interest due to their essential role in Wnt signaling, dysregulation of which has been reported to be associated with AD. Given the lack of information between the involvement of LRP5/6 in apoE4-induced pathology in AD, we have attempted to address this gap in Chapter 4 and 5.

1.4 ApoE receptors

1.4.1 Low density lipoprotein receptor family

The strong implication of apoE4 in AD pathogenesis raised the possibility that apoE4 might mediate its detrimental effects at least in part through its receptors.

ApoE receptors include the core members from LDL receptor family such as low density lipoprotein (LDL) receptor-related protein (LRP) 1, apoE receptor 2 (apoER2) as well as several more distantly related members like sorting protein-related receptor/lipoprotein receptor 11 (SorLA/LR11), LRP5 and LRP6 [108,109]. LDL receptor family members are a group of single transmembrane proteins located on the cell surface that recognizes and mediates endocytosis of several structurally diverse ligands. All receptors share several similar structural domains: Ligand-binding repeats, epidermal growth factor (EGF) precursor homology domains sensitive to pH, six-bladed β-propeller structure involved in pH dependent release of cargo, a transmembrane domain and a cytoplasmic tail with NPxY motifs (Figure 1-3) [110]. Most of the members are built from a unifying module of N-terminal Ligand-binding repeats followed by a C-terminal cluster of β-propeller structures. In the distantly related members, this module is inverted (LRP5 and LRP6) or combined with motifs that are not seen in the other receptors (SorLA/LR11) (Figure 1-3). Compared to the other members of this receptor family, LRP5 and LRP6 have been relatively less explored in AD pathology despite their functional importance in the Wnt signaling pathway.

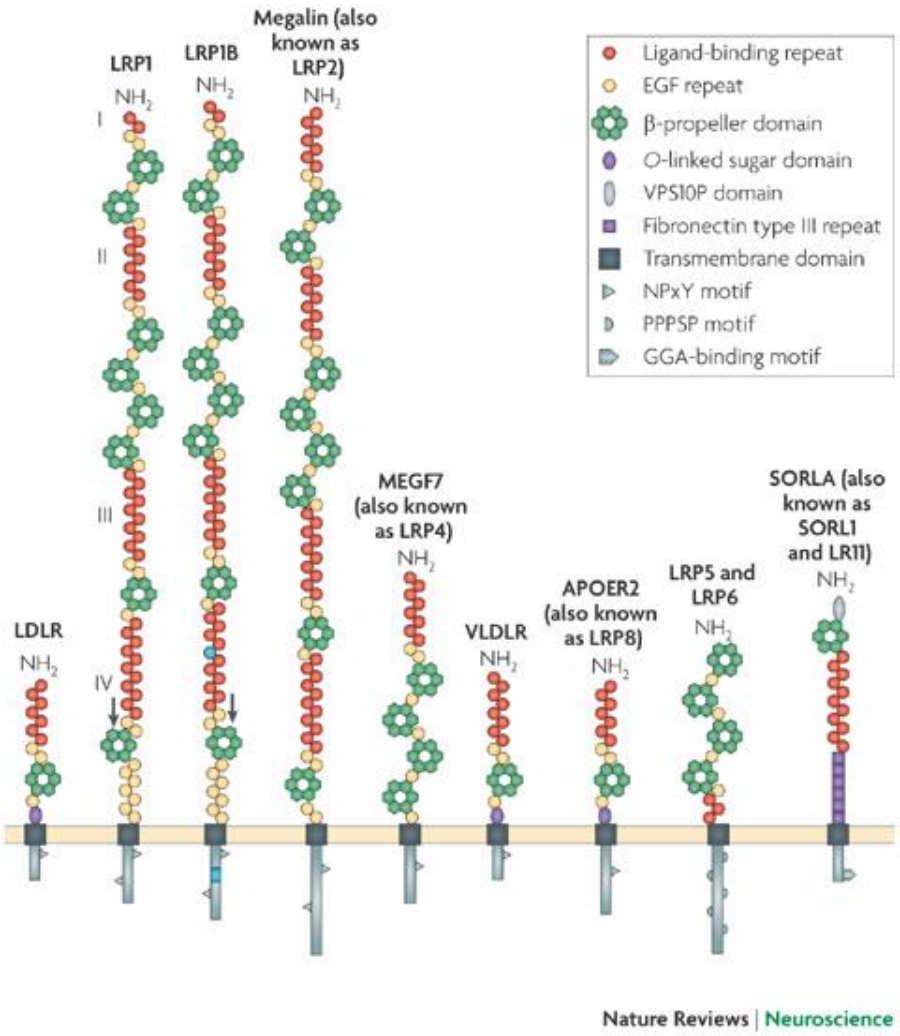

Figure 1-3. The structure of LDL receptor family members. The image was taken from Ref [111].

1.4.2 Low density lipoprotein-related protein 5 and 6

LRP5 and LRP6 are type I single transmembrane proteins with 1615 and 1613 amino acid residues respectively. They share 73% and 64% identity in extracellular and intracellular domains. The function of LRP5 and LRP6 were revealed with genetic studies of depletion and overexpression. Mice lacking LRP6 exhibited developmental defects that were similar to mutations of individual Wnt

genes [112]. *In vitro* co-immunoprecipitation assay and *in vivo Xenopus* embryo studies showed that LRP6 activated Wnt-Frizzled (Fz) signaling and induced Wnt responsive genes, whereas a dominant negative variant of LRP6 blocks signaling by Wnt or Wnt-Fz [113]. Later, Kelly et al. reported the similar reception role of LRP5 in Wnt signaling using mice with mutations in LRP5 [114]. Thus, LRP5 and LRP6 are the essential co-receptors to facilitate the transduction of Wnt signaling.

Wnt signaling is an autocrine and paracrine signaling pathway that has been implicated in many development processes including axis formation and midbrain development [115,116]. Wnt signaling pathway participates in the development of central nervous system and regulates the function of adult nervous system [117,118]. Aberrant regulated Wnt signaling has been associated with many diseases, including neurodegenerative disorders such as AD [119,120].

Among all the downstream pathways, only the canonical Wnt/β-catenin signaling pathway requires the action of LRP5 and LRP6. In the absence of Wnt ligands, a destruction complex composed of Axin, adenomatous polyposis coli (APC), glycogen synthase kinase (GSK) 3β and casein kinase 1 (CK1), phosphorylates the key regulator of this pathway, β-catenin [121]. Phosphorylated β-catenin is recognized and degraded by ubiquitin-proteasome system. Upon Wnt ligands

recognizing its receptor Fz on the cell surface, a complex is formed consisting of Wnt ligands, receptor Fz and co-receptor LRP5/6, leading to the association with CK1 [113,122]. This activates and recruits dishevelled (Dvl) to the cell plasma compartment. The activated Dvl displaces GSK3β from the destruction complex by recruiting GSK3 binding proteins (GBP)/Frat-1. Wnt stimulation inhibits the activity of GSK3β, resulting in the accumulation and nuclear translocation of β-catenin [123]. Inside the nucleus, β-catenin binds to T-cell specific transcription factor/lymphoid enhancer-binding factor 1 (TCF/LEF) by replacing histone deacetylase (HDAC) and transcriptional corepressor Groucho and activates the transcription of its target genes including *C-MYC, CYCLIN D1, AXIN2* that promote cell proliferation, differentiation, and tissue development [124] (Figure 1-4).

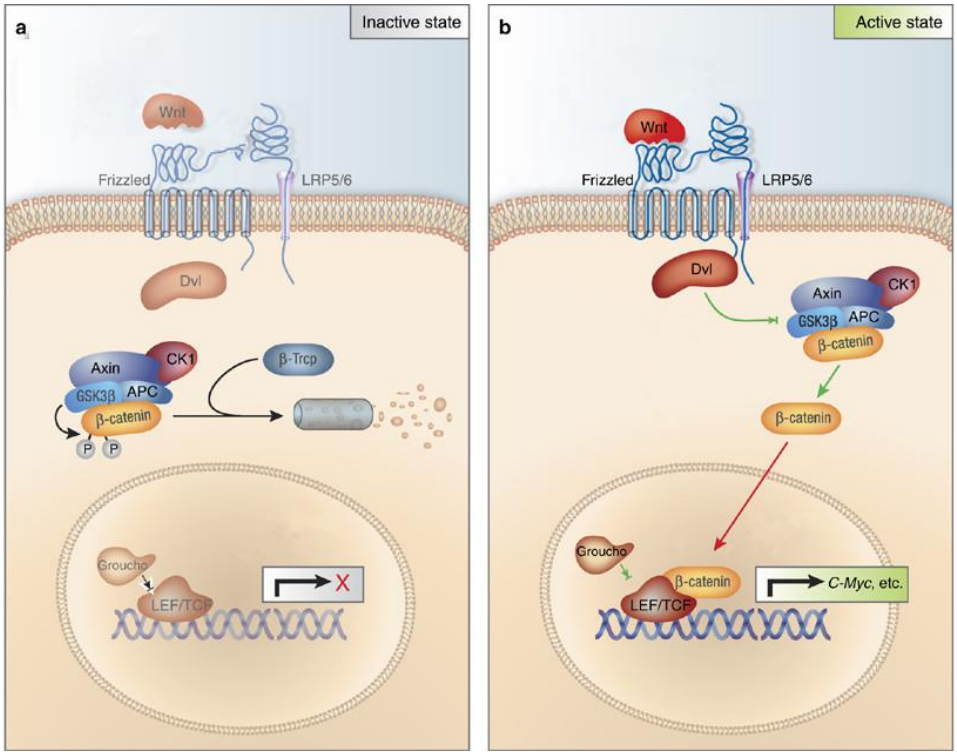

Figure 1-4. Schematic representation of the canonical Wnt/ β-catenin signaling pathway. This image was modified from Ref [125].

Although LRP5 and LRP6 are highly homologous proteins [126-128], they may not carry out equivalent functions. *LRP6*$^{-/-}$ mice were lethal and displayed mid/hindbrain defects which are the hallmarks for Wnt1-deficient mice. These mice revealed an excess of neural tissue and a corresponding loss of paraxial mesoderm, resembling to Wnt3a mutant mice. Mice depleted of LRP6 also had both anteroposterior and dorsoventral patterning defects, which were similar to mice carrying mutations in Wnt7a [112]. *LRP5*$^{-/-}$ mice, however, underwent normal embryogenesis and could grow into adulthood. These mice displayed osteoporosis-pseudoglioma [129] and abnormal cholesterol metabolism [130]. Thus, defects in *LRP6*$^{-/-}$ mice were much more severe than those in LRP5 deficient mice, though some functional redundancy was shown in both of the knockout mice. Mice with *LRP5; LRP6* double homozygous mutants failed to establish a primitive streak which resembled Wnt3 mutant mice and died earlier than *LRP6*$^{-/-}$ single knockout mice [114]. Taken together, LRP5 and LRP6 are involved in transducing the signaling by different Wnt ligands. Wnt3 relies on either LRP5 or LRP6 to exert the function, while Wnt1, Wnt3a and Wnt7a require primarily LRP6 rather than LRP5. The comparison among an allelic series of *LRP5; LRP6* knockout mice on the severity of developmental abnormalities indicated that LRP5 and LRP6 share overlapping function but LRP6 has a dominant role over LRP5 during embryonic development [114].

1.4.3 Dysregulated Wnt signaling in AD

Numerous studies have shown that Wnt/β-catenin signaling is dysregulated at different levels in AD [119,131-133]. The familial AD-linked *PSEN1* variant directly bound to β-catenin protein and formed multiprotein complexes, which resulted in reduced β-catenin accumulation and nuclear translocation [134-136]. LOAD risk factor apoE4 inhibited Wnt/β-catenin signaling and decreased β-catenin level [137]. Activated GSK3β, with a concomitant decrease in β-catenin levels, has been found in AD brains with NFT [138]. *In vivo* studies demonstrated that GSK3β transgenic mice displayed the sign of neurodegeneration and spatial learning deficits [139]. Recently, a genome-wide linkage study identified that the polymorphism of LRP6 is associated with LOAD [140]. Further molecular studies showed that this polymorphism *Ile* - 1062 → *Val* reduced Wnt/β-catenin activity in HEK293T cells. Subsequently, the splice variant LRP6Δ3 (LRP6 isoform skipping exon 3) was also reported to be associated with AD [141].

On the other hand, restoration of the repressed Wnt activity has been shown to have promising therapeutic effects in AD [142]. For example, activation of Wnt signaling by introducing Wnt ligands, Wnt3a or Wnt7a, overcame Aβ neurotoxicity in rat hippocampal neurons [143,144]. Similarly, lithium, the non-specific inhibitor of GSK3β, has been widely used in activating Wnt signaling to rescue neurodegeneration and improve behavioral impairments in rats injected with preformed Aβ fibrils [145]. Another possible approach of activating Wnt

signaling is to introduce or overexpress functional LRP5 and LRP6, however, not much work has been done in this regard. It is thus one of our aims in this thesis to evaluate the neuroprotective role of LRP5 and LRP6 against AD pathology and it has been discussed in Chapter 3.

1.5 Summary and concluding remarks

Due to the numerous failures of the current AD therapies in clinical trials, there is a need to better understand the underlying pathological mechanisms and to develop novel therapeutic drug targets. Despite acting as Wnt co-receptors and apoE4 receptors, the functional role of LRP5 and LRP6 in AD, however, still remains unclear. Thus, further knowledge of LRP5 and LRP6 will not only provide us with deeper understanding of AD pathology, but also help us in discovering novel therapeutic targets for the treatment of AD.

CHAPTER 2. HYPOTHESIS AND AIMS

A growing body of evidence has implicated the involvement of dysregulated Wnt signaling in the etiology of AD. Multiple Wnt components have been reported to be aberrantly modulated in AD. The recent studies of LOAD have pointed out the contribution of genetic variations of Wnt co-receptor LRP6 in the repressed Wnt activity. The functional role of Wnt co-receptors LRP5 and LRP6 in AD, however, still remains unclear. Thus, the overall goal of this study is to characterize the role of LRP5 and LRP6 in AD, with the objective of better understanding of the underlying mechanism and identifying novel Wnt-targeted therapies to prevent or delay AD development and progression.

In the first part of this thesis, we hypothesized that overexpression of LRP5 and LRP6 protects neuronal cells from cytotoxicity induced by hydrogen peroxide and reduces tau phosphorylation. Our hypothesis was based on several observations: First, LRP5 and LRP6 are the upstream co-receptors of Wnt signaling which plays an important role in regulating and maintaining the function of adult nervous system [117,118]. Second, activation of Wnt signaling either by Wnt ligands or GSK3β inhibitor has been shown to rescue neurodegeneration and improve behavioral impairment [143-145]. In addition, GSK3β has been implicated as one of the main tau phosphorylation kinases in the AD etiology [146,147]. As the direct modulators of GSK3β activity, LRP5 and LRP6 are

expected to affect the phosphorylation process of tau. Given these observations, overexpression of LRP5 and LRP6 is an attractive approach for improving neuronal cell survival and reducing tau phosphorylation.

To test our first hypothesis, we explored three specific aims:

(1) Establish the essential role of LRP5 and LRP6 in regulating Wnt/β-catenin activity and the expression of downstream proliferation genes.
(2) Assess the role of LRP5 and LRP6 in improving neuronal survival and protecting cells from oxidative stress.
(3) Characterize the role of LRP5 and LRP6 in reducing tau phosphorylation.

Other than functioning as Wnt co-receptors, LRP5 and LRP6 also structurally belong to LDL receptor family. Several members from LDL receptors have been shown to interact with apoE isoforms [111]. However, there is no direct evidence of the interaction between LRP5/6 and apoE. In addition, apoE4 has been reported to carry out its detrimental effect through dysregulating mitochondrial function [81,82]. As mitochondrial function is reflected and maintained by balanced mitochondrial dynamics, we were interested in assessing the effect of apoE4 on mitochondrial dynamics and whether this process was mediated by LRP5/6. Thus, in the second half of this thesis, we hypothesized that apoE4 disrupts normal mitochondrial dynamics through binding to LRP5/6.

To test this second hypothesis, we had three specific aims:

(1) Identify the interaction between Wnt co-receptors LRP5/6 and apoE isoforms.
(2) Evaluate the effect of apoE4 on mitochondrial dynamics in neuronal cell lines.
(3) Characterize the effect of the interaction between LRP5/6 and apoE4 on mitochondrial dynamics.

Work done to address three specific aims of the first hypothesis is included in Chapter 3, where we showed the neuroprotective role of Wnt co-receptors LRP5 and LRP6 against hydrogen peroxide-induced neurotoxicity and tau phosphorylation in SH-SY5Y neuroblastoma cells. The three aims of the second hypothesis are discussed in Chapter 4 and 5. In Chapter 4, we identify the interaction between LRP5/6 and all three common apoE isoforms and its isoform-specific effects on GSK3β activity. In Chapter 5, we report that apoE4 disrupts the normal mitochondrial dynamics and this abnormal disturbance is mediated through binding to LRP5/6.

Achieving the above aims not only provided us with deeper insights into the contributory role of LRP5/6 in AD, but also a new robust linkage between Wnt signaling and apoE4 pathology. This knowledge is useful for the subsequent development of LRP5 and LRP6 as the therapeutic targets for the treatment of AD.

CHAPTER 3. PROTECTIVE ROLE OF WNT SIGNALING CO-RECEPTORS LRP5/6 AGAINST HYDROGEN PEROXIDE-INDUCED NEUROTOXICITY AND TAU PHOSPHORYLATION IN SH-SY5Y NEUROBLASTOMA CELLS

3.1 Introduction

Among the factors associated to the pathogenesis of AD, growing amount of research suggests a vital role of dysregulated Wnt activity in the etiology of AD [133,134,137]. Multiple Wnt components have been reported to be altered in AD [119,131,132]. Central to these events is the GSK3β enzyme which plays an upstream role in the regulation of Wnt signaling activity, as well as a downstream mediator of tau phosphorylation as one of the major kinases. Failing to inhibit GSK3β activity leads to increased tau phosphorylation in primary culture of hippocampal neurons [147,148]. In addition to its role in tau pathology, the involvement of GSK3β in AD associated oxidative stress has also been widely studied. Abnormally activated GSK3β would reduce effectiveness of cellular defense systems, resulting in increased vulnerability to oxidative stress and eventually neuronal cell death [143,144]. Despite the important role of GSK3β in the pathogenesis of AD, currently there is no effective and safe therapeutic treatment targeting GSK3β.

LRP 5 and LRP6 are the membrane-bound Wnt co-receptors, which modulate Wnt signaling pathway through directly regulating the activity of GSK3β [149,150]. Upon binding to Wnt ligand, LRP5 and LRP6 inhibit the phosphorylation activity of GSK3β by recruiting Axin to plasma membrane and subsequently facilitate the accumulation of β-catenin and transcription of downstream target genes [149,151]. Research by De Ferrari et al. has suggested a link between LRP6 polymorphisms and LOAD through attenuating Wnt signaling [140] and a more recent publication reported that a novel LRP6 gene alternative splice variant in AD patients diminished Wnt signaling transduction [152]. However, the functional *in vitro* studies for understanding the role of LRP5/6 in AD pathology are still missing in cultured neuronal cell lines.

In this study, we evaluated the role of LRP5 and LRP6 in protecting neuronal cells against oxidative stress-induced cell death and reducing tau phosphorylation through regulating Wnt signaling. Our results show that overexpression of LRP5 and LRP6 in human neuroblastoma SH-SY5Y cells activated Wnt signaling and upregulated downstream proliferation genes. In contrast, silencing of LRP5 and LRP6 resulted in the repression of Wnt activity and expression of proliferative markers. Furthermore, we found that increasing protein expression of LRP5 and LRP6 overcame the cytotoxicity increased by oxidative stress and rescued SH-SY5Y from cell death. In addition, overexpressing LRP5 and LRP6 phosphorylated GSK3β at Serine (Ser) 9 residue and inhibited its activity, leading

to reduced tau phosphorylation. These data suggest that modulation of Wnt activity via the co-receptors LRP5 and LRP6 may serve as an attractive therapeutic strategy to enhance neuronal survival in neurodegenerative diseases such as AD.

3.2 Materials and Methods

3.2.1 Cell culture and reagents

All cell culture reagents were purchased from Sigma Chemical Co. (St. Louis, MO). Human neuroblastoma SH-SY5Y cells were cultured in Dulbecco's modified Eagle medium (DMEM) containing 10% fetal bovine serum (FBS), 100μg/mL streptomycin and 100units/mL of penicillin in a humidified chamber at 37°C, 5% CO_2. These cells were transfected with either vector alone (pcDNA3.1 or pCS2+) or plasmids expressing the full length LRP5 (a kind gift from Dr Georges Rawadi, Galapagos, France) or LRP6 (a kind gift from Dr. Xi He, Children's Hospital Boston, USA). Gene knockdown experiments were performed using double stranded short interfering RNA (siRNA) targeting LRP5 and LRP6 purchased from Dharmacon (Lafayette, CO): LRP5 On-Target Plus SmartPool siRNA, LRP6 On-Target Plus SmartPool siRNA and scrambled On-Target Plus non-targeting pool siRNA. TOPglow and pRL-CMV Renilla plasmids were purchased from Millipore (Bedford, MA). All transfection experiments were performed with Lipofectamine 2000 (Invitrogen, Carlsbad, CA) in OptiMEM (Invitrogen, Carlsbad, CA) according to the manufacturer's protocol. For the

collection of control L-cell conditioned medium and Wnt3a-conditioned medium (designated as LCM and WCM), both L-cells and L-cells stably transfected with a Wnt-3a expression factor (L-Wnt-3a cells) were kindly provided by Professor Victor Nurcombe (Institute of Medical Biology, A*STAR, Singapore) and maintained in DMEM supplemented with 10% FBS, 100µg/mL streptomycin, 100units/mL of penicillin and 400µg/mL of G418. WCM was prepared from Wnt-3a secreting L-Wnt-3a cells according to ATCC instructions.

3.2.2 Quantitative Real-Time PCR

Total RNA from SH-SY5Y cells was isolated using RNeasy Mini Kit (Qiagen, Valencia, CA), followed by on-column DNase treatment to remove genomic DNA contamination according to the manufacturer's instructions. RNA samples were reverse-transcribed into cDNA using Superscript III 1st strand Synthesis System Kit (Invitrogen, Carlsbad, CA) according to the manufacturer's instruction. Quantitative Real-Time PCR was performed with iQ SYBR Green Supermix (Bio-Rad Laboratories, Hercules, CA) on an iCycler iQ^{TM}5 Real-Time PCR detection system (Bio-Rad Laboratories, Hercules, CA). Relative change in gene expression was calculated using ΔΔCt method by iQ^{TM}5 Optical System software using GAPDH as an endogenous mRNA control. Primers used were as shown in Table 3-1.

Table 3-1 Primers used to determine the mRNA levels of GAPDH, Cyclin D1 and Axin2.

Primer Name	Sequence
GAPDH forward	5'-ATG TTC GTC ATG GGT GTG AA-3'
GAPDH reverse	5'- TGT GGT CAT GAG TCC TTC CA-3'
Cyclin D1 forward	5'-TGT TCG TGG CCT CTA AGA TGA AG-3'
Cyclin D1 reverse	5'-AGG TTC CAC TTG AGC TTG TTC AC-3'
Axin2 forward	5'-ACA ACA GCA TTG TCT CCA AGC AGC-3'
Axin2 reverse	5'-GCG CCT GGT CAA ACA TGA TGG AAT-3'

3.2.3 Dual luciferase reporter assay

SH-SY5Y cells ($2.5x10^5$) were seeded in 24-well plates overnight and transfected with 1μg LRP5 or LRP6 expression plasmids, 1μg reporter construct (TOPglow) and 0.04μg pRL-CMV Renilla control plasmids. For gene knockdown assays, 20nM siRNA was added in place of LRP5 or LRP6 expression plasmids. TOPglow plasmid contains four copies of the TCF binding site which is activated by β-catenin, whereas pRL-CMV Renilla is used for normalizing the cell count. After 6 hours of transfection, the medium was replaced with either LCM or WCM. Cells were harvested and lysed using 100μL 1 × reporter lysis buffer (Promega, Madison, WI) twenty-four hours post transfection and 20μL sample was transferred into Nunc-Immuno MicroWell 96 well polystyrene plate (Roskilde, Denmark). Luciferase activity was measured with the Dual-Luciferase Reporter Assay Kit (Promega, Madison, WI) according to the manufacturer's instruction, using 100μL Dual-Glo® luciferase assay reagent to measure the firefly luciferase

activity and 100μL Dual-Glo® Stop&Glo® reagent to determine the Renilla luminescence with a luminometer (Tecan, MTX Lab Systems Inc., Vienna, VA). All the readings were performed in triplicates and expressed as mean ± S.E.M. of the normalized ratios of Firefly to Renilla luciferase and as the percentage of samples transfected with respective vectors.

3.2.4 Western blotting analysis

Western blotting was used to analyze the protein levels of LRP5, LRP6, β-catenin, dephosphorylated β-catenin, cleaved caspase 3 and 7, GSK3β and phosphorylated tau. Cells transfected as above mentioned were washed with phosphate buffer saline (PBS) and solubilized in lysis buffer (25mM Tris, 2.5mM EDTA, 2.5mM EGTA, 100mM NaCl, 20mM $C_3H_7Na_2O_6P$, 20mM NaF, 1mM Na_3VO_4, 10mM $Na_4P_2O_7$, 0.5% deoxycholate, 1% Triton X-100, pH7.4) supplemented with protease inhibitor cocktail tablet (Roche Diagnostics, Germany). Samples (30μg protein per lane) were run on 8-15% polyacrylamide SDS gels and transferred onto polyvinylidene fluoride membranes (Bio-Rad Laboratories, Hercules, CA). Non-specific binding was blocked with 5% fat-free milk in TBST (Tris Buffer Saline with 0.1% Tween 20) at room temperature for 1 hour. Membranes were incubated with primary antibodies at 4˚C overnight, washed and incubated with secondary antibodies at room temperature for 1 hour, followed by washing for another 3 times. The protein bands were visualized with the ECL Western Blotting detection kit (Thermo Scientific, South Logan, UT). The primary antibodies used were: LRP5 (Invitrogen, Carlsbad, CA), LRP6 (Cell Signaling

Technology, Beverly, MA), β-catenin (Santa Cruz Biotechnology, Santa Cruz, CA), dephosphorylated β-catenin (Millipore, Bedford, MA), GSK3β (Cell Signaling Technology, Beverly, MA), PHF-Tau AT8 (Thermo Scientific, South Logan, UT), β-actin (Santa Cruz Biotechnology, Santa Cruz, CA), cleaved caspase 3 (Cell Signaling, Beverly, MA), and cleaved caspase 7 (Cell Signaling, Beverly, MA). Anti-mouse and anti-rabbit IgG secondary antibody conjugated with horseradish peroxidase were purchased from GE Healthcare Life Sciences, US. Several Western blotting results were quantified using ImageJ 1.47 (National Institutes of Health, Bethesda, MD).

3.2.5 Aβ25-35 and Aβ42 oligomer and fibril preparation

Aβ25-35 was purchased from Sigma Chemical Co. (St. Louis, MO) and Aβ42 was purchased from AnaSpec Inc. (Fremont, CA). 1,1,1,3,3,3-Hexafluoro-2-Propanol (HFIP, Sigma Chemical Co., St. Louis, MO) was added to Aβ peptide with the final peptide concentration of 1mM in the bottom of the vial through the rubber spetum with a 1mL syringe and a sharp needle. Aβ-HFIP solution was sonicated for 5 min before incubation at room temperature for one hour. The solution was then aliquoted as 10μL in 0.2mL sterile microcentrifuge tubes. The tubes were open and HFIP was allowed to evaporate overnight in the fume hood. A thin clear film was formed at the bottom of the tubes indicating good peptide quality. Dried peptide films were stored in -20˚C for further use. Upon using, DMSO was added into peptide films and vortexed to make 5mM Aβ stock. To

prepare Aβ oligomers, 5mM Aβ in DMSO was diluted with ice-cold phenol-free and serum-free F-12 cell culture media (Sigma Chemical Co., St. Louis, MO) to a final concentration of 100μM Aβ. The tube was vortexed for 15 sec and aged at 4˚C for indicated days. To prepare Aβ fibrils, 5mM Aβ in DMSO was diluted with ice-cold phenol-free and serum-free F-12 cell culture media (Sigma Chemical Co., St. Louis, MO) to a final concentration of 100μM Aβ. The tube was vortexed for 15 sec and aged at 37˚C for indicated days.

3.2.6 Cell viability analysis

SH-SY5Y cells were transfected with 10μg LRP5 or LRP6 plasmids in 10cm petri dish. For Aβ treatment, transfected cells were trypsinized and seeded with densities indicated in the result chapter in phenol-free FBS-free F12 medium. Cells were treated with a series of concentrations of Aβ25-35 and Aβ1-42 monomers, oligomers and fibrils for 24 hours, 48 hours and 72 hours. Cell viability was measured using Cell Counting Kit-8 solution (CCK-8, Dojindo Laboratories, Kumamoto, Japan) and CytoTox 96® Non-Radioactive Cytotoxicity Assay (Promega, Madison, WI). 10μL CCK-8 solution was added to each well of the 96-well plate and the plates were incubated in the CO_2 incubator for 4 hours. The absorbance of the formazan product was measured at 450nm using microplate reader (Tecan Infinite® 200 PRO, Männedorf, Switzerland). CytoTox 96® Non-Radioactive Cytotoxicity Assay was performed according to manufacturer's protocol. Briefly, 20μL Lysis Solution was added to target cell

maximum lactate dehydrogenase (LDH) release control. After 45 min, 50μL of the supernatant from each well of the assay plate was transferred to the corresponding well of a Nunc-Immuno MicroWell 96 well polystyrene plate (Roskilde, Denmark). 50μL of reconstitute Substrate Mix was added to each well and incubated at room temperature for 30 min, protected from light. 50μL of Stop Solution was added and absorbance was recorded at 490nm with microplate reader. For hydrogen peroxide treatment, transfected cells were trypsinized and seeded at a density of $1.5x10^4$ cells/well for 24h before being treated with 0-50μM hydrogen peroxide in WCM for 24 h. Cell viability was measured using 3-(4,5-dimethylthiazol-2-yl)-2,5-diphenyltetrazolium bromide (MTT) assay. MTT was dissolved in PBS to give a concentration of 5mg/mL. 20μL of MTT solution was then added into each well to yield a final volume of 220μL/well. Plates were incubated in the CO_2 incubator for 4 hours. Media were replaced with 100μL DMSO to dissolve formazan crystals with 20 min shaking on the orbital shaker. The absorbance of the formazan product was measured at 595nm using microplate reader. All the experiment was repeated three times and cell viability was represented as the percentage of the vehicle control.

3.2.7 Cell cycle analysis

SH-SY5Y cells were transfected and treated as described in Section 3.2.5 of this chapter. The effect of LRP5 and LRP6 overexpression on the cell cycle distribution was accessed by flow cytometry after staining the cells with

propidium iodide (PI). Transfected cells were fixed in 100μL of PBS and 400μL ice-cold 70% ethanol and stored in -20˚C overnight. On the following day, samples were washed with PBS once and stained in 500μL PBS with 16μL/mL PI and 240μL/mL RNase. Cell fluorescence was measured using the Dako Cytomation Cyan LX (Beckman Coulter, Brea, CA) and cell cycle analysis was performed with Summit 4.3 software (Beckman Coulter, Brea, CA).

3.2.8 Statistical analysis

All data was presented as an average of three independent experiments ± S.E.M. Statistical analysis was performed using Student's t test (SPSS, Chicago, IL) and significance was assumed at $p < 0.05$.

3.3 Results

3.3.1 LRP5 and LRP6 overexpression upregulates Wnt/β-catenin signaling and downstream proliferative genes in SH-SY5Y cells

To explore the functional role of Wnt co-receptors LRP5 and LRP6 in human neuroblastoma SH-SY5Y cells, we first overexpressed the co-receptors in SH-SY5Y cells and examined their effects on downstream Wnt signal transduction. As shown in Figure 3-1A, total and active (dephosphorylated) β-catenin protein levels were found to be elevated in LRP5- and LRP6-overexpressing SH-SY5Y

cells compared to control cells transfected with empty vectors, both in the absence and presence of Wnt3a ligands. In addition, we analyzed TCF/LEF transcriptional activities in the transfected cells using a TCF/LEF-responsive luciferase reporter vector (TOPglow) and found that the luciferase activities were significantly increased (Figure 3-1B). Compared to the vector control, TCF/LEF transcriptional activities were increased by approximately 10.7- and 76.6- fold in the presence of Wnt3a-conditioned media in LRP5 and LRP6 transfectants respectively. We next examined the expression of several Wnt downstream target genes involved in cell proliferation such as Axin2 and Cyclin D1 and observed a significant increase in gene expression with LRP5 and LRP6 overexpression. As shown in Figure 3-1C, the mRNA levels of Axin2 and Cyclin D1 were significantly increased by 39.4 ± 6.8% and 25.6 ± 1.0% respectively with LRP5 overexpression and 37.3 ± 6.2% and 40.2 ± 13.0% respectively with LRP6 overexpression in SH-SY5Y cells treated with Wnt3a ligands. These findings demonstrate that LRP5 and LRP6 overexpression are effective in transducing downstream Wnt signal transduction and target gene expression in SH-SY5Y cells.

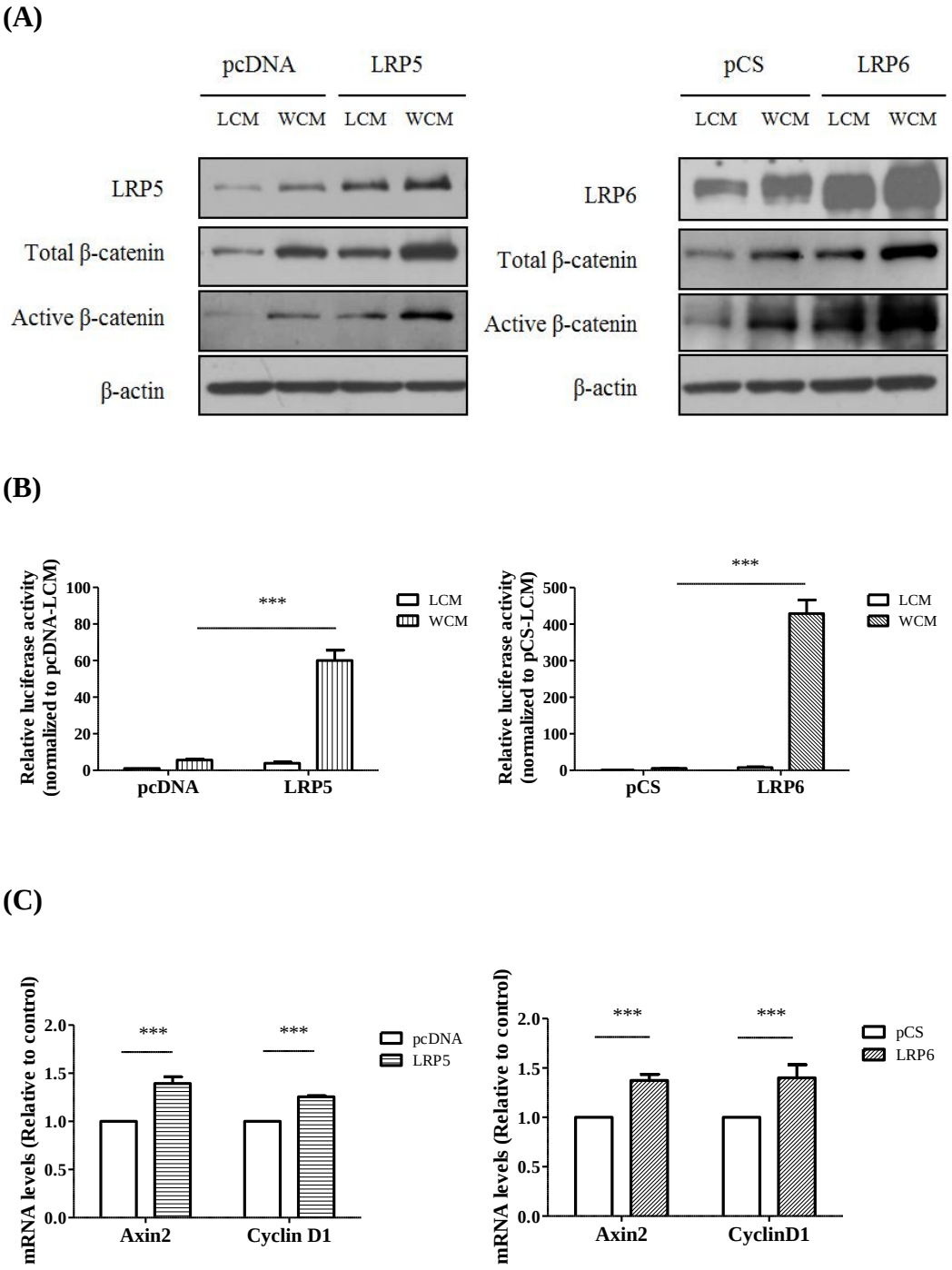

Figure 3-1. LRP5 and LRP6 overexpression upregulates Wnt/β-catenin signaling and downstream proliferative genes in SH-SY5Y cells. (A) SH-SY5Y cells were transfected with pcDNA3.1-LRP5 or pCS2+-LRP6 plasmids, followed by treatment of either LCM or WCM for 24 hours before harvested. Samples were solubilized with Western blotting lysis buffer and probed with specific antibodies, addressing the protein levels of LRP5/6, total β-catenin, active β-catenin, and β-actin. (B) SH-SY5Y cells were transfected with LRP5 or LRP6 expression plasmids together with TOPglow and pRL-

CMV Renilla plasmids and treated with LCM or WCM for 24 hours. Wnt3a-induced luciferase activities were measured with Dual–Luciferase Reporter Assay Kit. Values represented the average (n=3) ± S.E.M. of fold activation over control vectors (pcDNA3.1 or pCS2+) treated with LCM. (C) LRP5 and LRP6 overexpressed SH-SY5Y cells, treated with WCM for 24 hours, were harvested and subjected to quantitative Real Time PCR for relative mRNA level analysis of downstream target proliferative genes, Axin2 and Cyclin D1. The transcription levels were normalized to the respective GAPDH levels. Statistical differences were assessed using Student's t test (*$p<0.05$, **$p<0.01$, ***$p<0.001$).

3.3.2 Effect of siRNA knockdown of endogenous LRP5 and LRP6 on Wnt signaling in SH-SY5Y cells

We next performed gene knockdown experiments using siRNA to validate the functional role of LRP5 and LRP6 in regulating Wnt signaling. As shown in Figure 3-2A, total β-catenin protein level was reduced only in the presence of Wnt3a ligands when both co-receptors were suppressed. On the other hand, the decrease in active β-catenin protein levels was more significant than that of total β-catenin both in the presence and absence of Wnt3a stimulation. Correspondingly, TCF/LEF-dependent TOPglow reporter activity was significantly decreased by 68.4 ± 7.0% and 80.6 ± 2.7% in LRP5- and LRP6-knockdown cells respectively (Figure 3-2B). For the transcription of downstream survival genes such as Axin2 and Cyclin D1, mRNA levels were significantly downregulated by 28.7 ± 3.8% and 28.1 ± 6.6% respectively with LRP5 suppression and by 31.8 ± 2.7% and 41.5 ± 2.8% respectively with LRP6 suppression (Figure 3-2C). These results suggest that endogenous LRP5 and LRP6 co-receptors are functionally important in modulating Wnt signaling in SH-SY5Y cells.

(A)

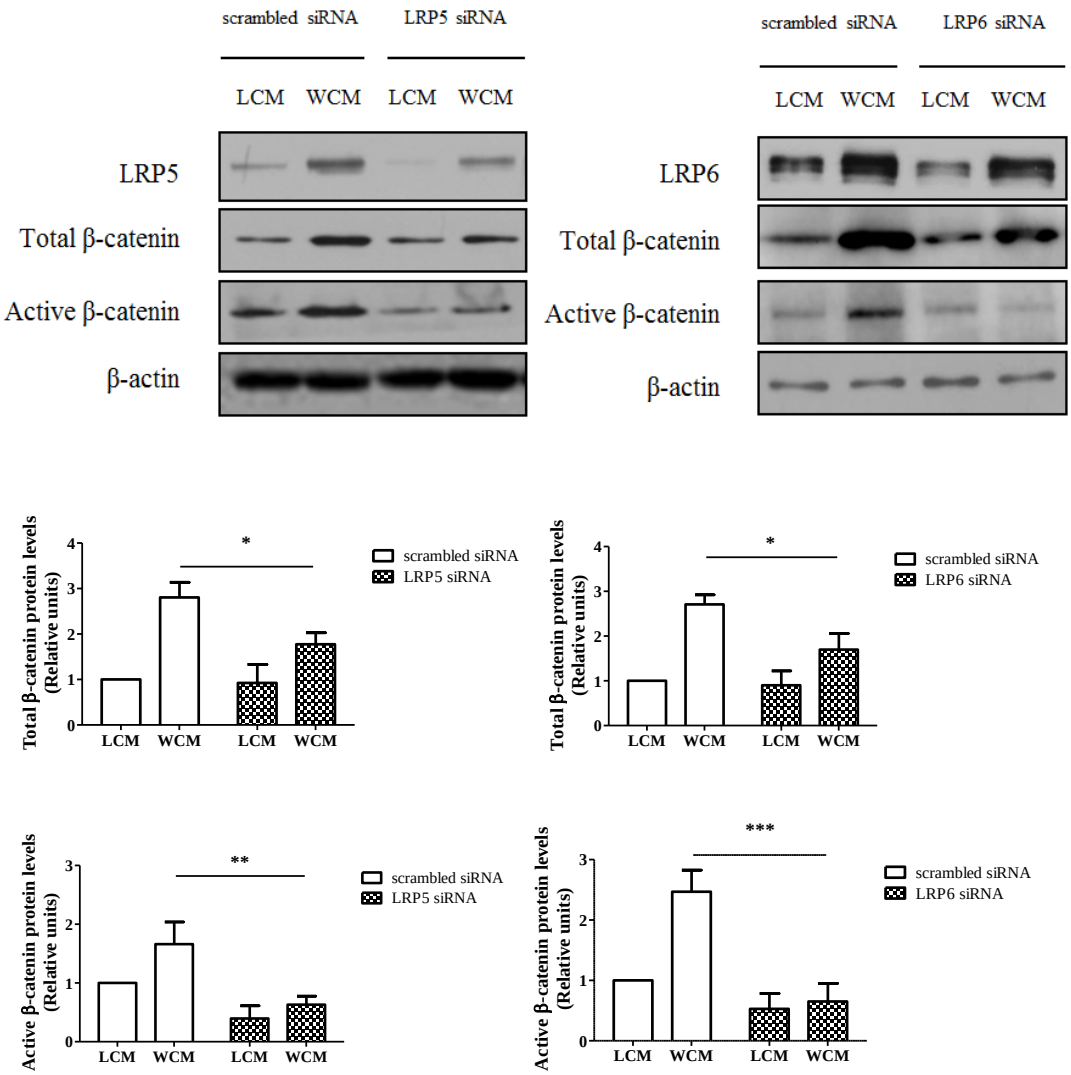
scrambled siRNA
LRP5 siRNA
LCM WCM LCM WCM
LRP5
Total β-catenin
Active β-catenin
β-actin
scrambled siRNA
LRP6 siRNA
LCM WCM LCM WCM
LRP6
Total β-catenin
Active β-catenin
β-actin
Total β-catenin protein levels (Relative units)
scrambled siRNA
LRP5 siRNA
LRP6 siRNA
Active β-catenin protein levels (Relative units)
LCM
WCM

(B)

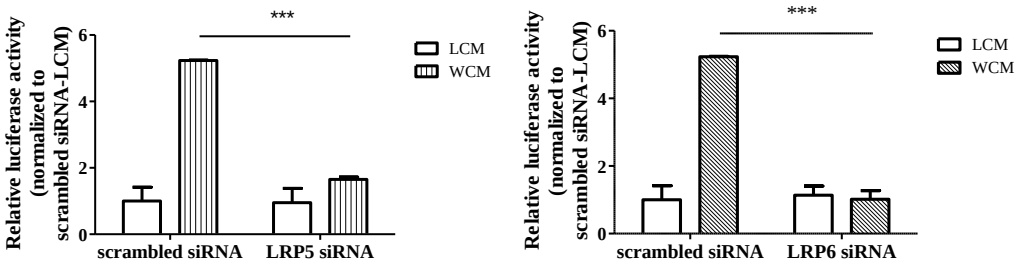
Relative luciferase activity (normalized to scrambled siRNA-LCM)
LCM
WCM
scrambled siRNA
LRP5 siRNA
LRP6 siRNA

(C)

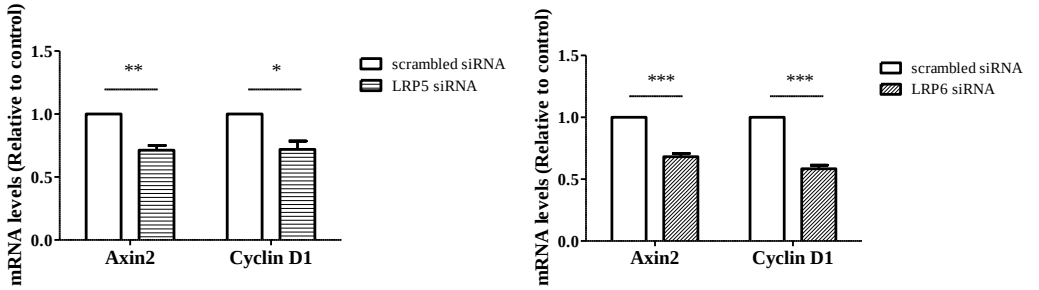

Figure 3-2. Knockdown of LRP5 or LRP6 in SH-SY5Y human neuroblastoma cells suppresses Wnt signaling and the transcription of downstream proliferation markers. (A) SH-SY5Y cells were transfected with 20nM scrambled, LRP5 or LRP6 siRNA and treated with either LCM or WCM for 24 hours before harvested. Samples were subjected to Western blotting lysis buffer and probed with anti-LRP5/6, anti-total β-catenin, anti-active β-catenin, and anti-β-actin antibodies. (B) SH-SY5Y cells were transfected with 20nM scrambled, LRP5 or LRP6 siRNA together with TOPglow and pRL-CMV Renilla plasmids and treated with LCM or WCM for 24 hours. Dual–Luciferase activities were measured and data was represented as the mean ± S.E.M. of fold activation over scrambled siRNA treated with LCM. (C) SH-SY5Y cells transfected with scrambled, LRP5 or LRP6 siRNA and treated with WCM for 24 hours, before subjected to quantitative Real Time PCR for relative mRNA level analysis of downstream target proliferative genes, Axin2 and Cyclin D1. The transcription levels were normalized to the respective GAPDH levels. Statistical differences were determined using Student's t test (*$p<0.05$, **$p<0.01$, ***$p<0.001$).

3.3.3 Generation of AD cell model with Aβ challenge

Overproduction and aggregation of Aβ has been proposed as the prime driver of AD [153]. Compared with other Aβ peptides, Aβ42 is the neurotoxic form and the main component of senile plaques. Therefore, we employed Aβ42 to induce toxicity in SH-SY5Y cells. To exclude the interference of FBS and phenol red in the cell culture medium, we introduced FBS-free, phenol red-free medium and determined the suitable cell count for seeding. SH-SY5Y cells with indicated cell counts ranging from $5x10^3$ to $5x10^5$ were seeded in 96-well plates and maintained

in FBS-free, phenol red-free F12 medium for 24 and 72 hours. 10% Triton-X100 were added as a positive control for 100% cell death. Cell viability was evaluated by CCK-8 and LDH cytotoxicity assays. As shown in Figure 3-3A, obvious and significant changes in CCK-8 and LDH readings were observed with cell counts of 10^5, $2x10^5$ and $5x10^5$. In addition, cell seeding of 10^5 provides 90% proper confluency under microscope. Therefore, cell count of 10^5 was used in the subsequent CCK-8 and LDH cytotoxicity assays. Since Aβ42 oligomers have emerged as the most toxic species, we aged Aβ42 monomers for 1 day into oligomers in F12 medium and treated SH-SY5Y cells with indicated concentrations for 24 hours and 72 hours as shown in Figure 3-3B. Despite the positive control suggested a significant decrease in cell viability, Aβ42 oligomers up to concentration of 5μM did not show any toxicity to the cells. Moreover, Aβ42 fibrils have also been indicated to induce progressive dystrophy and cell death in human cortical neurons [154]. Therefore, we introduced Aβ42 fibrils and increased the concentration to 10μM to examine cell viability. To preclude the possibility of interference, cells were starved in FBS-free, phenol-red F12 medium for 20 hours before Aβ was added. As shown in Figure 3-3C, both Aβ42 oligomers and fibrils did not have any effect on cell survival. We then tried to age Aβ42 for 7 days before added into incubation with SH-SY5Y cells. However, Aβ42 oligomers and fibrils still failed to induce any cytotoxicity even at the concentration of 50μM (Figure 3-3D). Among all the Aβ derivatives, Aβ25-35, is the shortest fragment that represents the biologically active region and retains the toxicity of the full-length Aβ peptide [155]. Hence, we aged Aβ25-35 for 1, 4, 7

days to form oligomers and fibrils at 4˚C and 37˚C respectively. 5, 10, 25 and 50μM of Aβ25-35 oligomers and fibrils were incubated with SH-SY5Y cells for 72 hours before assessment with CCK-8 and LDH assays. However, as shown in Figure 3-3E, no toxic effect was observed in the cells.

(A)

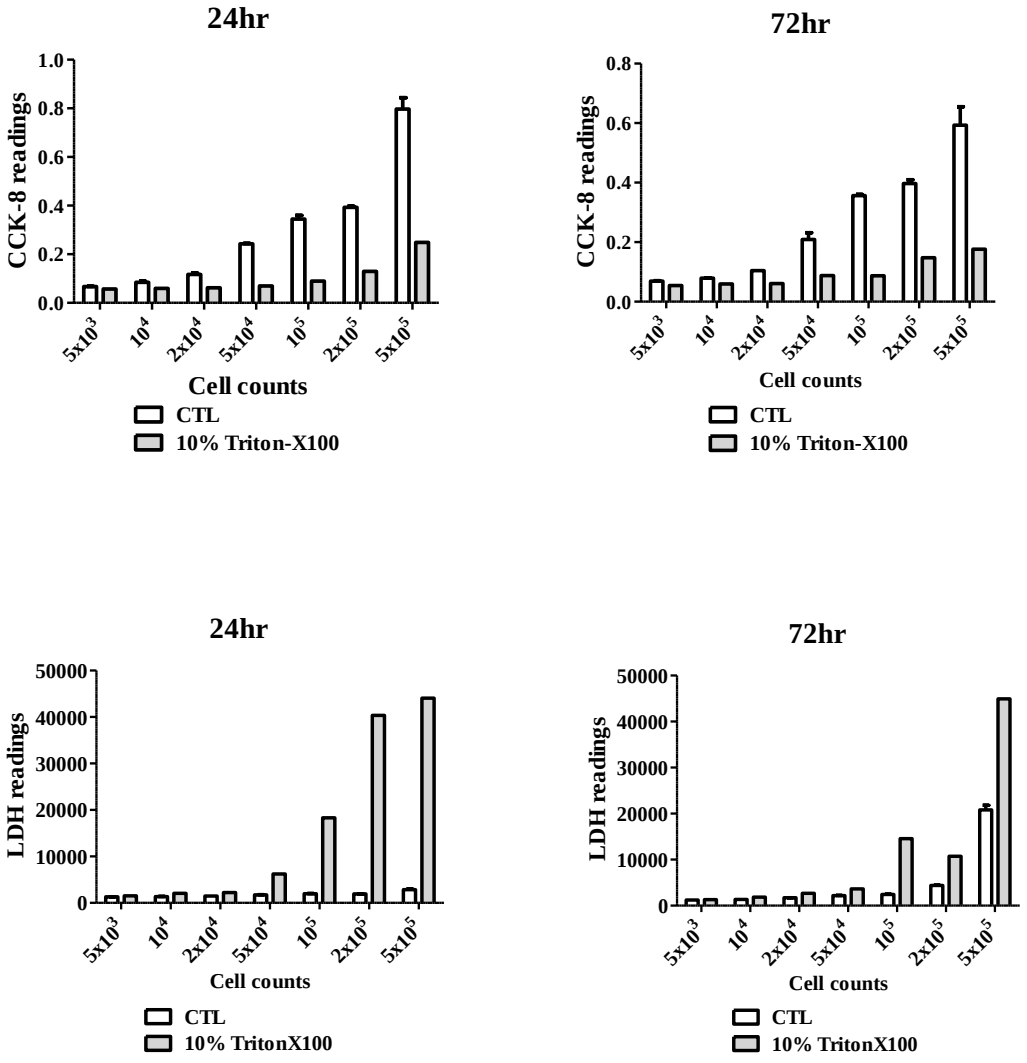

(B)

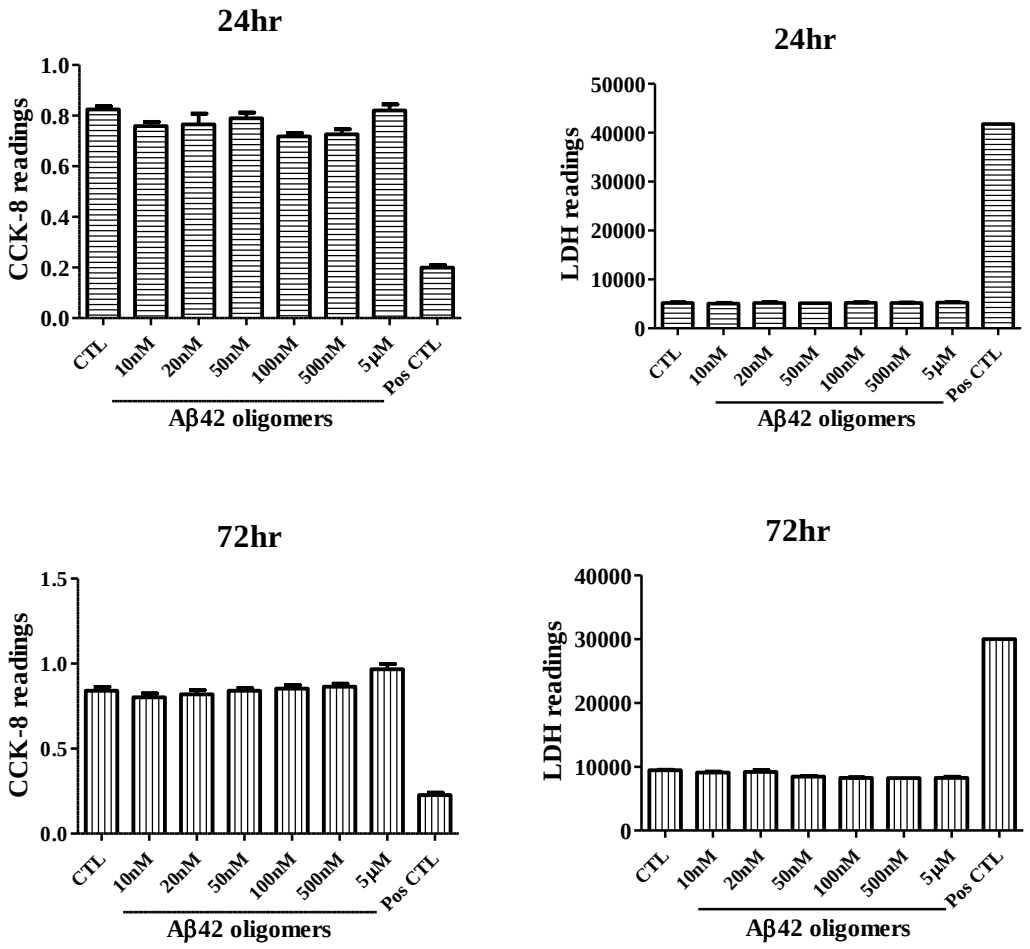
24hr
CCK-8 readings
1.0
0.8
0.6
0.4
0.2
0.0
CTL
10nM
20nM
50nM
100nM
500nM
5μM
Pos CTL
Aβ42 oligomers
24hr
LDH readings
50000
40000
30000
20000
10000
0
CTL
10nM
20nM
50nM
100nM
500nM
5μM
Pos CTL
Aβ42 oligomers
72hr
CCK-8 readings
1.5
1.0
0.5
0.0
CTL
10nM
20nM
50nM
100nM
500nM
5μM
Pos CTL
Aβ42 oligomers
72hr
LDH readings
40000
30000
20000
10000
0
CTL
10nM
20nM
50nM
100nM
500nM
5μM
Pos CTL
Aβ42 oligomers

(C)

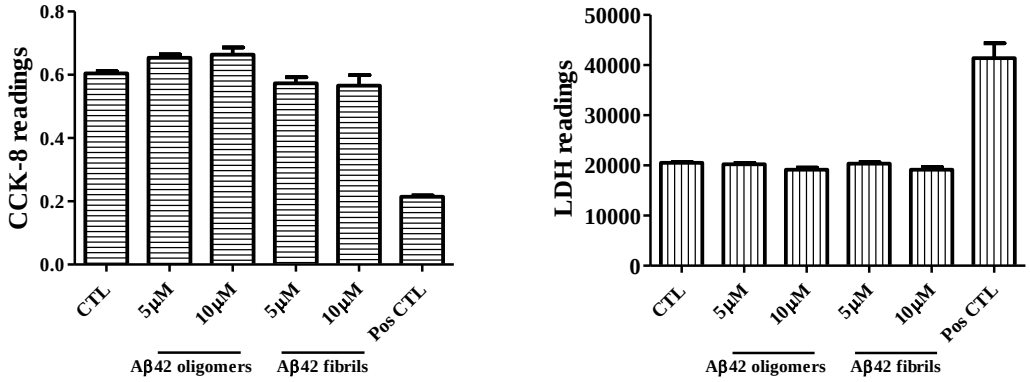
CCK-8 readings
0.8
0.6
0.4
0.2
0.0
CTL
5μM
10μM
5μM
10μM
Pos CTL
Aβ42 oligomers
Aβ42 fibrils
LDH readings
50000
40000
30000
20000
10000
0
CTL
5μM
10μM
5μM
10μM
Pos CTL
Aβ42 oligomers
Aβ42 fibrils

(D)

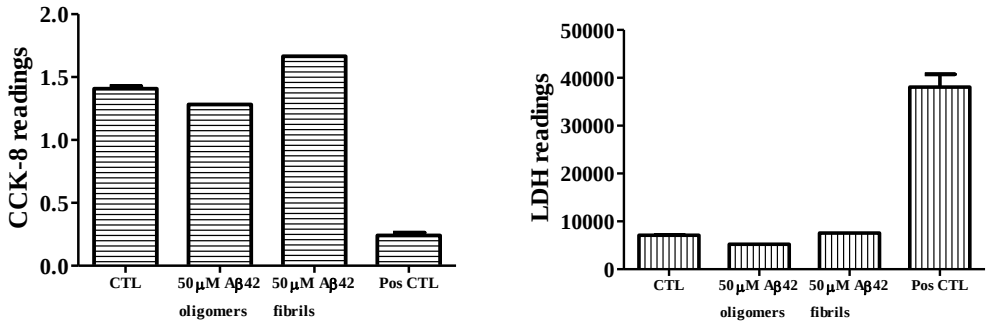
CCK-8 readings
2.0
1.5
1.0
0.5
0.0
CTL
50 μM Aβ42 oligomers
50 μM Aβ42 fibrils
Pos CTL
LDH readings
50000
40000
30000
20000
10000
0
CTL
50 μM Aβ42 oligomers
50 μM Aβ42 fibrils
Pos CTL

(E)

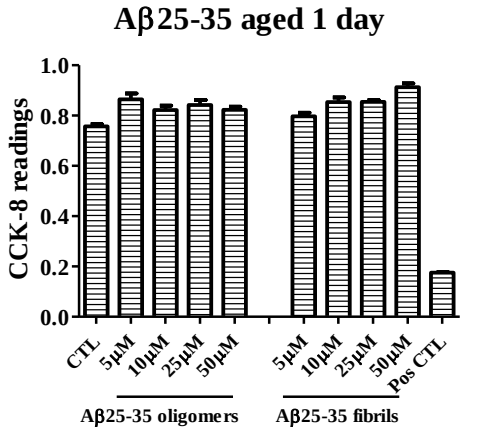
Aβ25-35 aged 1 day
CCK-8 readings
1.0
0.8
0.6
0.4
0.2
0.0
CTL
5μM
10μM
25μM
50μM
5μM
10μM
25μM
50μM
Pos CTL
Aβ25-35 oligomers
Aβ25-35 fibrils

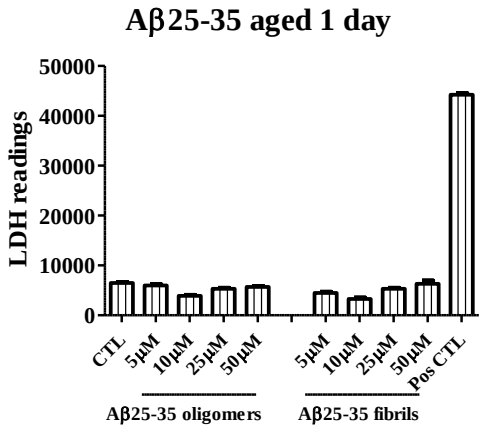
Aβ25-35 aged 1 day
LDH readings
50000
40000
30000
20000
10000
0
CTL
5μM
10μM
25μM
50μM
5μM
10μM
25μM
50μM
Pos CTL
Aβ25-35 oligomers
Aβ25-35 fibrils

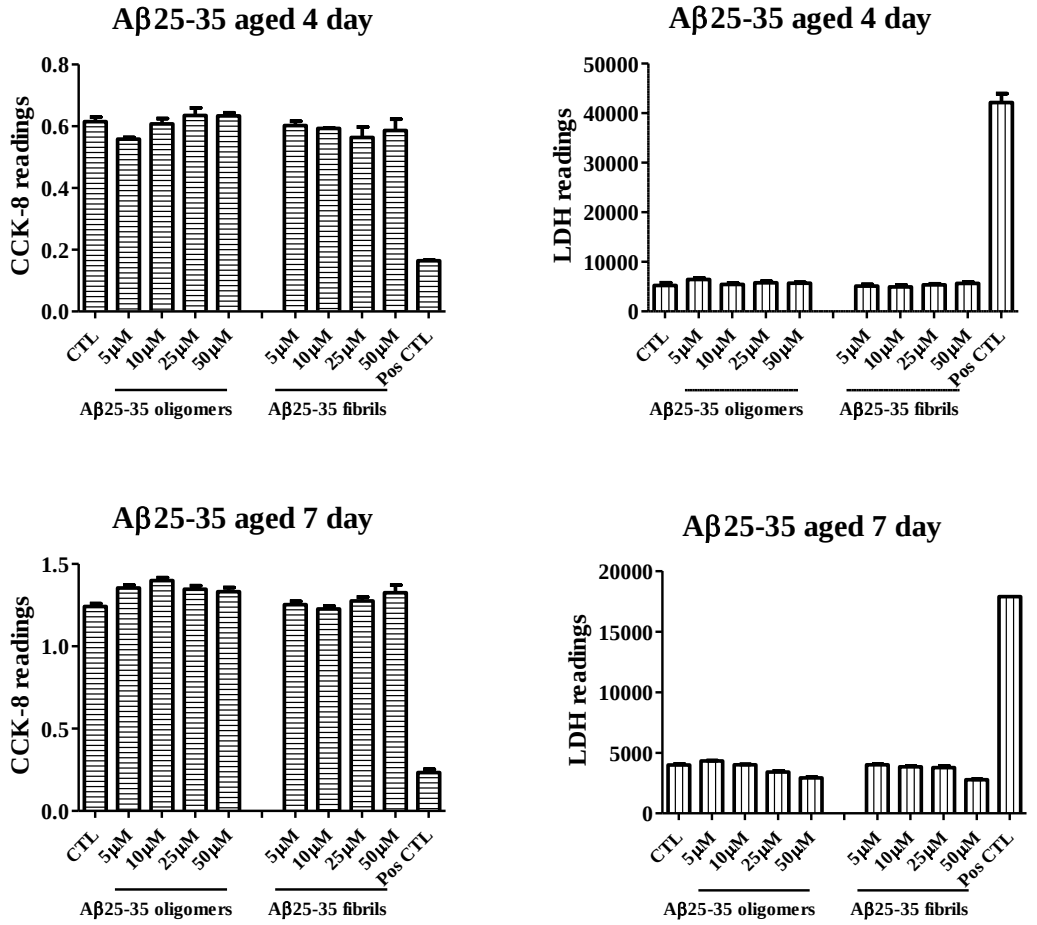

Figure 3-3. Generation of AD cell model with Aβ challenge. (A) SH-SY5Y cells with indicated cell counts were seeded in 96-well plates and incubated in FBS-free, phenol red-free F12 medium for 24 and 72 hours. 10% Triton-X100 was added 10 min before harvest as the positive control with 100% cell death. Cells were then subjected to CCK-8 cell viability and LDH cytotoxicity assays. (B) Aβ42 was aged at 4˚C for 1 day into oligomers. Indicated concentrations of Aβ42 oligomers were incubated with SH-SY5Y cells in FBS-free, phenol red-free F12 medium for 24 and 72 hours before examination with CCK-8 cell viability and LDH cytotoxicity assays. (C) Aβ42 was aged at 4˚C for 1 day into oligomers and aged at 37˚C for 1 day into fibrils. 5μM and 10μM Aβ42 oligomers and fibrils were added to SH-SY5Y cells for 72 hours. Cells were then subjected to CCK-8 cell viability and LDH cytotoxicity assays. (D) SH-SY5Y cells were starved in FBS-free, phenol red-free F12 medium for 20 hours before incubation for 72 hours with 50μM Aβ42 oligomers and fibrils aged for 7 days. Cells were then assessed for CCK-8 cell viability and LDH cytotoxicity. (E) Aβ25-35 was aged for 1, 4, 7 days into oligomers and fibrils. Indicated concentrations of Aβ25-35 oligomers and fibrils were added to pre-starved SH-SY5Y cells for 72 hours. Cells were then subjected to CCK-8 cell viability and LDH cytotoxicity assays.

3.3.4 LRP5 and LRP6 overexpression rescues SH-SY5Y cells from neurotoxicity caused by hydrogen peroxide-induced oxidative stress

After failing to generate AD cell model with Aβ challenge, we insulted cells with oxidative stress as the alternative AD model. Oxidative stress has been indicated to be an early event in AD [156]. In the post mortem AD brain, increased oxidative stress markers have been found to be associated with the loss of neuronal viability [157-159]. Moreover, Aβ has been reported to increase hydrogen peroxide level in cultured neuronal cells and cause cytotoxicity [160]. To induce oxidative stress in SH-SY5Y cells, cells were subjected to hydrogen peroxide treatment at concentrations ranging from 10 to 50μM and examined for cytotoxicity. Figure 3-4A showed that cell viability decreased in a concentration-dependent manner when cells were cultured with 10-50μM H_2O_2, as compared to vehicle control. LRP5 and LRP6 overexpression, however, were able to ameliorate this hydrogen peroxide-induced cell cytotoxicity at all concentrations used. To further confirm the protection against H_2O_2-mediated toxicity, cell cycle analysis of transfected cells was performed using flow cytometry. Hydrogen peroxide treatment resulted in increased Sub G0/G1 apoptosis population. However, the percentage of cells in the Sub G0/G1 phase was significantly reduced in LRP5- and LRP6-transfected cells following the same hydrogen peroxide treatment (Figure 3-4B). We further investigated the influence of the Wnt co-receptors on hydrogen peroxide-induced apoptosis by examining the expression of the key apoptotic mediators caspase 3 and 7. When SH-SY5Y cells were incubated with H_2O_2 alone, the cleavage of pro-caspase 3 and pro-caspase 7

into the active subunits was elevated in a concentration-dependent manner with hydrogen peroxide treatment (Figure 3-4C). In contrast, LRP5 and LRP6 overexpression was able to reduce the levels of cleaved caspase 3 and 7. Specifically, at 50μM H_2O_2 treatment, cleaved caspase 3 was decreased by 35.2% and 64.7% and caspase 7 was decreased by 66.5% and 79.6% by LRP5 and LRP6 overexpression respectively. The β-actin protein level, as an internal control, was almost the same in all samples.

(A)

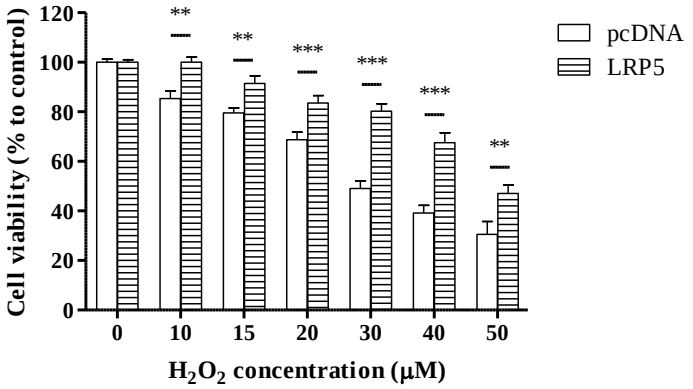

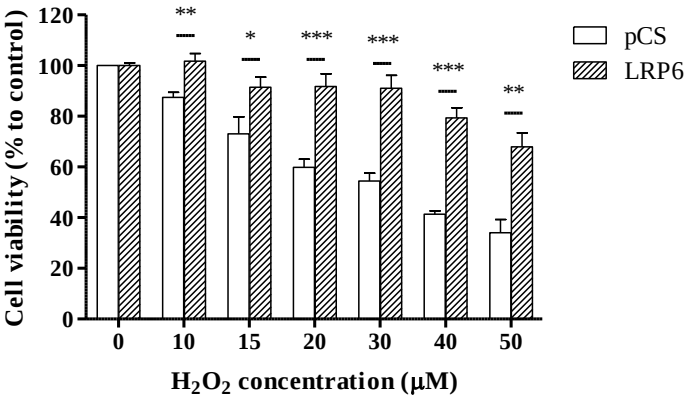

(B)

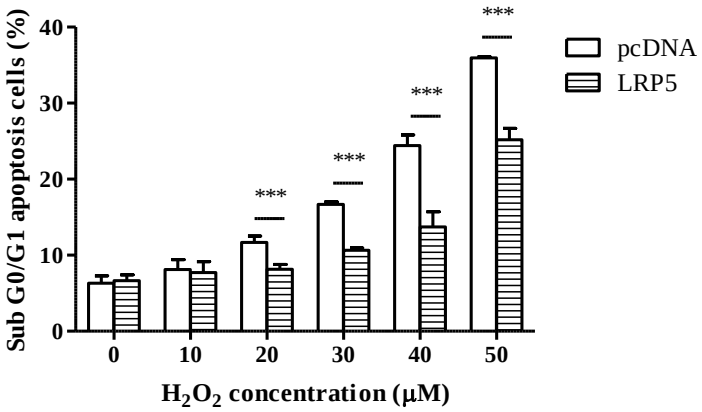
Sub G0/G1 apoptosis cells (%)
40
30
20
10
0
***
***
***
***
0
10
20
30
40
50
H2O2 concentration (μM)
pcDNA
LRP5

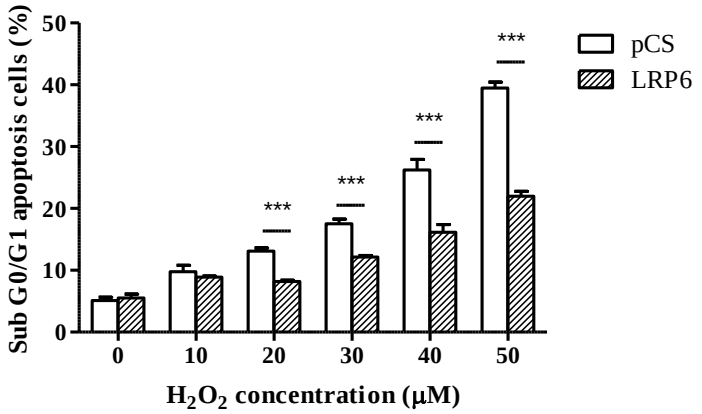
Sub G0/G1 apoptosis cells (%)
50
40
30
20
10
0
***
***
***
***
0
10
20
30
40
50
H2O2 concentration (μM)
pCS
LRP6

(C)

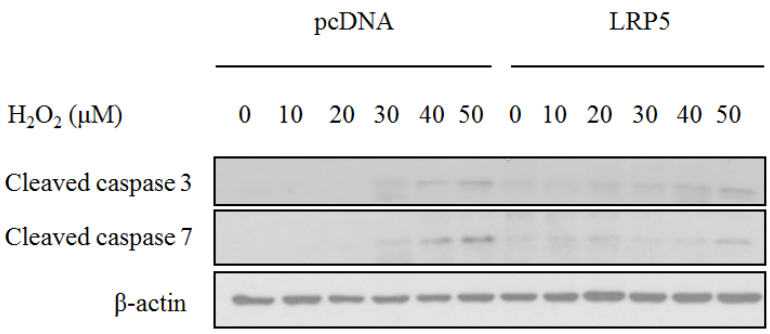
pcDNA
LRP5
H2O2 (μM)
0 10 20 30 40 50 0 10 20 30 40 50
Cleaved caspase 3
Cleaved caspase 7
β-actin

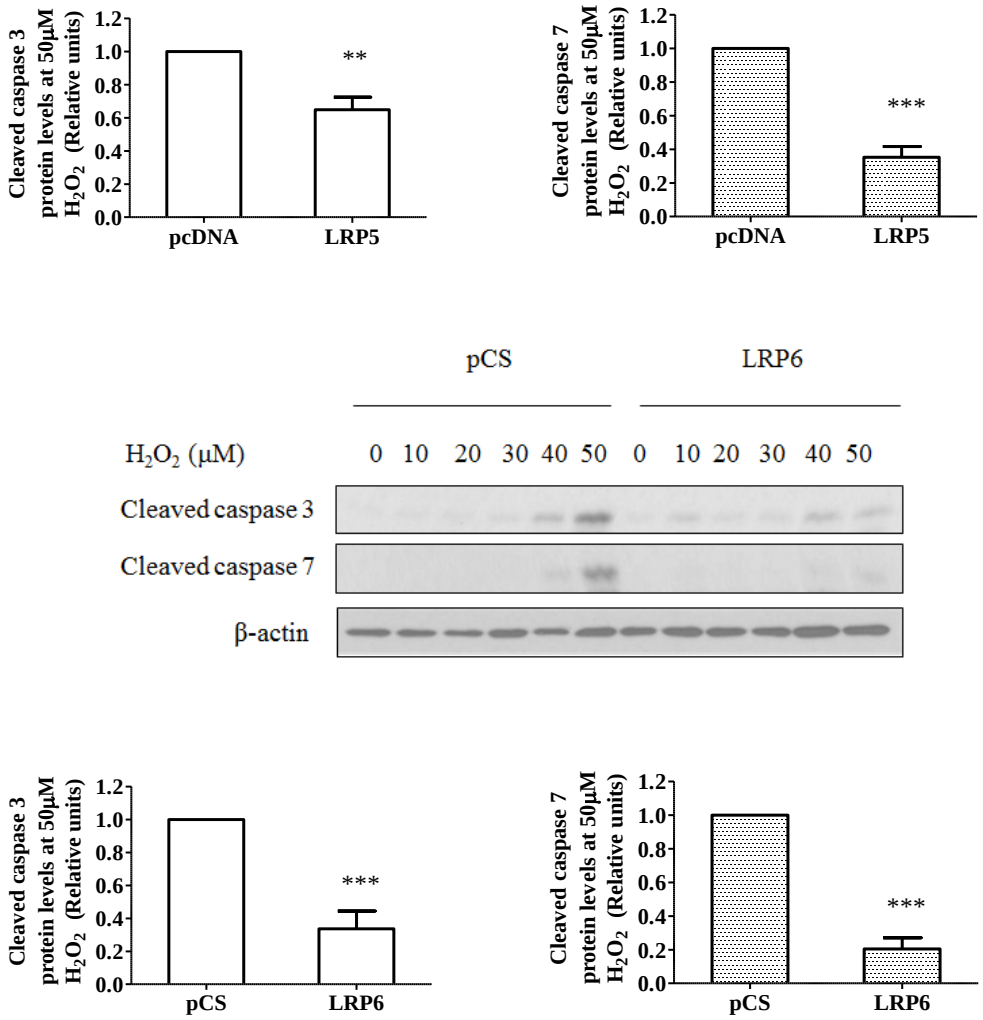

Figure 3-4. LRP5 and LRP6 overexpression rescues SH-SY5Y cells from neurotoxicity caused by hydrogen peroxide-induced oxidative stress. SH-SY5Y cells were transfected with pcDNA3.1-LRP5 or pCS2+-LRP6 plasmids and treated with various concentration of hydrogen peroxide in WCM for 24 hours before analyzed for cell viability assessment. (A) Cell viability was measured by MTT assay. The data were presented as the mean (% of non-treated group) ± S.E.M. LRP5 or LRP6 overexpression cells were compared to respective vector overexpression group in each treatment group and the statistical significance was measured with Student's t test (*$p<0.05$, **$p<0.01$, ***$p<0.001$). (B) Cells were stained with PI before subjected to flow cytometry for cell cycle analysis. The Sub G0/G1 apoptosis populations were plotted as the percentage of total cell counts and data were presented as mean ± S.E.M. from three independent experiments. The measurement of statistical significance was the same as described in (A). (C) Processing of pro-caspases 3 and 7 into active cleaved caspases were assessed by specific antibodies against active caspases 3 and 7. Quantitative densitometry of cleaved caspases 3 and 7 under the treatment of 50μM H_2O_2 was normalized to respective β-actin. The data represented the mean values ± S.E.M. and statistical significance was measured as above.

3.3.5 LRP5 and LRP6 overexpression inhibits GSK3β activity and reduces tau phosphorylation in SH-SY5Y cells

The presence of extracellular Wnt ligands activates Wnt signaling pathway and leads to the inhibition of GSK3β activity by phosphorylating GSK3β at Ser9 residue [143]. Consistent with this finding, our Western blotting result showed an increase in GSK3β Ser9 protein levels when Wnt3a ligands were present, indicating a decrease in GSK3β activity (Figure 3-5A). Since GSK3β has been identified as one of the main kinases phosphorylating tau at pathogenic residues implicated in AD [146,147], the decrease in GSK3β activity in our studies was also accompanied by a reduction in tau phosphorylation as examined using the phosphospecific antibody against tau Ser202/Thr205 (AT8) [161,162]. Remarkably, LRP5 and LRP6 overexpression augmented the reduction in GSK3β activity by 46.7% and 27.4% (1.9- and 1.4-fold increase in GSK3β Ser9 protein level) and reduced tau reactivity against the AT8 antibody further by 65.1% and 59.9% in the presence of Wnt3a ligands (Figure 3-5B).

(A)

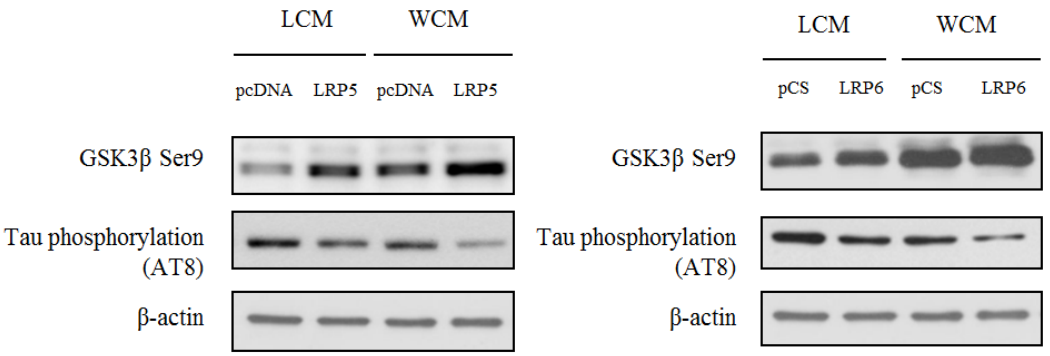

(B)

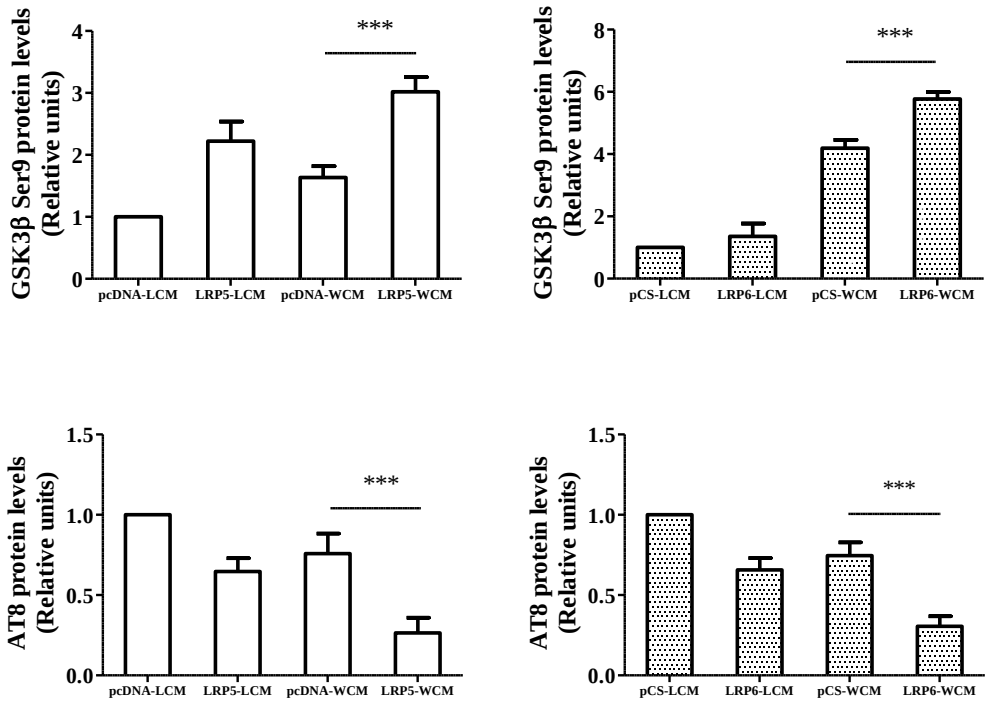

Figure 3-5. LRP5 and LRP6 overexpression inhibits GSK3β activity and reduces tau phosphorylation in SH-SY5Y cells. SH-SY5Y cells were transfected with LRP5 or LRP6 expression plasmids and treated with either LCM or WCM for 24 hours. (A) Cells were then subjected to Western blotting analysis and probed with anti-GSK3β Ser9 antibody or anti-phosphorylated tau AT8 antibody. (B) Quantitative densitometry of GSK3β Ser9 and Ser202/Thr205 phosphorylated tau was normalized to that of respective β-actin. The data represented the average ± S.E.M. and statistical significance was assessed with Student's t test (*$p<0.05$, **$p<0.01$, ***$p<0.001$).

3.4 Discussion

Aberrant Wnt inhibition has been implicated to play a vital role in the pathogenesis of AD in transgenic animal models as well as AD patients [133,134,137]. Activation of the repressed Wnt signaling by introducing Wnt ligands or inhibiting the activity of GSK3β has been shown to effectively rescue

neurodegeneration and improve behavioral impairments both *in vitro* and *in vivo* [143,144]. However, the link in transducing the upstream signaling from extracellular Wnt ligands to intracellular GSK3β still remains to be established. In this study, we found that overexpression of Wnt co-receptors LRP5 and LRP6 elevates cellular β-catenin protein level in the presence of Wnt ligands. Particularly, the increase of active β-catenin is more prominent. Active β-catenin is the dephosphorylated population that accumulates and translocates into nucleus to bind to TCF/LEF [123]. As a result, the transcription of downstream survival genes, Axin2 and Cyclin D1 [163,164], is upregulated. This finding suggests that LRP5 and LRP6 play an important role in positively regulating Wnt activity and facilitating the expression of proliferative genes. On the other hand, silencing of LRP5 or LRP6 results in reduced total and active β-catenin, and decreased transcription of downstream proliferative genes, which further supports the essential role of LRP5 and LRP6 in increasing neuronal survival gene expression through Wnt pathway.

To evaluate the neuroprotective role of LRP5 and LRP6 in AD, we introduced oxidative stress using hydrogen peroxide. Aβ aggregation-induced oxidative stress has been reported to be involved in AD by causing cytotoxicity [165-167]. Previously, it had been reported that activation of Wnt activity by Wnt3a ligand exerts a neuroprotective role in overcoming Aβ-induced oxidative stress and neurotoxic effects [143]. In the present study, our results indicate that hydrogen peroxide induced a significant reduction in cell viability in a dose-dependent manner, in concordance with the increase in the Sub G0/G1 apoptotic population.

Overexpression of LRP5 and LRP6 was able to restore cell viability and decrease apoptotic population at a concentration up to 50μM. Additionally, the protective effects of the two Wnt co-receptors were also evident through the protein levels of apoptotic mediators. Evaluation of caspase 3 and 7 activity clearly indicates that cells treated with hydrogen peroxide were affected by apoptosis at the concentration of 40 and 50μM. Taken together, our results highlight the importance of Wnt co-receptors LRP5 and LRP6 in rescuing neuronal cell from hydrogen peroxide-induced neurotoxicity and DNA fragmentation.

Tau hyperphosphorylation is an important hallmark for NFT formation and subsequent AD progression. GSK3β has been implicated as one of the main tau phosphorylation kinases in the AD etiology [138,139]. Studies have shown that inhibition of GSK3β activity, via either the GSK3β inhibitor lithium or Wnt ligands, reduced tau phosphorylation both *in vitro* and *in vivo* [168]. Since LRP5 and LRP6 are the direct regulators upstream of GSK3β in Wnt/β-catenin pathway, we examined the role of LRP5 and LRP6 in modulating the activity of GSK3β and tau phosphorylation. Our finding that overexpression of LRP5 and LRP6 inhibited GSK3β activity resulting in decreased levels of phosphorylated tau suggests that LRP5 and LRP6 protect cells from tau hyperphosphorylation through modulating GSK3β activity.

Although LRP5 and LRP6 are highly homologous and both serve as the co-receptors for Wnt cascade, numerous reports suggest that their role in regulating Wnt signaling may not be equivalent [114,150]. LRP6 deficient mice are perinatal lethal, whereas LRP5 knockout mice are viable and can grow into adulthood [112,129]. Here, we observed a more significant upregulation of β-catenin and downstream proliferation genes in the cells overexpresseing LRP6 than LRP5. Similarly, we found that knockdown of LRP6 repressed Wnt activity to a greater extent than knockdown of LRP5. As a result, LRP6 restored oxidative stress-induced neurotoxicity and tau phosphorylation to a greater extent than LRP5. Our results suggest that these two co-receptors both exhibit protective role against neurotoxicity and that more pronounced neuroprotective role was observed with LRP6.

3.5 Conclusion

In summary, we present the first molecular study that shows the neuroprotective role of Wnt co-receptors LRP5 and LRP6 in improving neuronal survival and reducing tau phosphorylation through upregulating Wnt signaling. Our findings suggest that Wnt co-receptors LRP5 and LRP6 could be further explored as novel therapeutic targets for AD.

CHAPTER 4. CHARACTERIZATION OF THE INTERACTION BETWEEN LRP5/6 AND APOLIPOPROTEIN E PROTEINS

4.1 Introduction

Although several susceptibility genes have been associated with AD, so far only apoE ε4 allele is recognized as the prime genetic risk factor for LOAD with high confidence [33,34]. The apoE gene is highly polymorphic, resulting in three common isoforms apoE2, apoE3 and apoE4 [53]. Compared to the prevalent apoE ε3 allele, ε4 increases AD risk while ε2 is regarded to be protective. ApoE2 and apoE3 are more efficient in redistributing lipids among CNS cells for normal lipid homeostasis, repairing injured neurons and maintaining synaptic connections while apoE4 may exert detrimental effects in the processes. These isoform-specific effects are mediated by its receptor, LDL receptor family.

As mentioned in Chapter 1, the LDL receptor family includes core members such as LRP1, apoER2, LDLR, as well as more distantly related ones such as LRP5, LRP6 and SorLA/LR11. So far only two members of this family have been linked with AD by human genetic studies, LRP1 [169] and LRP6 [140,152]. The distantly related members, LRP5 and LRP6, are the essential co-receptors of the Wnt/β-catenin pathway. As dysregulated Wnt signaling plays a vital role in AD pathology, it is possible that apoE exerts the isoform-specific neurobiological effects through LRP5 and LRP6. However, there is no direct evidence of the

interaction between LRP5/6 and apoE isoforms, albeit LRP5 has been reported to facilitate the internalization of apoE-enriched β-migrating very low density lipoprotein [170].

Therefore, in this chapter, we aimed to address the missing link between LRP5/6 and apoE isoforms and its effect on Wnt signaling. We herein identified the interaction between LRP5/6 and apoE isoforms with co-immunoprecipitation assays. Furthermore, we found that the interaction between LRP5 and apoE isoforms inhibited the activation ability of LRP5 on Wnt/β-catenin activity. In addition, the effects of the interaction on GSK3β were isoform-specific with apoE4 inducing the strongest inhibition. Taken together, the findings from this chapter not only provide a bridge linking Wnt signaling and apoE pathology together, but also present an interesting research direction for better understanding of the mechanisms underlying AD.

4.2 Materials and Methods

4.2.1 Cell culture and reagents

Cell culture and plasmid transfection with human neuroblastoma SH-SY5Y cells and HEK 293T cells were performed in the same manner as reported in Section 3.2.1 of Chapter 3. For overexpression plasmids, the source of pcDNA3.1–LRP5

and pCS2+–LRP6 was mentioned in Section 3.2.1 of Chapter 3. pCMV.–apoE2 and pCMV.–apoE4 were kindly given by Dr. Panagiotis Takis Athanasopoulos from University of Wolverhampton, United Kingdom.

4.2.2 Mutagenesis

200ng pCMV.–apoE2 plasmid was used as the DNA template to generate pCMV.–apoE3 using QuikChange™ Site-Directed Mutagenesis Kit (Stratagene, La Jolla, CA). Mutagenesis primers were designed as shown in Table 4-1. The following reaction mixture was prepared on ice (Table 4-2). The reaction tube was then placed on the thermal cycler Flexigene (Techne, Staffordshire, UK) with 30 sec-denaturation at 95˚C, followed by a total of 18 cycles consisting of 30 sec-denaturation at 95˚C, 1 min-annealing at 55˚C and 2 min-extension at 68˚C. At the end, the reaction was cooled down on ice for 2 min before DpnI restriction enzyme digestion at 37˚C for 1 hour to eliminate apoE2 template. 1μL of DpnI-treated DNA was then subjected to bacterial transformation.

Table 4-1 Primers used for site-directed mutagenesis from apoE2 to apoE3

Primer Name	Sequence
apoE2to3 forward	5'-GAT GAC CTG CAG AAG CGC CTG GCA GTG TAC-3'
apoE2to3 reverse	5'-GTA CAC TGC CAG GCG CTT CTG CAG GTC ATC-3'

Table 4-2 Reagents used for mutagenesis

Reagents	Volume
10x Pfu Buffer	5μL
pCMV.–apoE2 (100ng/μL)	2μL
apoE2to3 forward (100ng/μL)	1.25μL
apoE2to3 reverse (100ng/μL)	1.25μL
dNTP (10mM)	1μL
Turbo/Promega Pfu DNA	1μL
double-distilled H_2O (ddH_2O)	38.5μL
total	50μL

4.2.3 Bacterial transformation

1μL of mutagenesis product was transferred to a clean 1.5mL Eppendorf tube and mixed with 50μL DH5α bacterial strain on ice, followed by gently tapping. The bacteria-DNA mixture was incubated on ice for 30 min and then heat-shocked at 42˚C for 45 sec. The mixture was then cooled on ice for 2 min and added with 500μL pre-warmed LB Broth (Acumedia, Lansing, MI). The tube was shaken at 37˚C for 1 hour. Bacterial pellet was spun down under 4,000rpm for 5 min and 500μL supernatant was removed. The rest of supernatant was mixed with bacterial pellet and spread onto LB agar plate with 100μg/mL ampicillin. LB agar plate was then incubated at 37˚C overnight.

4.2.4 Restriction enzyme digestion

10μL out of 30μL plasmids with minipreparation (miniprep) was subjected to restriction enzymes double-digestion with 10 units of XhoI (New England Biolabs, Beverly, MA) and 10 units of HindIII (New England Biolabs, Beverly, MA) in a 20 μL reaction volume. The reaction mixture was incubated at 37˚C for 2 hours before being subjected to gel electrophoresis.

4.2.5 Agarose gel electrophoresis

1g agarose (Invitrogen, Carlsbad, CA) was weighed and dissolved into 100mL TAE (Tris-Acetate-EDTA) buffer (40mM Tris, 20mM acetate acid, 2mM EDTA, pH 8.3) in a 500mL conical flask. The agarose-TAE solution was stirred on a heated magnetic stirrer under 90˚C until completely melted. The melted agarose was allowed to cool sufficiently before adding SYBR® Safe DNA Gel Strain (Invitrogen, Carlsbad, CA) and pouring into a cast. A comb was placed in the cast to create wells for loading samples and gels were completely set before use. DNA samples were mixed with loading buffer (New England Biolabs, Beverly, MA) before transferring into the wells. 1kb DNA ladder (New England Biolabs, Beverly, MA) was loaded to indicate DNA molecular weight. Gel electrophoresis was performed under 120V for 30 min before visualization using ChemiDoc XRS$^+$ System (Bio-Rad Laboratories, Hercules, CA).

4.2.6 Western blotting analysis

Western blotting assay was performed with the same manner as described in Section 3.2.4 of Chapter 3 with modified lysis buffer (25mM Tris, 2.5mM EDTA, 2.5mM EGTA, 100mM NaCl, 20mM $C_3H_7Na_2O_6P$, 20mM NaF, 1mM Na_3VO_4, 10mM $Na_4P_2O_7$, 0.5% deoxycholate, 1% Triton X-100, pH7.4) supplemented with protease inhibitor cocktail tablet (Roche Diagnostics, Germany). ApoE antibody was purchased from Millipore (Billerica, MA). This apoE antibody was raised against a synthetic peptide corresponding to amino acids surrounding the polymorphic amino acid position 158 of apoE and recognizes all three human apoE isoforms.

4.2.7 Co-immunoprecipitation

0.5mL of total cell lysate containing 1mg of protein was incubated with apoE antibody and protein G agarose beads (Roche Diagnostics, Germany) at 4˚C on a turning roller overnight. The protein G agarose beads were washed with lysis buffer 3-4 times on the following day. Samples were then subject to SDS-PAGE gel and Western blotting.

4.2.8 Dual luciferase reporter assay

SH-SY5Y cells ($2.5x10^5$) were seeded in 24-well plates overnight and transfected with 1μg LRP5 or LRP6 expression plasmids, 1μg apoE2, apoE3 or apoE4 expression plasmids, 1μg reporter construct (TOPglow) and 0.04μg pRL-CMV Renilla control plasmids. After 6 hours of transfection, the medium was replaced with either LCM or WCM. Cells were harvested and the fluorescent activity was determined and calculated with the same manner as described in Section 3.2.3 of Chapter 3.

4.2.9 Statistical analysis

All data was presented as an average of three independent experiments ± S.E.M. Statistical analysis was performed using the one-way ANOVA with Dunnett's post-hoc analysis (SPSS, Chicago, IL) and significance was assumed at $p < 0.05$.

4.3 Results

4.3.1 Site-directed mutagenesis of pCMV.–apoE2 to generate pCMV.–apoE3

ApoE3 differs from apoE2 in amino acid residue 158, with apoE3 possessing Arg158 and apoE2 having Cys158. Therefore, to generate apoE3 plasmid, we performed site-directed mutagenesis with Turbo and Promega Pfu DNA polymerase using pCMV.–apoE2 as DNA template. As shown in Figure 4-1A,

after 18 cycles of amplification, a clear and abundant DNA band having similar molecular weight as pCMV.–apoE2 appeared in both mutagenesis products amplified by Turbo and Promega Pfu. 1μL of each mutagenesis product was then transformed into DH5α bacterial strains and three colonies each were picked up for restriction enzymes XhoI and HindIII double-digestion on the following day. As shown in agarose gel electrophoresis (Figure 4-1B), all the colonies presented one 1457bp and one 3274bp DNA bands as expected. Colony 1 amplified by Turbo Pfu and Colony 2 amplified by Promega Pfu were sent for sequencing to validate DNA sequences with apoE sequencing primers (Table 4-3). The sequencing results were aligned with Homo sapiens apoE3 sequence (NCBI Reference Sequence: NM_000041.2) with Basic Local Alignment Search Tool (BLAST) on the National Center for Biotechnology Information (NCBI) website. As shown in Figure 4-1C, the DNA sequence of apoE3 Colony 2 amplified by Promega Pfu (shown as Query 1 in the result) was concordant with the Homo sapiens apoE3 sequence (shown as Subject 1 in the result) from 541bp to 954bp. In Figure 4-1D, the DNA sequence of apoE3 Colony 2 amplified by Promega Pfu corresponds to 1bp–584bp of Homo sapiens apoE3 sequence, suggesting that the apoE3 plasmid from Colony 2 amplified by Promega Pfu possessed the correct apoE3 DNA sequence. Therefore, this colony of transformed bacteria was preserved in -80˚C for further use.

(A)

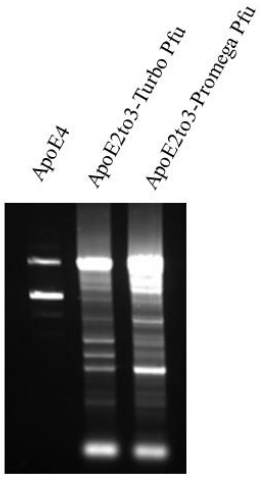

(B)

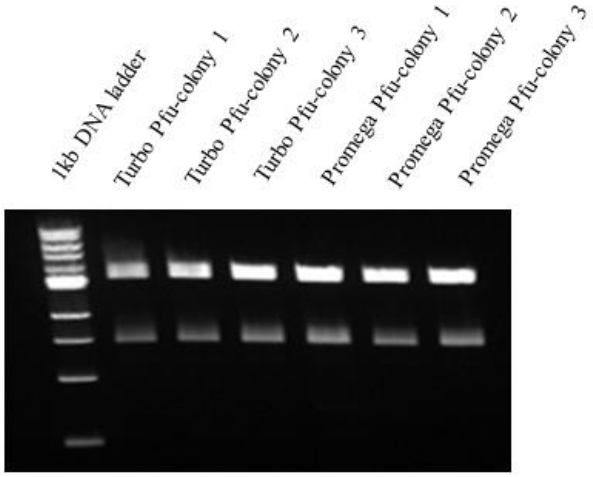

(C) Sequencing result with apoE forward primer

Range 1: 541 to 954 Graphics ▼ Next Match ▲ Previous Match

Score	Expect	Identities	Gaps	Strand
765 bits(414)	0.0	414/414(100%)	0/414(0%)	Plus/Plus

```
Query  1    CAGGCCGGGGCCCGCGAGGGCGCCGAGCGCGGCCTCAGCGCCATCCGCGAGCGCCTGGGG  60
            ||||||||||||||||||||||||||||||||||||||||||||||||||||||||||||
Sbjct  541  CAGGCCGGGGCCCGCGAGGGCGCCGAGCGCGGCCTCAGCGCCATCCGCGAGCGCCTGGGG  600

Query  61   CCCCTGGTGGAACAGGGCCGCGTGCGGGCCGCCACTGTGGGCTCCCTGGCCGGCCAGCCG  120
            ||||||||||||||||||||||||||||||||||||||||||||||||||||||||||||
Sbjct  601  CCCCTGGTGGAACAGGGCCGCGTGCGGGCCGCCACTGTGGGCTCCCTGGCCGGCCAGCCG  660

Query  121  CTACAGGAGCGGGCCCAGGCCTGGGGCGAGCGGCTGCGCGCGCGGATGGAGGAGATGGGC  180
            ||||||||||||||||||||||||||||||||||||||||||||||||||||||||||||
Sbjct  661  CTACAGGAGCGGGCCCAGGCCTGGGGCGAGCGGCTGCGCGCGCGGATGGAGGAGATGGGC  720

Query  181  AGCCGGACCCGCGACCGCCTGGACGAGGTGAAGGAGCAGGTGGCGGAGGTGCGCGCCAAG  240
            ||||||||||||||||||||||||||||||||||||||||||||||||||||||||||||
Sbjct  721  AGCCGGACCCGCGACCGCCTGGACGAGGTGAAGGAGCAGGTGGCGGAGGTGCGCGCCAAG  780

Query  241  CTGGAGGAGCAGGCCCAGCAGATACGCCTGCAGGCCGAGGCCTTCCAGGCCCGCCTCAAG  300
            ||||||||||||||||||||||||||||||||||||||||||||||||||||||||||||
Sbjct  781  CTGGAGGAGCAGGCCCAGCAGATACGCCTGCAGGCCGAGGCCTTCCAGGCCCGCCTCAAG  840

Query  301  AGCTGGTTCGAGCCCCTGGTGGAAGACATGCAGCGCCAGTGGGCCGGGCTGGTGGAGAAG  360
            ||||||||||||||||||||||||||||||||||||||||||||||||||||||||||||
Sbjct  841  AGCTGGTTCGAGCCCCTGGTGGAAGACATGCAGCGCCAGTGGGCCGGGCTGGTGGAGAAG  900

Query  361  GTGCAGGCTGCCGTGGGCACCAGCGCCGCCCCTGTGCCCAGCGACAATCACTGA  414
            ||||||||||||||||||||||||||||||||||||||||||||||||||||||
Sbjct  901  GTGCAGGCTGCCGTGGGCACCAGCGCCGCCCCTGTGCCCAGCGACAATCACTGA  954
```

(D) Sequencing result with apoE reverse primer

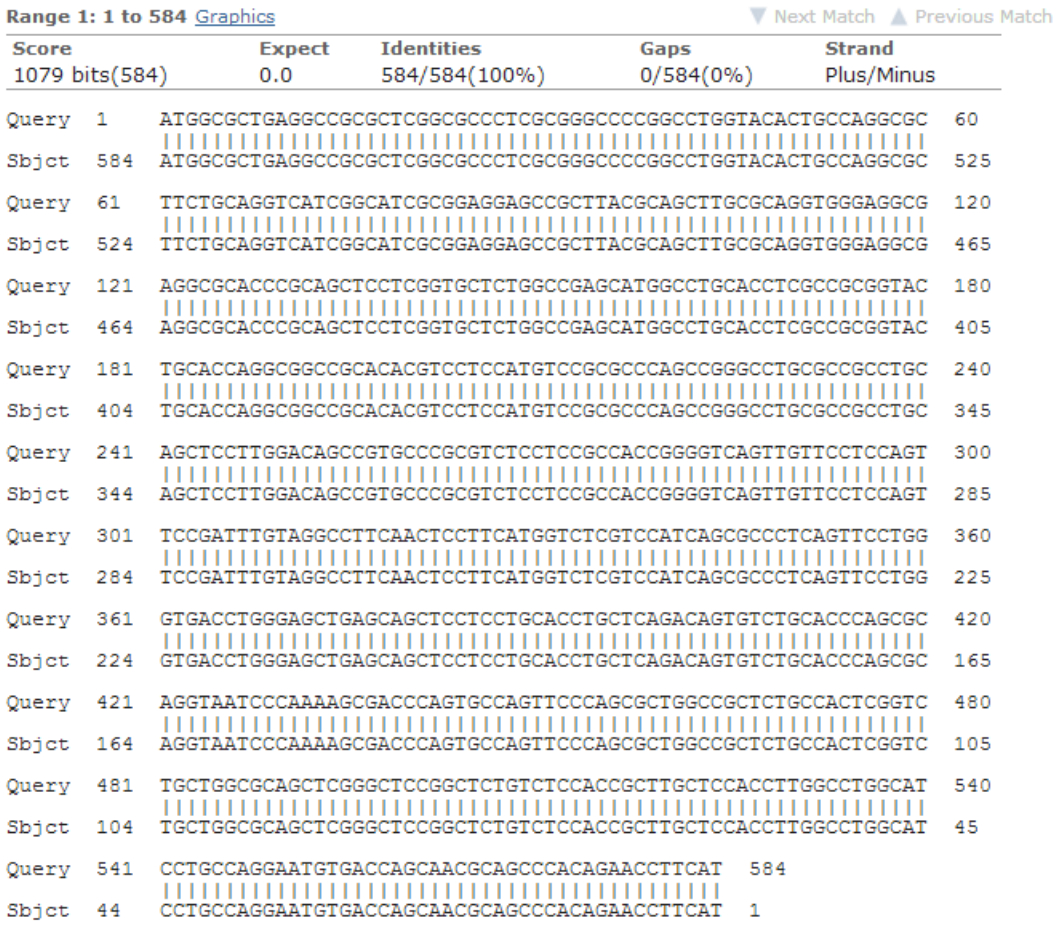

Range 1: 1 to 584 Graphics ▼ Next Match ▲ Previous Match

Score	Expect	Identities	Gaps	Strand
1079 bits(584)	0.0	584/584(100%)	0/584(0%)	Plus/Minus

```
Query  1    ATGGCGCTGAGGCCGCGCTCGGCGCCCTCGCGGGCCCCGGCCTGGTACACTGCCAGGCGC  60
           ||||||||||||||||||||||||||||||||||||||||||||||||||||||||||||
Sbjct  584  ATGGCGCTGAGGCCGCGCTCGGCGCCCTCGCGGGCCCCGGCCTGGTACACTGCCAGGCGC  525

Query  61   TTCTGCAGGTCATCGGCATCGCGGAGGAGCCGCTTACGCAGCTTGCGCAGGTGGGAGGCG  120
           ||||||||||||||||||||||||||||||||||||||||||||||||||||||||||||
Sbjct  524  TTCTGCAGGTCATCGGCATCGCGGAGGAGCCGCTTACGCAGCTTGCGCAGGTGGGAGGCG  465

Query  121  AGGCGCACCCGCAGCTCCTCGGTGCTCTGGCCGAGCATGGCCTGCACCTCGCCGCGGTAC  180
           ||||||||||||||||||||||||||||||||||||||||||||||||||||||||||||
Sbjct  464  AGGCGCACCCGCAGCTCCTCGGTGCTCTGGCCGAGCATGGCCTGCACCTCGCCGCGGTAC  405

Query  181  TGCACCAGGCGGCCGCACACGTCCTCCATGTCCGCGCCCAGCCGGGCCTGCGCCGCCTGC  240
           ||||||||||||||||||||||||||||||||||||||||||||||||||||||||||||
Sbjct  404  TGCACCAGGCGGCCGCACACGTCCTCCATGTCCGCGCCCAGCCGGGCCTGCGCCGCCTGC  345

Query  241  AGCTCCTTGGACAGCCGTGCCCGCGTCTCCTCCGCCACCGGGGTCAGTTGTTCCTCCAGT  300
           ||||||||||||||||||||||||||||||||||||||||||||||||||||||||||||
Sbjct  344  AGCTCCTTGGACAGCCGTGCCCGCGTCTCCTCCGCCACCGGGGTCAGTTGTTCCTCCAGT  285

Query  301  TCCGATTTGTAGGCCTTCAACTCCTTCATGGTCTCGTCCATCAGCGCCCTCAGTTCCTGG  360
           ||||||||||||||||||||||||||||||||||||||||||||||||||||||||||||
Sbjct  284  TCCGATTTGTAGGCCTTCAACTCCTTCATGGTCTCGTCCATCAGCGCCCTCAGTTCCTGG  225

Query  361  GTGACCTGGGAGCTGAGCAGCTCCTCCTGCACCTGCTCAGACAGTGTCTGCACCCAGCGC  420
           ||||||||||||||||||||||||||||||||||||||||||||||||||||||||||||
Sbjct  224  GTGACCTGGGAGCTGAGCAGCTCCTCCTGCACCTGCTCAGACAGTGTCTGCACCCAGCGC  165

Query  421  AGGTAATCCCAAAAGCGACCCAGTGCCAGTTCCCAGCGCTGGCCGCTCTGCCACTCGGTC  480
           ||||||||||||||||||||||||||||||||||||||||||||||||||||||||||||
Sbjct  164  AGGTAATCCCAAAAGCGACCCAGTGCCAGTTCCCAGCGCTGGCCGCTCTGCCACTCGGTC  105

Query  481  TGCTGGCGCAGCTCGGGCTCCGGCTCTGTCTCCACCGCTTGCTCCACCTTGGCCTGGCAT  540
           ||||||||||||||||||||||||||||||||||||||||||||||||||||||||||||
Sbjct  104  TGCTGGCGCAGCTCGGGCTCCGGCTCTGTCTCCACCGCTTGCTCCACCTTGGCCTGGCAT  45

Query  541  CCTGCCAGGAATGTGACCAGCAACGCAGCCCACAGAACCTTCAT  584
           ||||||||||||||||||||||||||||||||||||||||||||
Sbjct  44   CCTGCCAGGAATGTGACCAGCAACGCAGCCCACAGAACCTTCAT  1
```

Figure 4-1. Site-directed mutagenesis of pCMV.–apoE2 to generate pCMV.–apoE3. (A) pCMV.–apoE2 was used as DNA template to perform site-directed mutagenesis. Two types of High Fidelity Pfu DNA polymerase, Turbo Pfu and Promega Pfu, were employed to yield pCMV.–apoE3. After 18 cycles of amplification, 5μL mutagenesis products were subjected to 1% agarose gel electrophoresis for analysis. 200ng pCMV.apoE2 plasmid was loaded as an indicator of the correct molecular weight. (B) 1μL of both mutagenesis products were transformed into DH5α strains. The following day, three colonies each from Turbo and Promega Pfu amplification products were selected and plasmids were extracted with miniprep process before digestion with XhoI and HindIII. Colony 1 from Turbo Pfu amplification product and Colony 2 from Promega Pfu mutagenesis product were sent for sequencing. The sequencing results of Colony 2 amplified with Promega Pfu were presented in (C) and (D). The DNA sequence from mutagenesis product was shown as Query 1 and Homo sapiens apoE3 sequence was shown as Subject 1.

Table 4-3 Primers used for sequencing pCMV.apoE3.

Primer Name	Sequence
apoE forward	5'-CCT CCG CGA TGC CGA TGA CC -3'
apoE reverse	5'-CAC GCG GCC CTG TTC CAC C-3'

4.3.2 LRP5 and LRP6 interact with all three apoE isoforms

To determine the binding affinity between LRP5/6 and apoE isoforms, we performed co-immunoprecipitation assays. LRP5/6 expression plasmids together with apoE2, 3 or 4 were co-transfected into HEK293T cells. Cell lysates were immunoprecipitated down by apoE antibody and subjected to Western blotting assay. As shown in Figure 4-2A, LRP5 and LRP6 were detected in all the protein complexes pulled down by apoE antibody, which indicated the interaction between LRP5/6 and all three apoE isoforms. Since LRP5 is a less known Wnt co-receptor, we decided to focus our research on the interaction between LRP5 and apoE isoforms. To identify the interaction in neuronal cell lines, LRP5 and apoE isoforms were transiently co-transfected in human neuroblastoma SH-SY5Y cells. Figure 4-2B showed that LRP5 binds to apoE3 and 4 in SH-SY5Y cells with stronger binding affinity to apoE3.

(A)

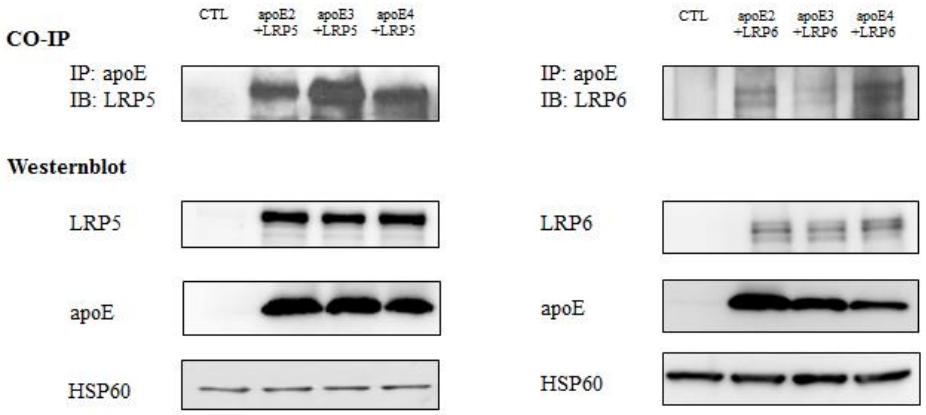

(B)

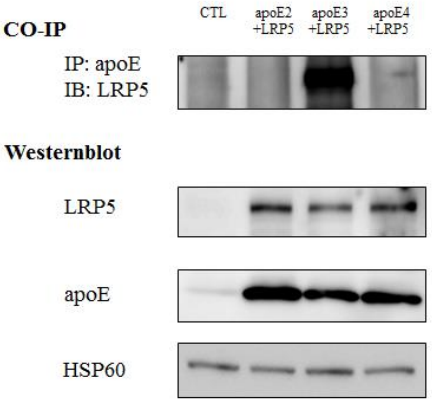

Figure 4-2. Detection of the interaction between apoE isoforms and LRP5/6. (A) HEK293T cells were overexpressed with LRP5 or 6 plasmids together with human apoE isoforms 2, 3, 4 plasmids. Equivalent lysates were immunoprecipitated (IP) with apoE antibody, followed by immunoblotting (IB) with LRP5 or 6 antibodies (upper panels). Total lysates were probed with specific antibodies, addressing the protein levels of LRP5/6, apoE 2/3/4, and β-actin. (bottom panel). (B) SH-SY5Y cells were overexpressed with apoE isoforms and LRP5 plasmid. The lysate was subjected to co-IP and Western blotting assays as described above.

4.3.3 The interaction between LRP5 and apoE isoforms disrupts the activation ability of LRP5

Since LRP5 acts as Wnt co-receptor to transduce Wnt signaling downstream, we asked the question whether binding with apoE isoforms would affect its ability to activate Wnt/β-catenin activities. TCF/LEF transcriptional activities in the SH-SY5Y cells co-transfected with LRP5 and apoE 2/3/4 were analyzed using a TCF/LEF-responsive luciferase reporter vector (TOPglow). In the absence of apoE isoforms, TCF/LEF transcriptional activities in the cells transfected with LRP5 were significantly increased compared to vector control. With the overexpression of apoE isoforms together with LRP5, however, TCF/LEF transcriptional activities were significantly decreased compared to the one transfected with LRP5 alone (Figure 4-3).

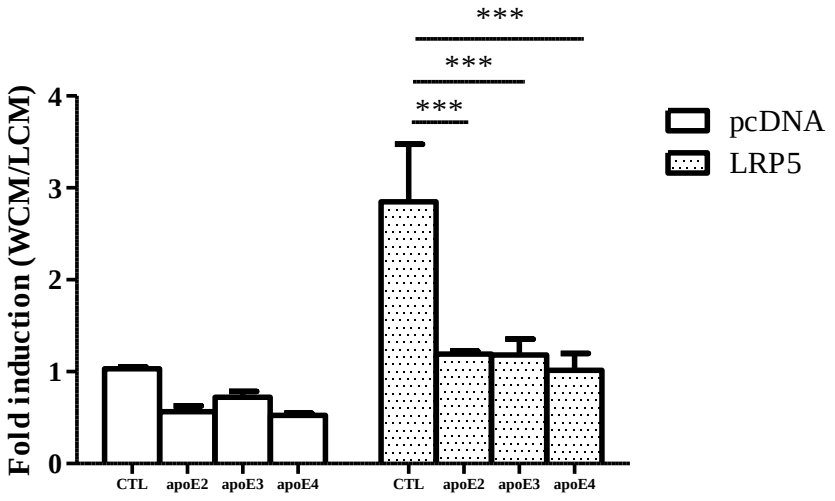

Figure 4-3. The interaction between LRP5 and apoE isoforms disrupts the activation ability of LRP5. SH-SY5Y cells were transfected with apoE isoforms and LRP5 expression plasmids together with TOPglow and pRL-CMV Renilla plasmids and treated with LCM or WCM for 24 hours. Wnt3a-induced luciferase activities were measured with Dual–Luciferase Reporter Assay Kit. Fold induction was presented in the

bar graph as of luciferase readings of WCM treatment over LCM treatment. Values represented the average (n=3) ± S.E.M.. Statistical differences were assessed using one-way ANOVA with Dunnett's post-hoc analysis (*p<0.05, **p<0.01, ***p<0.001).

4.3.4 Effect of the interaction between LRP5 and apoE isoforms on GSK3β activity

GSK3β is another major player in AD pathology whose activity is partially regulated by Wnt signaling. Therefore, we assessed whether GSK3β activity was affected by the interaction between LRP5 and apoE isoforms. Consistent with the finding in Chapter 3, Western blotting showed an increase in GSK3β Ser9 protein levels when LRP5 was overexpressed, indicating a decrease in GSK3β activity. For cells transfected with apoE isoforms alone, we observed a decrease in GSK3β activity in apoE4 overexpressing cells, but not in those transfected with apoE2 and apoE3. When LRP5 was co-expressed together with apoE isoforms, a significant decrease in GSK3β activity was observed in apoE3 and apoE4 expressing cells whereas no significant protein level change was seen for apoE2 transfectants with the presence of LRP5 (Figure 4-4).

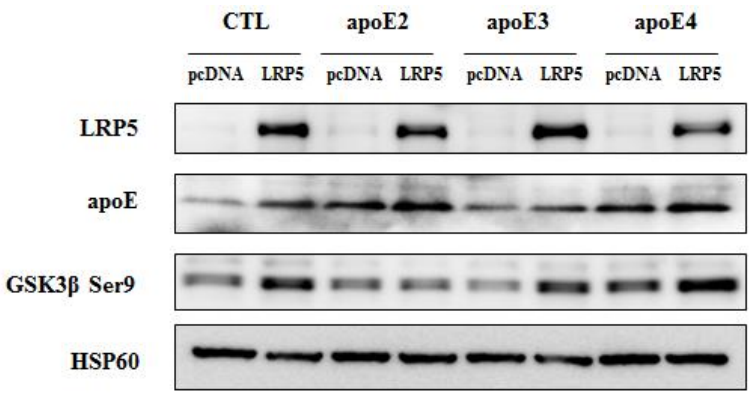

Figure 4-4. Effect of the interaction between LRP5 and apoE isoforms on GSK3β activity. SH-SY5Y cells were transfected with LRP5 together with apoE isoforms expression plasmids. Cells were then subjected to Western blotting analysis and probed with anti-LRP5, anti-apoE, anti-GSK3β Ser9 or anti-β-actin antibodies.

4.4 Discussion

LDL receptor family constitutes a group of structurally related cell surface receptors that recognize and bind to several structurally diverse extracellular ligands [108,109]. LDL receptor family has recently emerged as prominent players in neurodegenerative diseases due to its role as apoE receptors. However, the mechanism underlying this genetic predisposition is still largely unknown. On the other hand, abnormally regulated Wnt signaling has recently received significant attention for its role in AD pathology. LRP5 and LRP6, the distantly related members of LDL receptor family, also function as the essential Wnt co-receptors. However, the direct evidence of the binding between LRP5/6 and apoE isoforms still remains to be established.

We herein show for the first time that LRP5 and LRP6 bind to all three common apoE isoforms in HEK293T cells. In neuronal cell lines, SH-SY5Y human neuroblastoma cells, LRP5 strongly bound to apoE3 while a relatively weak interaction was observed between LRP5 and apoE4. The interaction between LRP5 and apoE2 was not seen in SH-SY5Y cells, which might be due to the low affinity beyond the detection limit.

Since LRP5 is the important Wnt co-receptor and apoE4 has been reported to inhibit Wnt7a-induced TCF/LEF transcriptional activity [137], we examined whether the interaction between LRP5 and apoE isoforms had any effect on Wnt signaling. Consistent to the previous studies with Wnt7a, our results showed that transfected apoE2, 3, and 4 reduced Wnt3a luciferase activities compared to basal conditions. However, Caruso et al. reported that apoE4 displayed a strong inhibitory effect in Wnt signaling whereas in our results the inhibitory effects were comparable among all the isoforms [137]. This might be due to the differences between Wnt ligands since it has been previously showed that Wnt3a and Wnt7a have different binding specificities for Fzs [171]. Furthermore, our results demonstrated that expression of apoE isoforms together with LRP5 abolished the activation ability of LRP5 on Wnt signaling. Taken together, our observation indicated that apoE isoforms regulate Wnt signaling and the interaction between LRP5 and apoE isoforms disrupts the co-activation ability of LRP5 and Fz.

Another important mediator of Wnt signaling is GSK3β, which has also been implicated in different aspects of AD pathophysiology. In addition to its ability to phosphorylate tau, GSK3β activity has been shown to influence neuronal proliferation and differentiation [172]. Defects in above processes lead to an impairment of memory which is one of the main features of AD. To address the issue whether the interaction between LRP5 and apoE isoforms affects GSK3β activity, we performed Western blotting assay and determined the protein amount of Ser9 phosphorylated GSK3β. Our results first showed that apoE4 decreased GSK3β activity significantly while apoE2 and apoE3 did not. Second, the interaction between LRP5 and apoE regulated GSK3β activity in an isoform-specific manner. A further reduction in GSK3β activity was seen when apoE4 was co-transfected with LRP5. ApoE3 was able to inhibit GSK3β activity only when LRP5 was co-expressed, whereas apoE2 did not show any inhibitory effect even with the enforced expression of LRP5. The GSK3β activity results in Figure 4-4 were not concordance with Wnt3a-induced TCF/LEF transcriptional activities in Figure 4-3, probably due to the absence of exogenous Wnt ligands and differences in the cell harvest time. As demonstrated by Cedazo-Minguez et al., recombinant apoE3 and apoE4 activated GSK3β at 1 hour [173]. At 5 hours, however, the activation effect was not seen with apoE3 while an inhibitory effect was observed with apoE4 [173]. Therefore, detailed studies with different transfection durations are needed to further understand the effect of this interaction on GSK3β.

4.5 Conclusion

Taken together, our results provide direct evidence on the interaction between Wnt co-receptors LRP5/6 and all three common apoE isoforms, namely apoE2, apoE3 and apoE4. This piece of data not only proves that LRP5 and LRP6 are the receptors of apoE isoforms, but also provides a link between Wnt signaling and apoE pathology. In addition, we also showed that the interaction between LRP5 and apoE isoforms disrupts the activation ability of LRP5 and exerts isoform-specific effects on GSK3β activity. The findings from this chapter provide an interesting direction in understanding the mechanism underlying AD pathology and further studies focused on pathogenic apoE4 will be explored in the next chapter.

CHAPTER 5. APOLIPOPROTEIN E4 DISRUPTS NORMAL MITOCHONDRIAL DYNAMICS THROUGH BINDING TO LOW-DENSITY LIPOPROTEIN RECEPTOR-RELATED PROTEIN 5/6 IN SH-SY5Y CELLS

5.1 Introduction

Mitochondria are highly dynamic organelles, adopting different shapes from giant tubular network to small punctate pattern of separated mitochondria through fusion and fission processes [174,175]. In addition to morphology, fusion and fission processes also regulate mitochondrial functions including energy production, generation of ROS and cell survival [176]. Due to high dependence on mitochondrial energy production and complex morphology, neurons are especially sensitive to mitochondrial dysfunction [177]. Alterations in mitochondrial dynamics significantly impair neuronal functions which have been associated with neurodegenerative diseases including AD [106,107,178].

Mitochondrial fusion is a two-step process, with outer membrane fusion followed by inner membrane fusion. These events result in the mixing of membranes, intermembrane space and matrix [179]. In mammals, two large transmembrane GTPases, Mfn 1 and 2, are essential for mediating outer membrane fusion [180,181]. These two Mfns form homotypic and heterotypic complexes, which provide a mechanism for organelle tethering [96,182]. Subsequently, it is possible that GTP hydrolysis-driven conformational changes mediate the outer membranes

to fuse. Another GTPase, OPA1, is required for mediating inner membrane fusion. Cells depleted of either Mfns or OPA1 completely lose the ability of mitochondrial fusion [96,183] (Figure 5-1). On the other hand, mitochondrial fission process is mediated by two classes of proteins. The protein in the first class, Drp1, mostly resides in cytosol, which is recruited to the mitochondrial fission puncta by the second class of molecules including Fis1 (Figure 5-1). Drp1 is a central player essential for mitochondrial fission in most types of cells. Knockdown with RNA interference or expression of a dominant-negative variant of Drp1 leads to extensions in the length of mitochondrial tubules [99,102]. Similar to dynamin, the GTPase domain in Drp1 is likely to hydrolyze GTP and provide mechanical force to assemble into high-order helical structures [184,185]. The self-assemble spiral structures correspond to the Drp1 puncta on mitochondria and cause a large constriction [186-188].

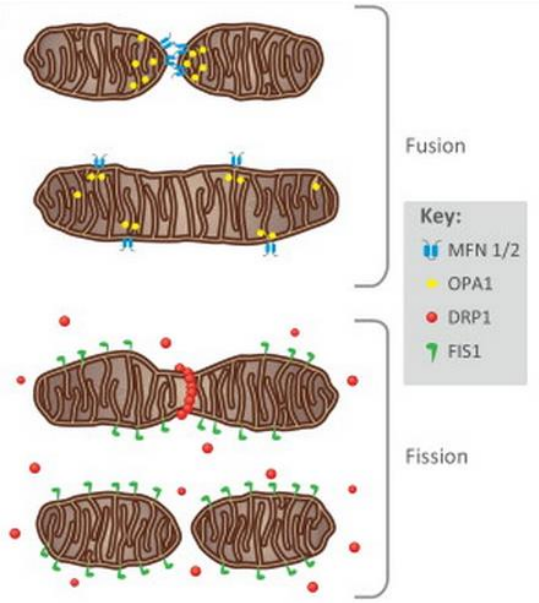

Figure 5-1. Schematic representation of mitochondrial fusion and fission processes. This image was taken from Ref [189].

Despite growing evidence suggesting that mitochondrial fusion and fusion processes are disrupted in AD neurons, the molecular basis underlying the abnormalities in mitochondrial dynamics remains to be investigated. The main genetic risk factor for LOAD apoE4 has been repeatedly reported to induce mitochondrial dysfunction [81,83,190]. Therefore, it is noteworthy to know whether apoE4 also participates in abnormally regulating mitochondrial dynamics.

In this study, we showed that overexpression of apoE4 in SH-SY5Y human neuroblastoma cells increased the levels of mitochondrial fission proteins Drp1 and Fis1 and reduced the level of mitochondrial fusion protein Mfn2. Subsequently, we observe that mitochondria displayed swollen and fragmented morphology under the confocal microscopy. To understand this mechanism underlying mitochondrial fission, we demonstrate a direct interaction between apoE4 and LRP5/6 in both HEK293T and SH-SY5Y cell lines using co-immunoprecipitation assay. This interaction could be disrupted by LRP5/6 inhibitor DKK1. Using DKK1 to dissociate apoE4 and LRP5/6, we observed a reduction in the elevated protein levels of Drp1 and Fis1 and an increase in the repressed Mfn2 protein level. This dissociation subsequently led to the restoration of the normal mitochondrial dynamics. Taken together, our data suggest that apoE4 alters mitochondrial dynamics through binding to LRP5/6 and disruption of this interaction might be a potential therapeutic strategy for AD patients carrying apoE4.

5.2 Materials and Methods

5.2.1 Cell culture and reagents

SH-SY5Y human neuroblastoma cells and HEK 293T cells were cultured and transfected with the same manner as reported in Section 4.2.1 of Chapter 4.

5.2.2 Polymerase Chain Reaction (PCR)

ApoE4 fragment (apoE4 1-272) was amplified with specific primers (Table 5-1) using a Thermal Cycler (Techne, Staffordshire, UK). Amplification reagents were prepared in a sterile 0.2mL tube on ice as follows (Table 5-2). The amplification tube was placed in the Thermo Cycler and denatured at 95˚C for 10 min, followed by 30 cycles of amplification with DNA denaturation at 95˚C for 1 min, primer annealing at 62˚C for 1 min, and primer extension at 72˚C for 1 min. At the end, a total of 10 min extension at 72˚C was performed.

Table 5-1 Primers used for amplification of apoE4 fragment

Primer Name	**Sequence**
apoE4 fragment forward	5'-CCC AAG CTT GGG ATG AAG GTT CTG TGG GCT GCG-3'
apoE4 fragment reverse	5'-CAT GGA TCC ATG TTA GGC CTG CAG GCG TAT CTG CTG-3'

Table 5-2 Reagents used for PCR amplification

Reagents	Volume
10x Pfu Buffer	5μL
pCMV.–apoE4 (0.1μg/μL)	1μL
apoE4 fragment primer forward	1.5μL
apoE4 fragment primer reverse	1.5μL
dNTP (10mM)	1μL
Pfu DNA polymerase	1μL
ddH_2O	39μL
Total	50μL

5.2.3 Restriction enzyme digestion

To generate linear DNA for ligation, 0.5μg pcDNA3.1 vector and 15μL apoE4 fragment PCR product were digested with 10 units of HindIII (New England Biolabs, Beverly, MA) and 10 units of BamHI (New England Biolabs, Beverly, MA) at 37˚C for 5 hours. For plasmids or fragments verification, around 1 μg DNA was double-digested by 10 units of HindIII (New England Biolabs, Beverly, MA) and 10 units of BamHI (New England Biolabs, Beverly, MA) at 37˚C for 2 hours.

5.2.4 Alkaline phosphatase digestion

Alkaline phosphatase digestion was performed before ligation to remove 5'-phosphate group and avoid self-ligation. 1μL Calf Intestinal Alkaline Phosphatase

(CIP) (New England Biolabs, Beverly, MA) was diluted with 4μL ddH_2O. 1μL of diluted CIP was added into 20μL of restriction enzyme digestion product. The mixture was incubated at 37˚C for 2 hours.

5.2.5 Agarose gel electrophoresis

Agarose gel electrophoresis was performed with the same manner as reported in Section 4.2.4 of Chapter 4.

5.2.6 Gel extraction

Gel extraction was performed with QIAquick Gel Extraction Kit (Qiagen, Valencia, CA) according to manufacturer's protocol. Briefly, when adequate separation of bands occurred in gel electrophoresis, DNA fragments of interest were carefully excised under UV light ensuring as much agarose gel as possible has been removed. Gel slices were weighed in a clean 1.5mL microcentrifuge tube. Three volume of Buffer QG to one volume of gel (a gel slide of mass 0.1g equals to 0.1mL) was added into microcentrifuge tube and incubated at 50˚C until the gel completely melted. One gel volume of isopropanol was added and mixed into the tube before being loaded onto the column. Column bounded DNA was washed with Buffer QG and PE, followed by elution with nuclease-free water.

5.2.7 DNA ligation

DNA ligation was performed with a 10μL reaction volume with T4 DNA ligase (Promega, Madison, WI). Restriction enzyme-digested and CIP-treated apoE4 fragment and pcDNA3.1 vector were transferred to a clean 0.5mL microcentrifuge tube supplemented with 10x ligation buffer. 1μL T4 ligase was then added to the tube. The prepared ligation mixture was incubated at room temperature for 4 hours before being subjected to bacterial transformation.

5.2.8 Bacterial transformation

10μL of ligate was transferred to a clean 1.5mL Eppendorf tube and mixed with 50μL DH5α bacterial strain on ice, followed by gently tapping. Bacterial transformation was performed with the same manner as described in Section 4.2.3 of Chapter 4.

5.2.9 Western blotting analysis

Western blotting assay was performed with the same manner as described in Section 3.2.4 of Chapter 3. Additional antibodies were: apoE (Millipore, Billerica, MA), Drp1 (BD Transduction Laboratories, Franklin Lakes, New Jersey), Fis1 (Alexis Biochemicals Corp., San Diego, CA), OPA1 (BD Transduction Laboratories, Franklin Lakes, New Jersey), Mfn1 (Santa Cruz Biotechnology,

Santa Cruz, CA), and Mfn2 (Abcam, Cambridge, MA). ApoE antibody was raised against a synthetic peptide corresponding to amino acids surrounding the polymorphic amino acid position 158 of apoE, therefore this antibody was able to recognize apoE4 (1-272) fragment.

5.2.10 Co-immunoprecipitation

The co-immunoprecipitation procedure was the same as reported in Section 4.2.6 of Chapter 4.

5.2.11 Confocal fluorescence microscopy

SH-SY5Y cells ($5x10^5$) were seeded on coverslips inside a 6-well plate overnight and transfected with 3μg LRP5 or LRP6 and 3μg apoE4 expression plasmids. After washing with PBS, cells were incubated with MitoTracker Red CMXRos (Invitrogen, Carlsbad, CA) for 10 min in the CO_2 incubator, followed by fixation in 4% w/v paraformaldehyde for 10 min and permeabilization in 0.1% v/v TritonX-100 in PBS for 20 min. Samples were then blocked with 1% w/v bovine serum albumin (BSA) for 1 hour at room temperature. Primary antibodies (1:200 dilution) in 0.1% w/v BSA were added into the petri dishes. After washing 3 times with PBS, cells were incubated with secondary antibodies Alexa Fluor 488 goat anti-mouse IgG (Invitrogen, Carlsbad, CA), Alexa Fluor 568 goat anti-mouse IgG (Invitrogen, Carlsbad, CA), Alexa Fluor 488 goat anti-rabbit IgG (Invitrogen,

Carlsbad, CA) or Chromeo™ 642 anti-Rabbit IgG - H&L (Abcam, Cambridge, MA) for another 1 hour. After washing with PBS 3 times, the coverslips were reversed and mounted onto slides. Fluorescence images were obtained using confocal microscopy Fluoview Fv10 (Olympus, Tokyo, Japan).

5.2.12 Mitochondrial morphology analysis

Quantitative analysis of mitochondrial morphology was achieved using Image J software [191,192]. All images were captured with 60x objective. Images of 10 random fields were acquired from each treatment set at room temperature. The acquired mitochondrial raw images were thresholded optimally to minimize the noise and processed into binary pixels. The grayscale images were then subjected to shape distributor plugin analysis. Form Factor (FF, the reciprocal of circularity value) and Aspect Ratio were employed as indexes of mitochondrial interconnectivity. A circularity value ($4\pi \bullet \text{area}/\text{perimeter}^2$) of 1 represents circular and unbranched mitochondria. As the mitochondria elongate and branch, the circularity value decreases and approaches to 0. An Aspect Ratio (AR, major axis/minor axis) of 1 indicates a perfect circle and higher aspect ratio values indicate more elliptical and elongated mitochondria.

5.2.13 Colocalization analysis

For colocalization studies, 10 images of random fields for each treatment set were captured with 60x objective. Samples were recorded separately in each dye-

corresponding channel. Pearson's correlation coefficient (PCC), the correlation of the intensity values of the two different color pixels in a dual-channel image, was calculated by Fluoview Fv10-ASW to determine protein-protein colocalization.

5.2.14 Detection of mitochondrial transmembrane potential

SH-SY5Y cells ($2.5x10^5$) were seeded in 24-well plates and transfected with 1μg apoE4 and 1μg LRP5 or LRP6 expression plasmids. After 24 hours of transfection, cells were incubated with 5μg/mL JC-1 fluorescence dye. 250nM staurosporine (STS) (Sigma-Aldrich, St Louis, MO) was added 8 hours before JC-1 incubation as the positive control treatment group. Plates were incubated in the CO_2 incubator for half an hour. Then cells were washed with PBS twice before transferred to a Nunc-Immuno MicroWell 96 well black polystyrene plate (Roskilde, Denmark). JC-1 forms aggregates in the healthy mitochondria which display strong red fluorescent intensity with excitation and emission at 560nm and 595nm, respectively. In unhealthy cells, JC-1 exists in monomeric form which shows strong green fluorescence intensity with excitation and emission at 484nm and 535nm, respectively. The absorbance of the red and green fluorescence was measured using a microplate reader (Tecan Infinite® 200 PRO, Männedorf, Switzerland). JC-1 ratio was calculated by dividing the readings of red fluorescence intensity over those of green fluorescence intensity. The experiment was repeated three times and data were expressed as the average ± S.E.M.

5.2.15 Statistical analysis

Statistical significance was determined by Student's t test or Dunnett's One-way ANOVA (SPSS, Chicago, IL). $p < 0.001$ (***), $p < 0.01$ (**), $p < 0.05$ (*) were considered to be significant.

5.3 Results

5.3.1 Molecular cloning of apoE4 fragment plasmid

Due to unique structure, apoE4 is cleaved into C-terminal-truncated fragment apoE4 (1-272) inside neurons. This fragment has been found to induce cytotoxicity in cultured neuronal cells and cause behavioral deficits in transgenic mice [193-195]. Hence, to investigate the detrimental effect of apoE4 and apoE4 fragment, we designed primers annealing to 1-272 amino acids of apoE4 and performed PCR amplification with pCMV.–apoE4 plasmid as template. pcDNA3.1 vector and apoE4 fragment PCR product were digested with HindIII and BamHI and treated with CIP to remove 5' phosphate group before gel electrophoresis. A linear pcDNA3.1 vector with molecular weight of 5,428bp and a clear apoE4 fragment DNA band of 816bp were seen (Figure 5-1A). The DNA fragments of interest were excised under UV light and extracted using QIAquick Gel Extraction Kit. Extracted fragments were verified on 1% agarose (Figure 5-1B). Next, pcDNA3.1 vector and apoE4 fragment were ligated under room temperature with T4 DNA ligase for 4 hours, followed by bacterial transformation.

On the following day, ten colonies were picked up to identify the correct clones for apoE4 fragment. Plasmids were extracted and digested with HindIII and BamHI, followed by gel electrophoresis. As shown in Fig. 5-1C, Colony 1, 2, 3, and 5 presented DNA bands at 816bp, the correct molecular weight for the apoE4 fragment. Therefore, the first colony was selected and preserved in 15% glycerol under -80˚C.

(A)

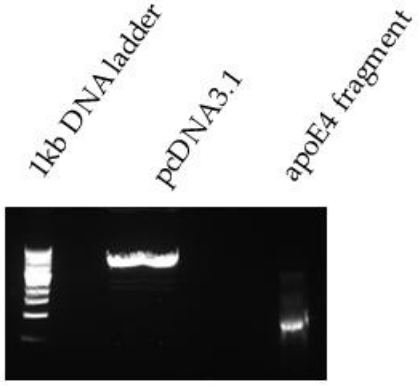

(B)

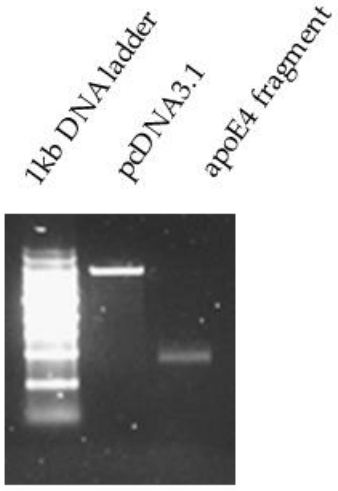

(C)

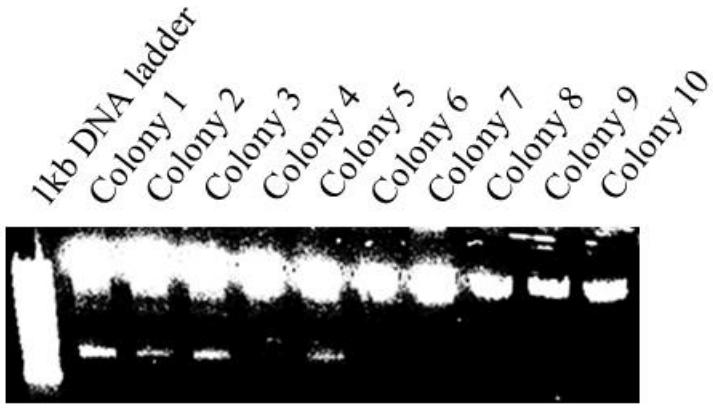

Figure 5-2. Molecular cloning of apoE4 fragment plasmid. (A) pCMV.–apoE4 was used as PCR template to amplify apoE4 fragment (1-272) with the annealing temperature of 62˚C. pcDNA3.1 vector and apoE4 fragment PCR product were subjected to restriction enzymes double-digestion with HindIII and BamHI. Samples were incubated with CIP to remove 5' phosphate group and loaded onto 1% agarose gel for gel electrophoresis. (B) Correct DNA bands were excised carefully from the agarose gel under UV light. Excised gels were solubilized and subjected to QIAquick Gel Extraction Kit to obtain DNA fragments. After extraction, purified DNA fragments were subjected to gel electrophoresis for validation. (C) Purified pcDNA3.1 vector and apoE4 fragment were ligated at room temperature for 4 hours before transformed into DH5α bacterial strains. Ten colonies were selected and subjected to miniprep. Extracted plasmids were digested with HindIII and BamHI, followed by gel electrophoresis for verification.

5.3.2 Overexpression of apoE4 and apoE4 fragment perturbs mitochondrial dynamics

ApoE4 has been reported to exert a detrimental effect on mitochondrial metabolism [196-198] and mitochondrial function [77]. Mitochondrial function is regulated and reflected by its dynamics. In addition, mitochondrial morphology and dynamics are also found to be impaired in the brains of AD patients [106,107]. Therefore, we examined whether apoE4 would affect mitochondrial dynamics. As shown in Figure 5-2A, the levels of mitochondrial fission proteins Drp1 and Fis1 were increased, while the expression of mitochondrial fusion protein Mfn2 was repressed in cells overexpressed with apoE4 compared to control cells transfected with empty vector. To analyze mitochondrial morphology, cells were stained with MitoTracker Red CMXRos and visualized under confocal microscope. Figure 5-2B showed that swollen mitochondria with short tubules were observed in cells overexpressing apoE4 and apoE4 fragment, suggesting an imbalance in mitochondrial fusion and fission. Statistical analysis of FF values that determine the interconnectivity of the mitochondria and AR values that measure the length

of the mitochondria from three independent experiments was performed. Results showed that cells overexpressed with apoE4 and apoE4 fragment have significantly lower FF values (mean ± S.E.M, n=10) and AR values (mean ± S.E.M, n=10) as compared to control cells (Figure 5-2C).

(A)

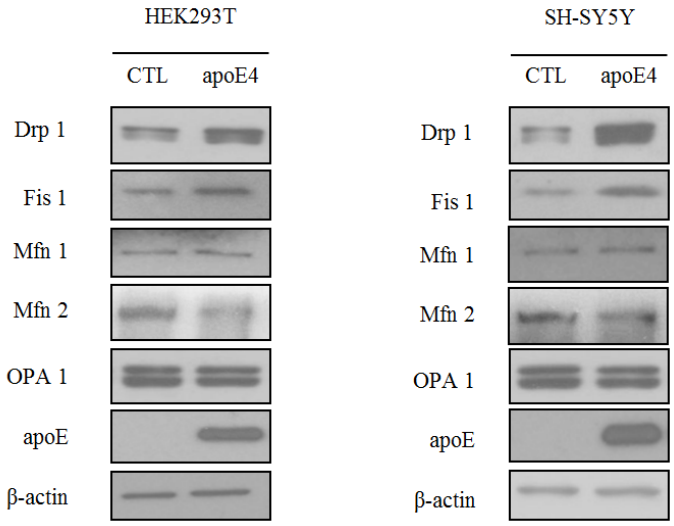

(B)

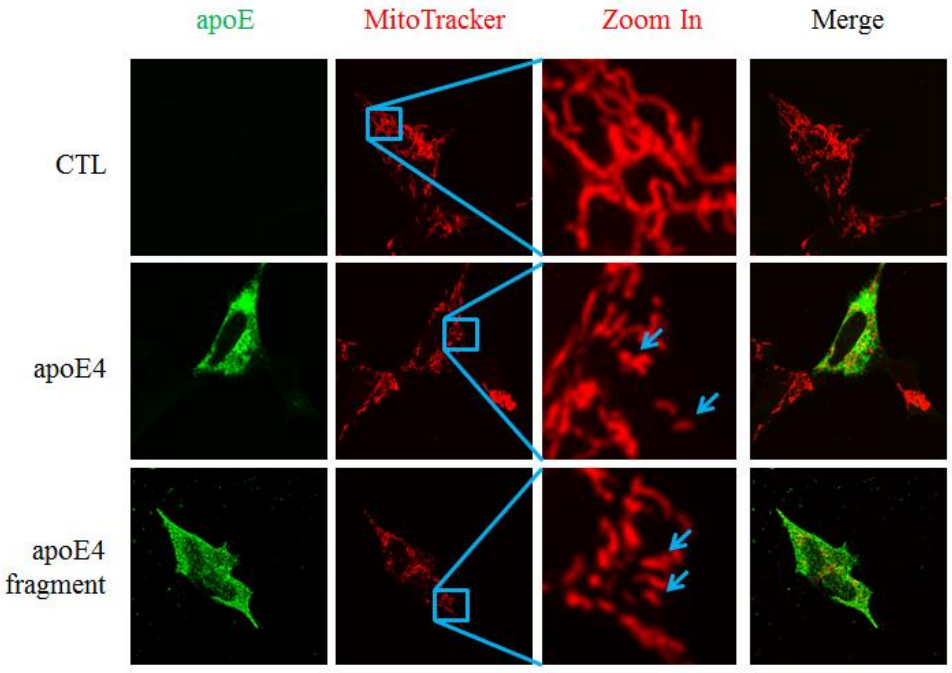

(C)

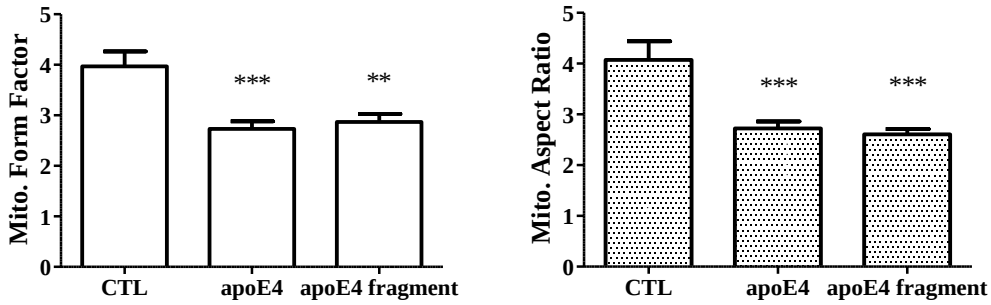

Figure 5-3. ApoE4 and apoE4 fragment induce abnormalities in mitochondrial dynamics. (A) SH-SY5Y cells were transfected with pCMV.–apoE4 or pCMV. vector. Samples were solubilized with Western blotting lysis buffer and probed with specific antibodies, addressing the protein levels of mitochondrial fission proteins Drp1, Fis1 and fusion proteins Mfn1, Mfn2, OPA1. (B) SH-SY5Y cells were transfected with human apoE4 or apoE4 fragment expression plasmids. Twenty four hours after transfection, cells were stained with MitoTracker Red CMXRos, fixed in paraformaldehyde and permeabilized in TritonX-100. ApoE4 and apoE4 fragment proteins were probed with apoE primary antibody and detected by Alexa Fluor 488 anti-mouse IgG. Fluorescent signals were visualized under confocal microscope. (C) Mitochondrial morphology was determined by FF and AR using Image J software shape distributor plugin. The data represented average (n=10) ± S.E.M. and statistical significance was assessed with Student's t test (*$p<0.05$, **$p<0.01$, ***$p<0.001$).

5.3.3 ApoE4 and apoE4 fragment interact with LRP5/6

In the previous chapter, we have demonstrated the interaction between apoE4 and LRP5/6 in both HEK293T and SH-SY5Y cells. Here, we explored the interaction further with apoE4 fragment. As shown in co-immunoprecipitation assay with HEK293T cells (Figure 5-3A), we were able to detect LRP5 and LRP6 in the protein complexes pulled down by apoE antibody, which confirmed the interaction between apoE4 and LRP5/6 shown in the last chapter. In addition, it also demonstrated an interaction between LRP5/6 and apoE4 fragment. Furthermore, LRP5/6 and apoE4 were transiently co-transfected in human

neuroblastoma cells SH-SY5Y. Similarly, LRP5 and LRP6 were detected in the protein complex immunoprecipitated by apoE antibody in SH-SY5Y cells (Figure 5-3B). Next, we performed confocal microscopy to determine whether apoE4 colocalized with LRP5/6. SH-SY5Y cells were transfected with LRP5/6 and apoE4 or respective vectors and probed with fluorescence-conjugated antibodies. The overlay image showed a colocalization between apoE4 (in red) and LRP5/6 (in green) (Fig. 5-3C). PCC values that quantify the degree of colocalization between fluorophores were calculated using Fluoview Fv10-ASW. For cells overexpressing apoE4 and LRP5, PCC value was determined to be 0.944 ± 0.006 (Table 5-3), suggesting a strong colocalization of the two proteins; similarly, a very strong colocalization were seen between apoE4 and LRP6 with PCC values to be 0.958 ± 0.025 (Table 5-4).

(A)

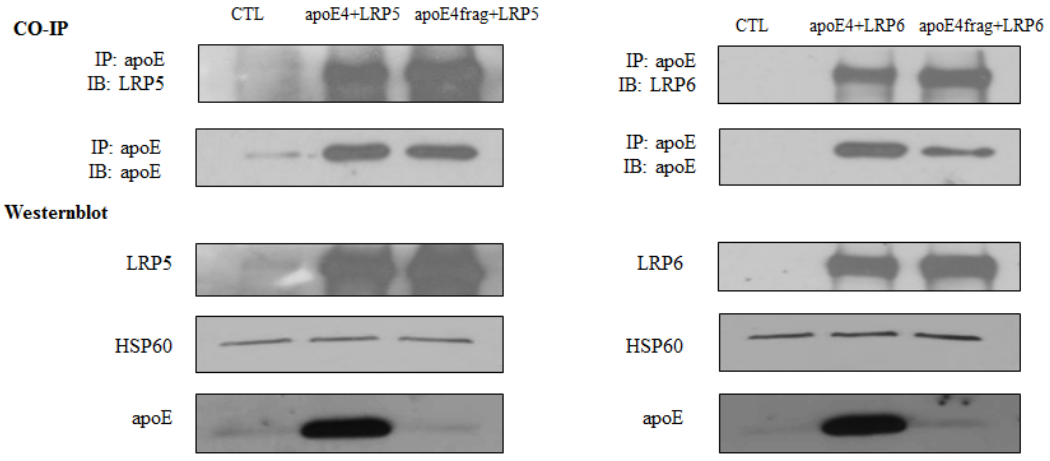

(B)

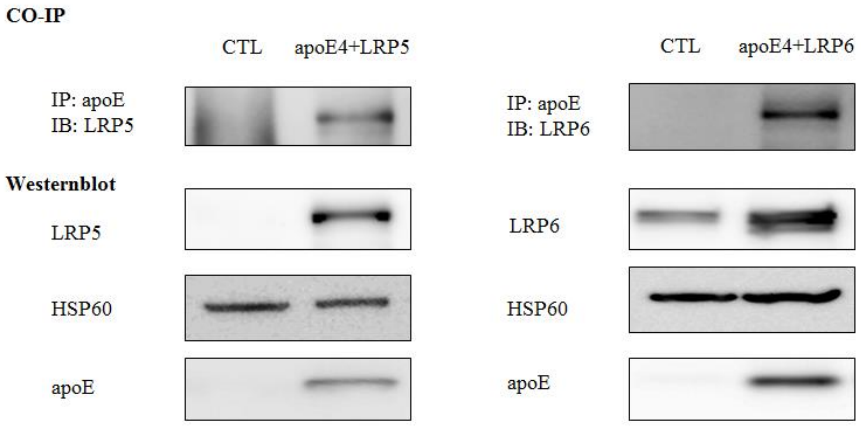
CO-IP
CTL
apoE4+LRP5
CTL
apoE4+LRP6
IP: apoE
IB: LRP5
IP: apoE
IB: LRP6
Westernblot
LRP5
LRP6
HSP60
HSP60
apoE
apoE

(C)

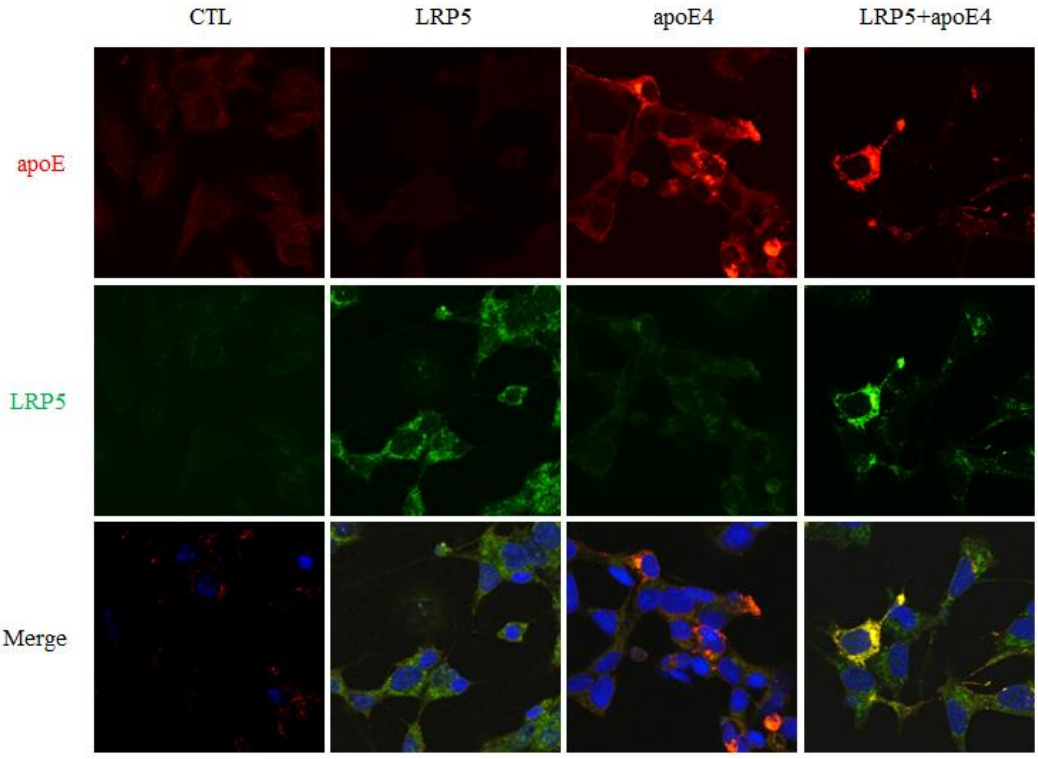
CTL
LRP5
apoE4
LRP5+apoE4
apoE
LRP5
Merge

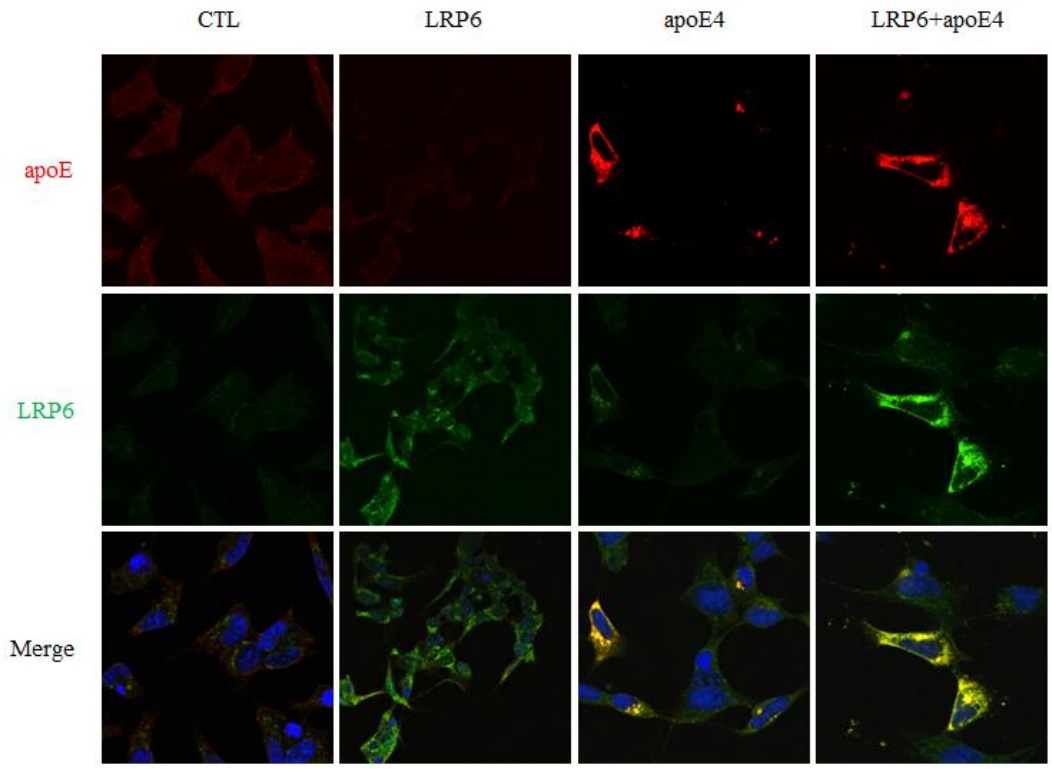

Figure 5-4. Detection of the interaction between apoE4/apoE4 fragment and LRP5/6. (A) HEK293T cells were overexpressed with human wild-type apoE4 or apoE4 fragment together with LRP5 or 6 plasmids. Equivalent lysates were immunoprecipitated with apoE antibody, followed by immunoblotting with LRP5 or 6 antibodies (upper panels). Total lysates were probed for the indicated proteins (bottom panel). (B) SH-SY5Y cells were overexpressed with human wild-type apoE4 and LRP5/6 plasmids. The lysate was subjected to co-IP and Western blotting assays as described above. (C) SH-SY5Y cells were overexpressed with apoE4 and LRP5/6, and fixed with paraformaldehyde followed by permeabilization using TritonX-100. The samples were then probed with specific primary antibodies for apoE and LRP5/6, followed by secondary antibodies Alexa Fluor 568 goat anti-mouse IgG (recognizing apoE) and Alexa Fluor 488 goat anti-rabbit IgG (recognizing LRP5/6). The colocalization was measured by PCC using Fluoview Fv10-ASW and data was presented as the mean (n=10) ± S.E.M..

Table 5-3 Statistical analysis of the degree of colocalization between apoE4 and LRP5.

Experimental Group	PCC (Mean ± S.E.M.)
CTL	0.743 ± 0.020
LRP5	0.727 ± 0.020
apoE4	0.849 ± 0.010
apoE4 + LRP5	0.944 ± 0.006

Table 5-4 Statistical analysis of the degree of colocalization between apoE4 and LRP6.

Experimental Group	PCC (Mean ± S.E.M.)
CTL	0.750 ± 0.015
LRP6	0.295 ± 0.020
apoE4	0.772 ± 0.041
apoE4 + LRP6	0.958 ± 0.025

5.3.4 DKK1 disrupts the interaction between apoE4 and LRP5/6 in a dose-dependent manner

DKK1 is a secreted protein that antagonizes Wnt/beta-catenin signaling by inhibiting LRP5/6 [199]. The ectodomain of LRP5/6 contains four β-propeller/EGF-like domain repeats [127,200]. The binding of LRP6 to its ligand Wnt9b requires the first two repeats of β-propeller/EGF-like domain and the last two repeats are required for Wnt3a binding [201]. A crystal structural study showed that DKK1 C-terminal domain binds to the last two repeats and DKK1 N-

terminal domain binds to the first two repeats of LRP6, demonstrating that DKK1 can inhibit both receptor binding domains [202]. Therefore, we postulated that DKK1 might inhibit the interaction between apoE4 and LRP5/6. We overexpressed apoE4 and LRP5/6 in HEK293T cells, followed by treatment of 0, 20, 50, 100ng/mL DKK1 for 24 hours. Co-immunoprecipitation assay showed that DKK1 dissociated the interaction in a dose-dependent manner (Figure 5-4A). As DKK1 significantly dissociates the interaction at a concentration of 100ng/mL, we subsequently used this concentration of DKK1 to treat SH-SY5Y cells. An obvious disturbance of the interaction was observed in SH-SY5Y cells treated with 100ng/mL DKK1 for 24 hours (Figure 5-4B). Confocal fluorescence microscopy analysis was performed to verify the changes in the colocalization of apoE4 and LRP5/6 (Figure 5-4C). With the treatment of DKK1, PPC values were significantly decreased from 0.944 ± 0.006 to 0.830 ± 0.015 for apoE4 and LRP5 (Table 5-5); and reduced from 0.958 ± 0.025 to 0.817 ± 0.075 for apoE4 and LRP6 (Table 5-6).

(A)

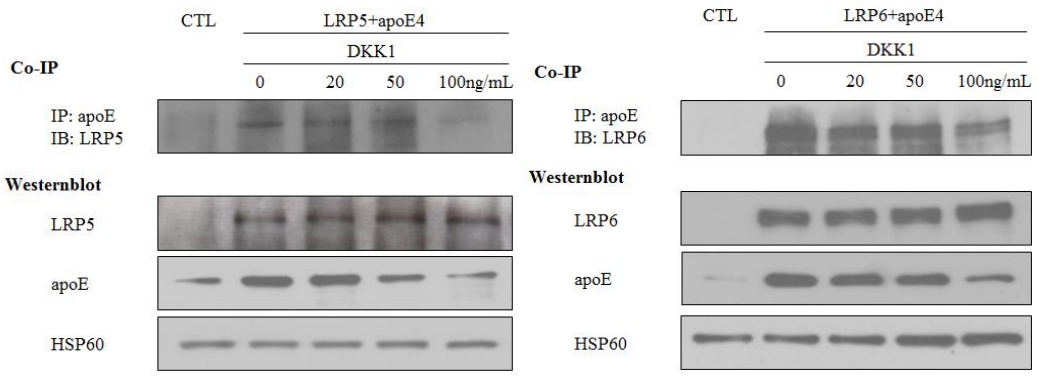

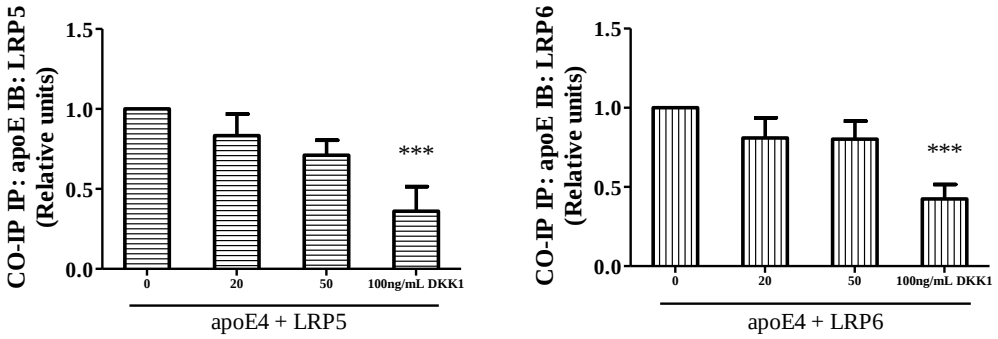
CO-IP IP: apoE IB: LRP5
(Relative units)
1.5
1.0
0.5
0.0
***
0
20
50
100ng/mL DKK1
apoE4 + LRP5
CO-IP IP: apoE IB: LRP6
(Relative units)
1.5
1.0
0.5
0.0
***
0
20
50
100ng/mL DKK1
apoE4 + LRP6

(B)

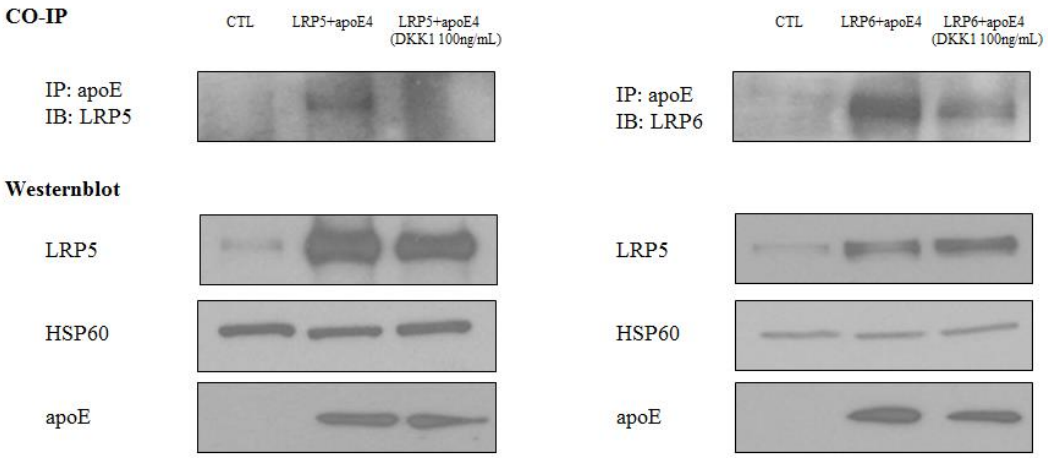
CO-IP
CTL
LRP5+apoE4
LRP5+apoE4
(DKK1 100ng/mL)
IP: apoE
IB: LRP5
CTL
LRP6+apoE4
LRP6+apoE4
(DKK1 100ng/mL)
IP: apoE
IB: LRP6
Westernblot
LRP5
HSP60
apoE
LRP5
HSP60
apoE

(C)

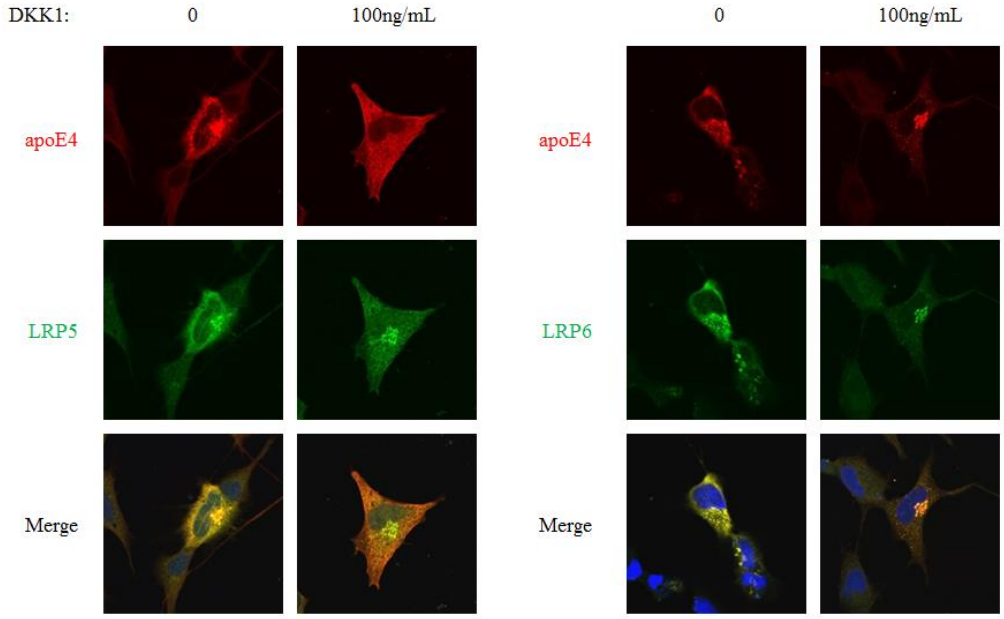
DKK1:
0
100ng/mL
0
100ng/mL
apoE4
LRP5
Merge
apoE4
LRP6
Merge

(D)

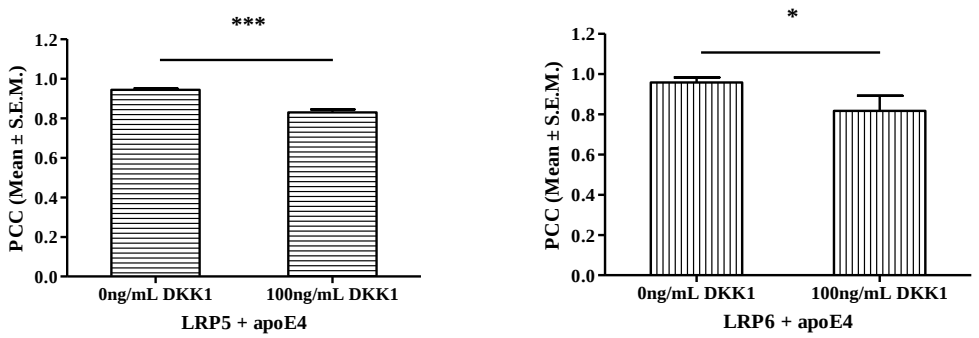

Figure 5-5. DKK1 disrupts the interaction between apoE4 and LRP5/6 in both HEK293T cells and SH-SY5Y cells. (A) HEK293T cells were overexpressed with apoE4 and LRP5/6 plasmids, followed by treatment with 0, 20, 50, 100ng/mL DKK1 for 24 hours. Equivalent lysates were immunoprecipitated with apoE antibody, followed by immunoblotting with LRP5 or 6 antibodies (upper panels). Total lysates were probed for the indicated proteins (bottom panel). (B) SH-SY5Y cells were co-transfected with apoE4 and LRP5/6 expression plasmids before treatment with 0 and 100ng/mL DKK1 for 24 hours. The lysate was subjected to co-IP and Western blotting assays as described above. (C) SH-SY5Y cells were overexpressed with apoE4 and LRP5/6, followed by treatment with 0 and 100ng/mL DKK1 for 24 hours before being harvested. Cells were fixed with paraformaldehyde and permeabilized using TritonX-100. The samples were then probed with specific primary antibodies for apoE and LRP5/6, followed by secondary antibodies Alexa Fluor 568 goat anti-mouse IgG (recognizing apoE) and Alexa Fluor 488 goat anti-rabbit IgG (recognizing LRP5/6). (D) The degree of colocalization was determined by PCC values calculated using Fluoview Fv10-ASW. Data was presented as the average (n=10) ± S.E.M. and statistical significance was assessed with Student's t test (*$p<0.05$, **$p<0.01$, ***$p<0.001$).

5.3.5 Dissociation of apoE4 and LRP5/6 restores perturbed mitochondrial dynamics

To understand the mechanism underlying apoE4-induced abnormalities in mitochondrial dynamics, we analyzed the mitochondrial fusion and fission protein levels in apoE4 and LRP5/6 co-expressed SH-SY5Y cells treated with DKK1. As shown in Figure 5-5A, we found a reduction in the elevated mitochondrial fission proteins Drp1 and Fis1 levels and an increase in the repressed mitochondrial

fusion protein Mfn2. Under the confocal microscopy, collapsed and fragmented mitochondria around the nucleus were seen in cells overexpressed with apoE4 and LRP5/6, whereas mitochondria in the SH-SY5Y cells treated with DKK1 remained filamentous and distributed across the cells (Figure 5-5B). FF and AR values showed that cells overexpressing apoE4 and LRP5/6 under the treatment of DKK1 have higher FF values (mean ± S.E.M, n=10) and AR values (mean ± S.E.M, n=10) as compared to cells without DKK1 treatment (Figure 5-5C).

(A)

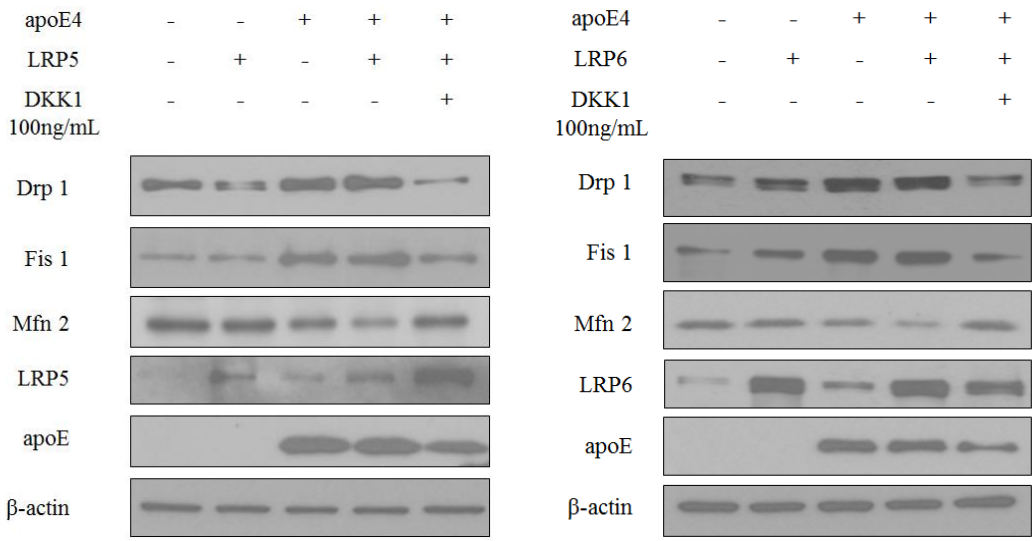

(B)

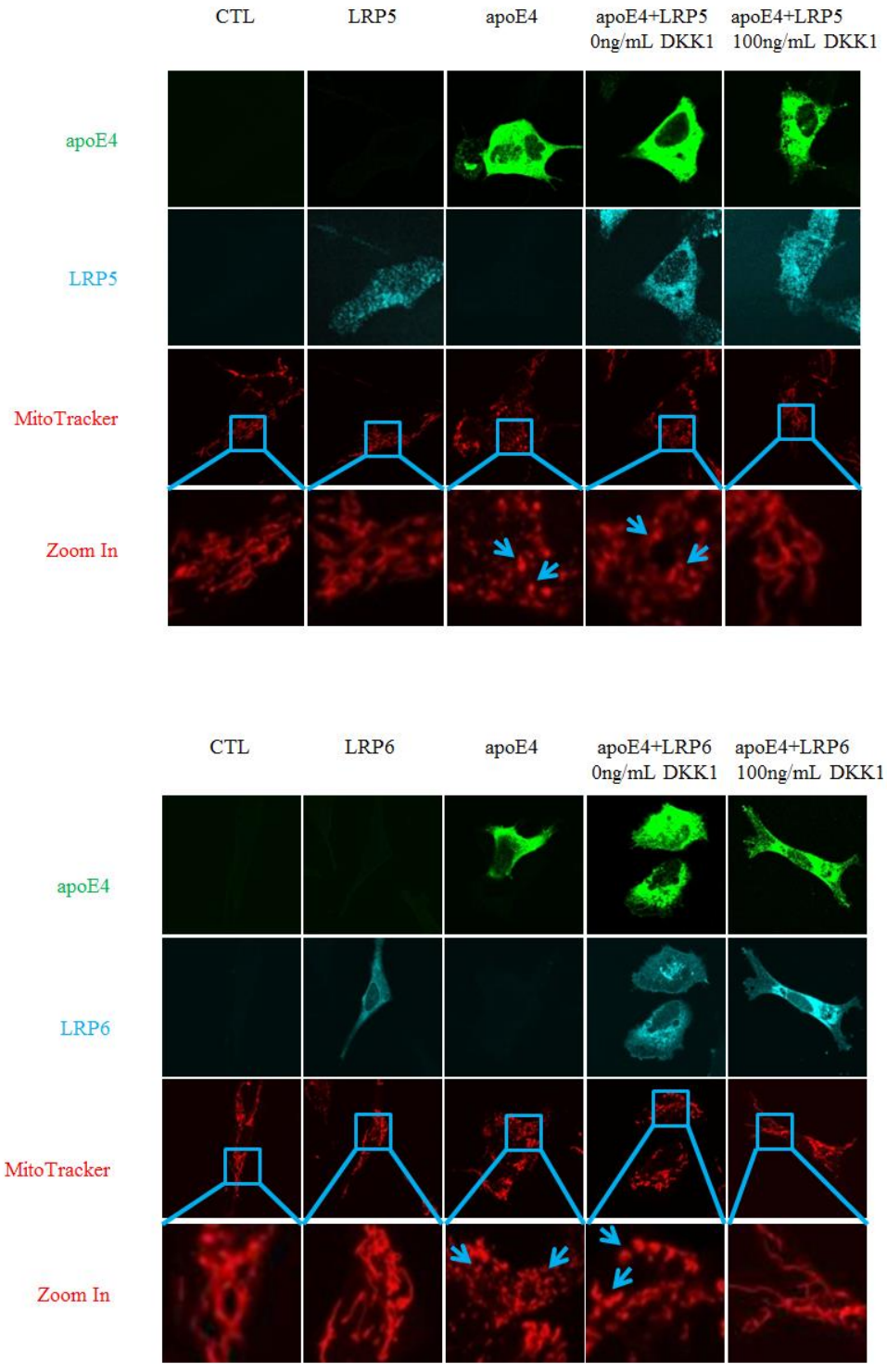
CTL
LRP5
apoE4
apoE4+LRP5 0ng/mL DKK1
apoE4+LRP5 100ng/mL DKK1
apoE4
LRP5
MitoTracker
Zoom In
CTL
LRP6
apoE4
apoE4+LRP6 0ng/mL DKK1
apoE4+LRP6 100ng/mL DKK1
apoE4
LRP6
MitoTracker
Zoom In

(C)

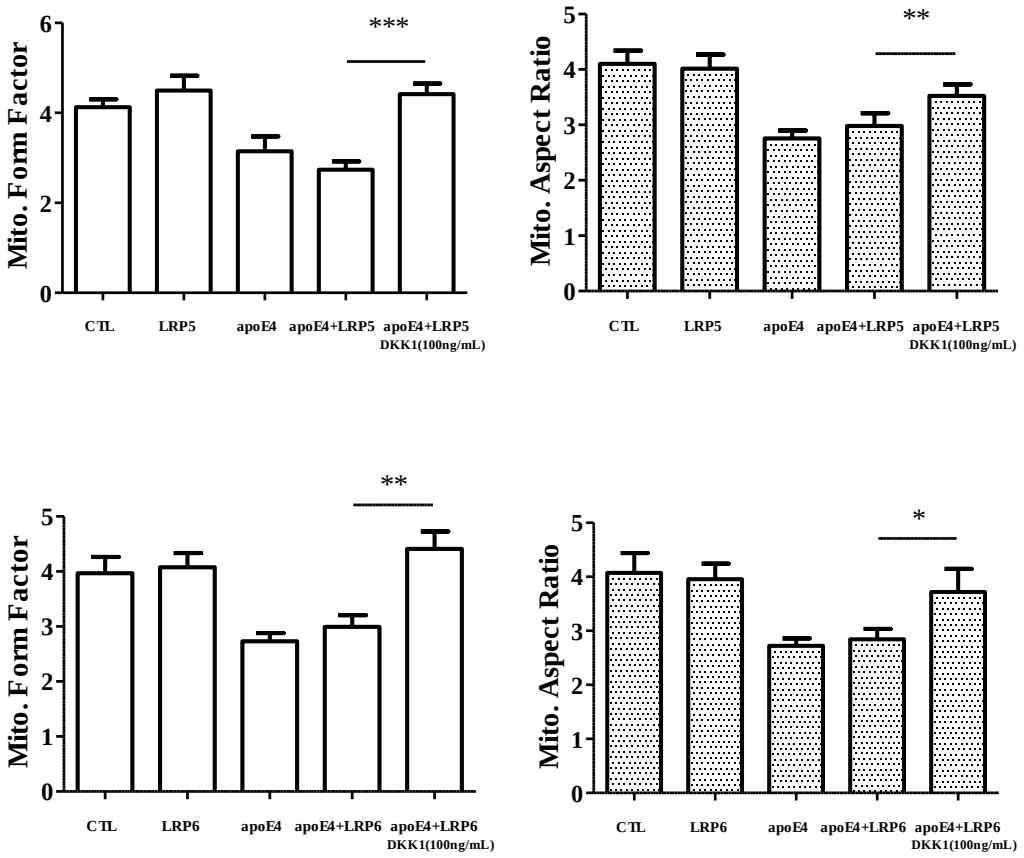

Figure 5-6. Dissociation of apoE4 and LRP5/6 restores perturbed mitochondrial dynamics back to normal. SH-SY5Y cells were co-transfected with apoE4 and LRP5/6 plasmids and treated with 0, 100ng/mL DKK1 for 24 hours. (A) Cell lysates were subjected to Western blotting assay, probing with specific antibodies for Drp1, Fis1, Mfn2, apoE, LRP5/6 and β-actin. (B) Cells were stained with MitoTracker Red CMXRos for 10 min before fixation with paraformaldehyde and permeabilization by TritonX-100. Samples were then probed with specific antibodies for apoE and LRP5/6, followed by secondary antibodies Alexa Fluor 488 goat anti-mouse IgG (recognizing apoE) and Chromeo™ 642 goat anti-rabbit IgG (recognizing LRP5/6). (C) AR values and FF values were calculated using Image J software shape distributor plugin to determine mitochondrial morphology. Data represented the average (n=10) ± S.E.M. and statistical significance was assessed with Student's t test (*$p<0.05$, **$p<0.01$, ***$p<0.001$).

5.3.6 Knockdown of LRP5/6 abolishes apoE4-induced disruption in mitochondrial dynamics

To confirm the functional role of LRP5/6 in apoE4-induced abnormalities in mitochondrial dynamics, we performed gene knockdown experiments using siRNA on apoE4 overexpressing SH-SY5Y cells. Confocal microscopy was performed to examine mitochondrial morphology. As expected, SH-SY5Y cells overexpressed with apoE4 possessed swollen and fragmented mitochondria clumped around nuclei. To eliminate the possibility that DKK1 itself affects mitochondrial morphology, we treated apoE4 overexpressing SH-SY5Y cells with 100ng/mL DKK1. As seen in Figure 5-6A, the morphology of mitochondria in cells overexpressing apoE4 under the treatment of DKK1 was similar to that of apoE4 transfected SH-SY5Y cells without DKK1 treatment, suggesting DKK1 did not affect mitochondrial dynamics. Silencing of LRP5 and LRP6, however, were able to elongate mitochondrial units and distribute mitochondria across the whole cells. Statistical analysis of FF and AR values showed that depletion of LRP5 and LRP6 in the cells overexpressed with apoE4 lowered FF (mean ± S.E.M., n=10) and AR (mean ± S.E.M, n=10) as compared to cells without LRP5/6 repression (Figure 5-6B).

(A)

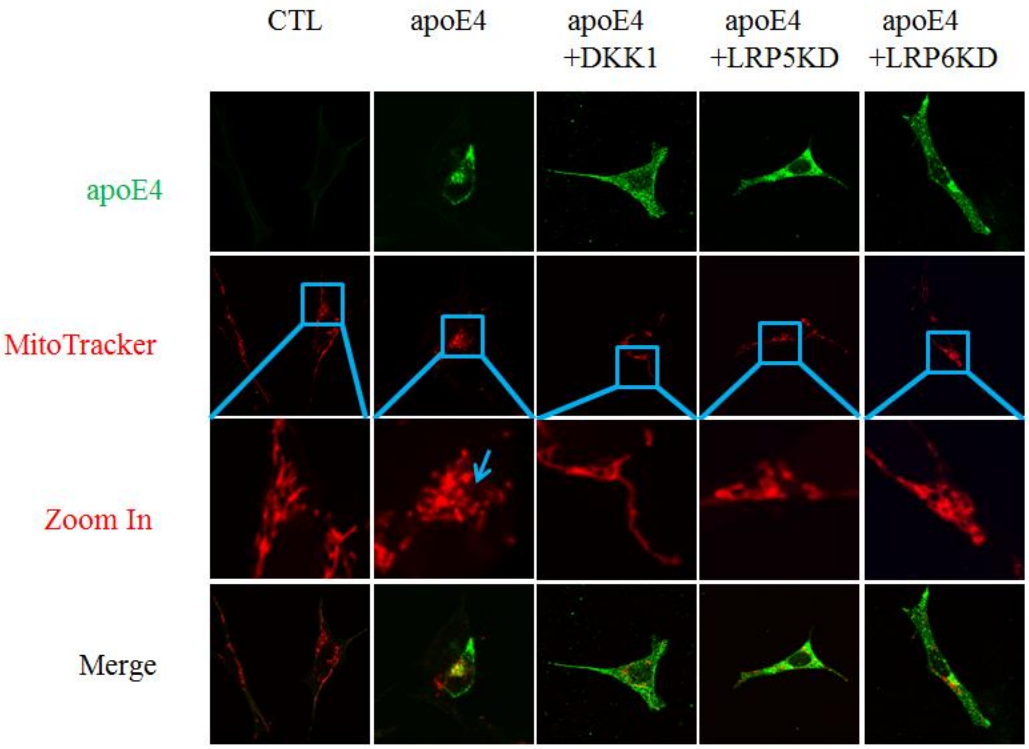

(B)

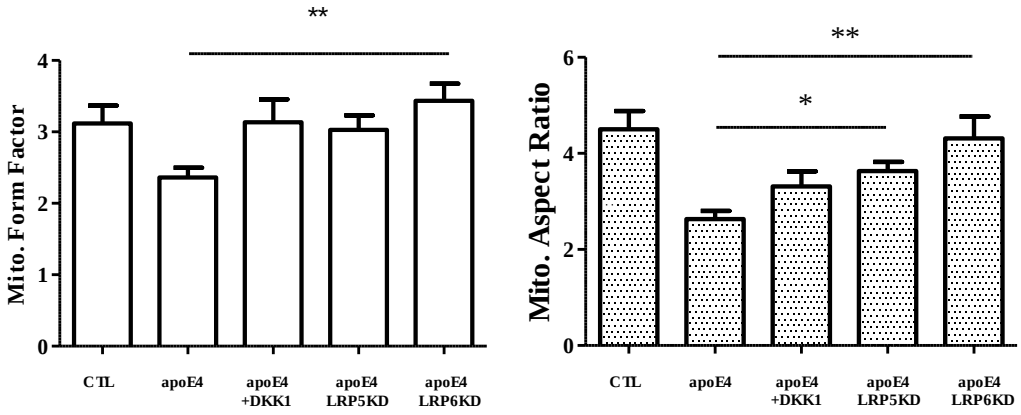

Figure 5-7. Knockdown of LRP5/6 abolishes apoE4-induced disruption in mitochondrial dynamics. (A) SH-SY5Y cells were co-transfected with apoE4 plasmid and LRP5/6 siRNA before stained with MitoTracker Red CMXRos. Cells overexpressed with empty vector, apoE4 alone or apoE4 followed by treatment of DKK1 were used as control groups. Samples were fixed with paraformaldehyde and permeabilized by TritonX-100. Cells were then probed with anti-apoE antibody and detected with Alexa Fluor 488 goat anti-mouse IgG. (B) AR values and FF values were calculated using Image J software shape distributor plugin to determine mitochondrial morphology. Data was presented as the average (n=10) ± S.E.M. and statistical significance was assessed

with one-way ANOVA with Dunnett's post-hoc analysis (*p<0.05, **p<0.01, ***p<0.001).

5.3.7 Overexpression of apoE4 does not affect mitochondrial transmembrane potential

In addition to mitochondrial morphology and size, mitochondrial dynamics also regulates mitochondrial functions. Studies have shown that the activities of mitochondrial complexes III and IV were affected in apoE4-induced toxicity [81]. Since complex III and IV are related to the maintenance of mitochondrial transmembrane potential, we examined the effect of apoE4 on mitochondria transmembrane potential. SH-SY5Y cells were transfected with apoE4 plasmids, followed by staining with JC-1 fluorescence dye, an indicator of mitochondrial transmembrane potential ($\Delta\Psi m$). The green JC-1 monomers selectively enter into mitochondria and reversibly form aggregates with intense red fluorescence in the healthy cells with high $\Delta\Psi m$. As expected, the treatment of STS induced a significant decrease in mitochondrial potential. On the other hand, there were no significance differences in JC-1 ratio (aggregates over monomers) when apoE4 was overexpressed (Figure 5-7A). To determine if the interaction between apoE4 and LRP5/6 could possibly affect mitochondrial transmembrane potential, we co-transfected apoE4 and LRP5/6 in SH-SY5Y cells, followed by the treatment of DKK1 to dissociate the interaction. As shown in Figure 5-7B, no significant changes in $\Delta\Psi m$ were observed among the treatment groups except for the positive control group STS.

(A)

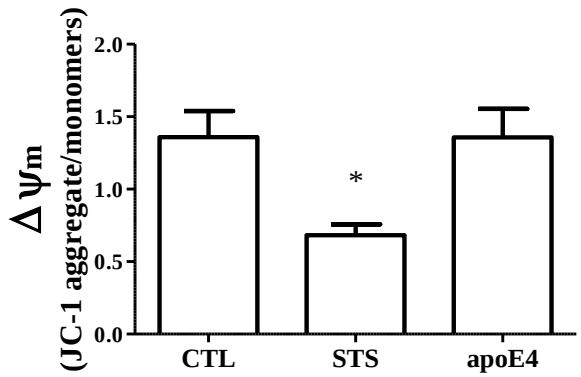

(B)

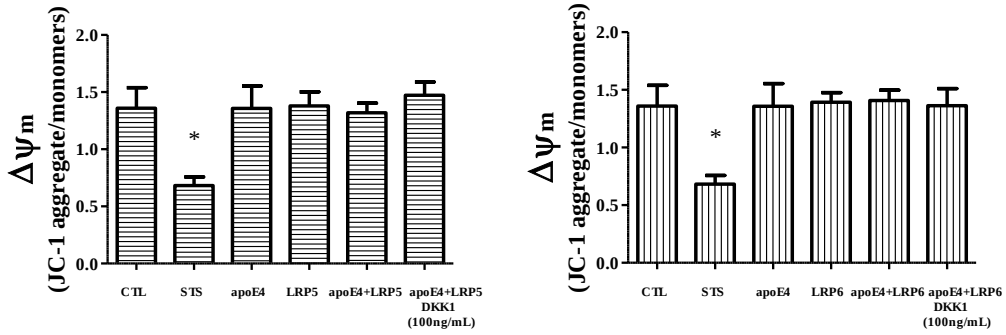

Figure 5-8. Overexpression of apoE4 does not affect mitochondrial transmembrane potential. (A) SH5Y cells were overexpressed with human wild type apoE4 plasmids or pCMV.vector, followed by incubation with JC-1 mitochondrial transmembrane potential dye. JC-1 ratio was obtained by dividing JC-1 aggregate fluorescence by monomer fluorescence. The treatment of 250nM STS for 8 hours was used as a positive control to indicate the decrease in JC-1 ratio. (B) SH-SY5Y cells were transfected with designated expression plasmids before incubation with JC-1 fluorescence dye. Data represented the average (n=10) ± S.E.M. and statistical significance was assessed with one-way ANOVA with Dunnett's post-hoc analysis (*$p<0.05$, **$p<0.01$, ***$p<0.001$).

5.4 Discussion

This study shows for the first time that apoE4 increases the levels of mitochondrial fission proteins Drp1 and Fis1 and decreases the level of mitochondrial fusion protein Mfn2. A subsequent elongated morphology of

mitochondria was observed, indicating unbalanced mitochondrial fusion and fission. We also report for the first time that apoE4 and its fragment bound to LRP5 and LRP6 *in vitro*. The interaction between apoE4 and LRP5/6 was disrupted by LRP5/6 inhibitor DKK1 in a dose-dependent manner. Furthermore, dissociation of apoE4 and LRP5/6 by DKK1 reduced the elevated Drp1 and Fis1 protein levels and increased the repressed protein level of Mfn2, leading to restoration of normal mitochondrial dynamics. However, neither apoE4 nor the interaction/dissociation between apoE4 and LRP5/6 affected mitochondrial transmembrane potential. Taken together, LRP5/6 acts as a receptor for apoE4 in causing abnormalities of mitochondrial fusion and fission.

Our findings suggest that apoE4 exerts its detrimental effect at least in part through perturbing mitochondrial dynamics. ApoE4 has been reported to induce mitochondrial dysfunction in AD patients [77]. Differential mitochondrial protein levels were seen in hippocampal tissue of apoE3 and apoE4 transgenic mice [84] as well as in apoE ε4 carriers and non-carriers [85]. However, no previous studies have implicated the role of apoE4 in mitochondrial fusion and fission, despite multiple lines of evidence indicating the mitochondrial dynamics to be perturbed in AD. Morphometric analysis revealed that mitochondria not only decreased in number but also enlarged in size in AD neurons [78]. The finding of enlarged and swollen mitochondria was also observed in AD cybrid cells [92] and fibroblasts from LOAD patients [106]. However, there are some discrepancies in the analysis of mitochondrial dynamics-related protein levels. Wang et al. reported a

significantly decreased level of Drp1 in 19.3% of sporadic AD fibroblasts along with elongated mitochondria accumulation in the perinuclear area [93]. The group also showed that an overexpression of wild-type Drp1 in the fibroblasts rescued mitochondrial abnormalities [93]. Moreover, studies with detailed immunoblot analysis indicated that the levels of Drp1, OPA1, Mfn1 and Mfn2 were significantly decreased whereas the level of Fis1 was increased in AD brain [107]. In contrast to the above reported studies, Manczak et al. showed an increased expression of Drp1 and a reduction in that of Mfn1 and Mfn2 in AD patients [203]. Our results reported that apoE4 increased the protein levels of Drp1 and Fis1 and decreased that of Mfn2, which corresponds to the observation in AD subjects made by Manczak et al. However, the link between apoE4 and mitochondrial dynamics-related protein levels has still yet to be verified with further studies using primary neurons and *in vivo* models. Although the mitochondrial protein levels have been analyzed, there are still some discrepancies regarding the effect of apoE4 on mitochondrial integrity. Chang et al. reported that mitochondrial potential and integrity was impaired by apoE4 through the lipid- and receptor-binding regions [80]. However, the studies by Nakamura et al. showed that overexpression of apoE4 had no effects on $\Delta\Psi m$ [81]. Supporting the observation in the latter study, our results showed that the presence of apoE4 did not affect $\Delta\Psi m$. Whether other mitochondrial functions are affected as a result of abnormal mitochondrial dynamics induced by apoE4, will require additional mitochondrial functional studies to be performed.

Although we have identified apoE4-mediated changes in the mitochondrial morphology and disruptions in mitochondrial dynamics related protein levels, the mechanism underlying these abnormalities remains unclear. One possible pathway may be through binding to its receptors, members of LDL receptor family. Up till now, only two members of the family, LRP1 and LRP6, have been reported to genetically associate with AD. The polymorphism of LRP1 is a minor risk factor for AD [169,204], whereas LRP6 polymorphism *Val1062* has been reported to act synergistically with apoE4 ε4 allele [140]. Our study confirmed the direct interaction between apoE4 and LRP5/6 at the protein levels. Using DKK1 as an inhibitor to dissociate the binding, we were able to restore the disrupted levels of mitochondrial dynamics-related proteins and altered mitochondrial morphology back to normal. However, neither the interaction nor the dissociation between apoE4 and LRP5/6 showed any significant effects on mitochondrial transmembrane potential. Taken together, our study shows that apoE4 dysregulates mitochondrial fusion and fission processes via binding to LRP5 and LRP6.

5.5 Conclusion

To summarize, results in this chapter showed for the first time that apoE4 carries out its detrimental effect in neuronal cells through disrupting mitochondrial dynamics and this process is regulated by LRP5/6. With the increasingly important role of mitochondria in neurobiology and AD physiopathology,

dissociating the interaction between apoE4 and LRP5/6 could be explored as the potential therapeutic strategy for inhibiting apoE4-induced pathology in AD.

CHAPTER 6. CONCLUSION AND FUTURE PERSPECTIVES

The overall goal of this thesis was to understand the functional role of LRP5 and LRP6 in the pathology and etiology of AD. To achieve the overall goal, we proposed two hypotheses to investigate the potential implication of these two proteins in the mechanism of AD with neuronal cell lines.

In Chapter 3, we addressed **the first hypothesis** wherein we reported that overexpression of LRP5 and LRP6 has a neuroprotective role in improving cell survival and reducing tau phosphorylation in neuronal cells. In Aim 1, we showed that overexpression of LRP5 and LRP6 upregulated Wnt activity. As a result, mRNA levels of proliferative markers Axin2 and Cyclin D1 were significantly increased with LRP5 and LRP6 overexpression in SH-SY5Y cells treated with Wnt3a ligands. In contrast, Wnt activity was significantly decreased in LRP5- and 6- knockdown cells respectively. For the transcription of downstream survival genes Axin2 and Cyclin D1, mRNA levels were significantly downregulated with LRP5 and LRP6 repression. Moreover in Aim 2, we reported that LRP5 and LRP6 overexpression were able to ameliorate hydrogen peroxide-mediated cytotoxicity at all concentrations used. The protective role of LRP5 and LRP6 was further confirmed by reduced Sub G0/G1 apoptotic population. We also observed decreased levels of cleaved caspase 3 and 7 in the LRP5- and 6-overexpressed cells. Lastly in Aim 3, LRP5 and LRP6 overexpression reduced

GSK3β activity and decreased phosphorylated tau protein. Thus, we have successfully proven our hypothesis that overexpression of LRP5 and LRP6 protects neuronal cell from cytotoxicity induced by hydrogen peroxide and reduces tau phosphorylation in SH-SY5Y cells.

The present work has raised several issues to be pursued in future investigations. We demonstrated that overexpression of LRP5 and LRP6 protected SH-SY5Y cells from oxidative stress-induced cell death. Although implicated in the pathogenesis of AD, oxidative stress has been suggested to result from Aβ aggregation. The accumulation of Aβ in the brain has been widely accepted to be one of the possible causes for neurodegeneration in AD. In the present study, the attempt to establish AD cell model with Aβ challenge was not successful with no significant cell death. Despite hydrogen peroxide was used as an alternative, Aβ challenge provides a more suitable AD model. Therefore, one future direction could be to optimize and establish Aβ-challenged AD model. In addition, given that the Wnt signaling pathway is involved in normal cell growth, continuous activation of this signaling pathway may result in excessive neuronal stimulation, probably leading to tumorigenesis. Thus, it would be a potential challenge to ensure the selectivity of therapeutic strategies against pathological cells specifically to avoid tumorigenic side effects of overstimulating Wnt pathway. The findings in Chapter 3 suggested that modulating Wnt signaling through overexpression of LRP5 and LRP6 is a promising approach for AD therapy.

However, this hypothesis has only been proven in human neuroblastoma SH-SY5Y cells. Future studies with a wider range of neuroblastoma cell lines, primary neurons harvested from transgenic mice and AD patient cell samples are required to confirm and supplement our findings to better clarify the potential of LRP5 and LRP6 as therapeutic targets. Furthermore, despite our *in vitro* experiments showed some encouraging results, the *in vivo* efficacy of this approach needs to be confirmed in AD transgenic mouse models.

In Chapter 4 and 5 (discussing **the second hypothesis**), we evaluated the interactions of apoE isoforms with LRP5/6 and apoE4-mediated abnormalities in mitochondrial dynamics. In Aim 1, we detected the presence of LRP5 and LRP6 in the protein complex pulled down by apoE antibody, which indicated the interaction between LRP5/6 and apoE4 in both HEK293T and SH-SY5Y cells. Moreover, the interaction between apoE isoforms and LRP5 abolished the activation ability of LRP5 and exerted isoform-specific effects on GSK3β activity. In Aim 2, our results indicated that overexpression of apoE4 increased the protein levels of mitochondrial fission proteins Drp1 and Fis1 and reduced that of mitochondrial fusion protein Mfn2 compared to SH-SY5Y cells overexpressing empty vector. Under the confocal microscope, cells overexpressing apoE4 were observed to present short tubules and clumps of tangled mitochondria surrounding the nucleus, in contrast to the normal mitochondria with a combination of short and long filament-like structures distributed throughout the cell. The presence of

clumps and fragmented mitochondria indicated an imbalance in mitochondrial fusion and fission. Furthermore in Aim 3, we identified that the Wnt antagonist DKK1 dissociated the binding between apoE4 and the two receptors in a dose-dependent manner. With the treatment of DKK1, we observed that the disrupted mitochondrial morphology was restored back to filamentous structures distributed across the cells and the degree of mitochondrial clustering was less intense as compared to those without treatment. Hence, our results have proven that apoE4 alters mitochondrial dynamics through binding to LRP5/6.

In Chapter 4, we only showed the binding of apoE isoforms and their effects on Wnt signaling as well as GSK3β activity, with LRP5 in neuronal cells. The binding ability of LRP6 and the effects on Wnt signaling needs to be evaluated with further studies. In addition, Cedazo-Minguez et al. reported that the effect of apoE3 and apoE4 on GSK3β activity is time-dependent [173]. Thus, the effect of interaction between apoE isoforms and LRP5/6 in regulating GSK3β activity and tau phosphorylation should be evaluated at different time points. The present study focused on evaluating the effect of apoE isoforms on Wnt activity or GSK3β by transfecting cells with expression plasmids encoding for the three isotypes. Since apoE proteins are mainly secreted by astrocytes and target the receptors on neurons in the physiological condition, a more relevant model of future studies on the mechanism would be to treat neuronal cells with medium collected from astrocyte transfecting with apoE isoforms. In Chapter 5, our

findings indicated that apoE4 caused the imbalance in mitochondrial fusion and fission processes through binding to LRP5 and LRP6. However, the effect of the interaction between other apoE isoforms and LRP5/6 on mitochondrial dynamics still remains unclear. Questions such as whether apoE2/3 carries out beneficial effects in maintaining mitochondrial dynamics and the role of the interaction between apoE2/3 and LRP5/6 on this beneficial effect should be addressed in order to have a better understanding of the differential effects of apoE isoforms in AD. In addition, in this chapter we reported that dissociation of apoE4 and LRP5/6 with LRP5/6 antagonist DKK1 restores the disturbance in mitochondrial dynamics. Another approach to disrupt the interaction is to identify an apoE4 antagonist to free up apoE4 bound LRP5/6, abolishing the detrimental effect on mitochondrial dynamics. Moreover, despite aberrantly regulated mitochondrial functions being repeatedly associated with AD in neuronal cells as well as AD patient samples [81,83], the underlying mechanism has not been fully understood. Our preliminary results failed to show that the interaction between apoE4 and LRP5/6 had any significant effect on mitochondrial transmembrane potential. This may possibly be due to the lack of optimization in transfection and treatment duration or because this interaction is involved in the early stage of mitochondrial dysfunction. Thus, an optimized study needs to be conducted to assess the effect of this interaction on mitochondria integrity. Lastly, the unique conformation of apoE4 makes it more susceptible to misfolding and instability, resulting in proteolysis and the generation of neurotoxic apoE fragment to a greater extent than other apoE isoforms, which has been reported to be involved in

mitochondrial dysfunction, cytoskeletal alterations and neuronal cell death [80,81]. Our results showed that apoE4 fragment also bound to LRP5/6. However, the involvement of apoE4 fragment in the downstream detrimental effect on mitochondrial dynamics needs to be confirmed with the evaluation of mitochondrial dynamics related protein levels and mitochondrial morphology. Moreover, whether this interaction is involved in the internalization and cleavage of apoE4 into fragment requires further studies to quantify the fragment under the treatment of DKK1.

The results from Chapter 5 might seem to be discrepant with the beneficial effect of LRP5/6 concluded from Chapter 3. However, in Chapter 3 the beneficial effect of LRP5 was observed in the presence of exogenous Wnt3a ligands, but not apoE4. In addition, the endogenous apoE levels were beyond limit of detection, suggesting the effect of endogenous apoE proteins are marginal compared with that of exogenous Wnt3a ligands. In Chapter 5, when both apoE4 and LRP5 were overexpressed, LRP5 was occupied by apoE4 with no presence of exogenous Wnt3a ligands. The beneficial effect of endogenous Wnt3a on LRP5 was masked by the detrimental effect of exogenous apoE4 on LRP5. Therefore, it is likely that LRP5 has a dual role, beneficial to neuronal cell survival with the presence of Wnt3a but toxic when interacting with apoE4.

In conclusion, the findings of this thesis have not only helped in identifying the dual functional role of Wnt co-receptors LRP5 and LRP6 in AD, but have also indicated that LRP5 and LRP6 could be explored and developed as novel therapeutic targets for AD.

BIBLIOGRAPHY

1. Berchtold NC, Cotman CW (1998) Evolution in the conceptualization of dementia and Alzheimer's disease: Greco-Roman period to the 1960s. Neurobiol Aging 19: 173-189.

2. Goate A, Chartier-Harlin MC, Mullan M, Brown J, Crawford F, et al. (1991) Segregation of a missense mutation in the amyloid precursor protein gene with familial Alzheimer's disease. Nature 349: 704-706.

3. Selkoe DJ (1998) The cell biology of beta-amyloid precursor protein and presenilin in Alzheimer's disease. Trends Cell Biol 8: 447-453.

4. Shankar GM, Walsh DM (2009) Alzheimer's disease: synaptic dysfunction and Abeta. Mol Neurodegener 4: 48.

5. Bloom GS (2014) Amyloid-beta and tau: the trigger and bullet in Alzheimer disease pathogenesis. JAMA Neurol 71: 505-508.

6. Thies W, Bleiler L (2013) 2013 Alzheimer's disease facts and figures. Alzheimers Dement 9: 208-245.

7. Bartus RT, Dean RL, 3rd, Beer B, Lippa AS (1982) The cholinergic hypothesis of geriatric memory dysfunction. Science 217: 408-414.

8. Cummings JL, Back C (1998) The cholinergic hypothesis of neuropsychiatric symptoms in Alzheimer's disease. Am J Geriatr Psychiatry 6: S64-78.

9. Francis PT, Palmer AM, Snape M, Wilcock GK (1999) The cholinergic hypothesis of Alzheimer's disease: a review of progress. J Neurol Neurosurg Psychiatry 66: 137-147.

10. Birks J (2006) Cholinesterase inhibitors for Alzheimer's disease. Cochrane Database Syst Rev: CD005593.

11. McShane R, Areosa Sastre A, Minakaran N (2006) Memantine for dementia. Cochrane Database Syst Rev: CD003154.

12. Myhrer T (1998) Adverse psychological impact, glutamatergic dysfunction, and risk factors for Alzheimer's disease. Neurosci Biobehav Rev 23: 131-139.

13. Galimberti D, Scarpini E (2011) Disease-modifying treatments for Alzheimer's disease. Ther Adv Neurol Disord 4: 203-216.

14. Chiang K, Koo EH (2014) Emerging therapeutics for Alzheimer's disease. Annu Rev Pharmacol Toxicol 54: 381-405.

15. Gauthier S, Aisen PS, Ferris SH, Saumier D, Duong A, et al. (2009) Effect of tramiprosate in patients with mild-to-moderate Alzheimer's disease: exploratory analyses of the MRI sub-group of the Alphase study. J Nutr Health Aging 13: 550-557.

16. Bilikiewicz A, Gaus W (2004) Colostrinin (a naturally occurring, proline-rich, polypeptide mixture) in the treatment of Alzheimer's disease. J Alzheimers Dis 6: 17-26.

17. Salloway S, Sperling R, Keren R, Porsteinsson AP, van Dyck CH, et al. (2011) A phase 2 randomized trial of ELND005, scyllo-inositol, in mild to moderate Alzheimer disease. Neurology 77: 1253-1262.

18. Faux NG, Ritchie CW, Gunn A, Rembach A, Tsatsanis A, et al. (2010) PBT2 rapidly improves cognition in Alzheimer's Disease: additional phase II analyses. J Alzheimers Dis 20: 509-516.

19. Siemers E, Skinner M, Dean RA, Gonzales C, Satterwhite J, et al. (2005) Safety, tolerability, and changes in amyloid beta concentrations after administration of a gamma-secretase inhibitor in volunteers. Clin Neuropharmacol 28: 126-132.

20. Imbimbo BP, Giardina GA (2011) gamma-secretase inhibitors and modulators for the treatment of Alzheimer's disease: disappointments and hopes. Curr Top Med Chem 11: 1555-1570.

21. Tong G, Wang JS, Sverdlov O, Huang SP, Slemmon R, et al. (2012) Multicenter, randomized, double-blind, placebo-controlled, single-ascending dose study of the oral gamma-secretase inhibitor BMS-708163 (Avagacestat): tolerability profile, pharmacokinetic parameters, and pharmacodynamic markers. Clin Ther 34: 654-667.

22. Vellas B, Sol O, Snyder PJ, Ousset PJ, Haddad R, et al. (2011) EHT0202 in Alzheimer's disease: a 3-month, randomized, placebo-controlled, double-blind study. Curr Alzheimer Res 8: 203-212.

23. Gilman S, Koller M, Black RS, Jenkins L, Griffith SG, et al. (2005) Clinical effects of Abeta immunization (AN1792) in patients with AD in an interrupted trial. Neurology 64: 1553-1562.

24. Brody DL, Holtzman DM (2008) Active and passive immunotherapy for neurodegenerative disorders. Annu Rev Neurosci 31: 175-193.

25. Wisniewski T, Konietzko U (2008) Amyloid-beta immunisation for Alzheimer's disease. Lancet Neurol 7: 805-811.

26. Dodel R, Neff F, Noelker C, Pul R, Du Y, et al. (2010) Intravenous immunoglobulins as a treatment for Alzheimer's disease: rationale and current evidence. Drugs 70: 513-528.

27. Gura T (2008) Hope in Alzheimer's fight emerges from unexpected places. Nat Med 14: 894.

28. Martinez A, Perez DI (2008) GSK-3 inhibitors: a ray of hope for the treatment of Alzheimer's disease? J Alzheimers Dis 15: 181-191.

29. Griffin WS (2006) Inflammation and neurodegenerative diseases. Am J Clin Nutr 83: 470S-474S.

30. Reddy VP, Zhu X, Perry G, Smith MA (2009) Oxidative stress in diabetes and Alzheimer's disease. J Alzheimers Dis 16: 763-774.

31. Adlard PA, Bush AI (2006) Metals and Alzheimer's disease. J Alzheimers Dis 10: 145-163.

32. Gamba P, Testa G, Sottero B, Gargiulo S, Poli G, et al. (2012) The link between altered cholesterol metabolism and Alzheimer's disease. Ann N Y Acad Sci 1259: 54-64.

33. Bertram L, Lill CM, Tanzi RE (2010) The genetics of Alzheimer disease: back to the future. Neuron 68: 270-281.

34. Genin E, Hannequin D, Wallon D, Sleegers K, Hiltunen M, et al. (2011) APOE and Alzheimer disease: a major gene with semi-dominant inheritance. Mol Psychiatry 16: 903-907.

35. Wilson CA, Doms RW, Lee VM (1999) Intracellular APP processing and A beta production in Alzheimer disease. J Neuropathol Exp Neurol 58: 787-794.

36. Haass C, Hung AY, Schlossmacher MG, Teplow DB, Selkoe DJ (1993) beta-Amyloid peptide and a 3-kDa fragment are derived by distinct cellular mechanisms. J Biol Chem 268: 3021-3024.

37. Hardy JA, Higgins GA (1992) Alzheimer's disease: the amyloid cascade hypothesis. Science 256: 184-185.

38. Hong-Qi Y, Zhi-Kun S, Sheng-Di C (2012) Current advances in the treatment of Alzheimer's disease: focused on considerations targeting Abeta and tau. Transl Neurodegener 1: 21.

39. Yu JT, Tan L, Hardy J (2014) Apolipoprotein E in Alzheimer's disease: an update. Annu Rev Neurosci 37: 79-100.

40. Farrer LA, Cupples LA, Haines JL, Hyman B, Kukull WA, et al. (1997) Effects of age, sex, and ethnicity on the association between apolipoprotein E genotype and Alzheimer disease. A meta-analysis. APOE and Alzheimer Disease Meta Analysis Consortium. JAMA 278: 1349-1356.

41. Van Den Heuvel C, Thornton E, Vink R (2007) Traumatic brain injury and Alzheimer's disease: a review. Prog Brain Res 161: 303-316.

42. Rosendorff C, Beeri MS, Silverman JM (2007) Cardiovascular risk factors for Alzheimer's disease. Am J Geriatr Cardiol 16: 143-149.

43. Sharp ES, Gatz M (2011) Relationship between education and dementia: an updated systematic review. Alzheimer Dis Assoc Disord 25: 289-304.

44. Barnes DE, Yaffe K (2011) The projected effect of risk factor reduction on Alzheimer's disease prevalence. Lancet Neurol 10: 819-828.

45. Liu CC, Kanekiyo T, Xu H, Bu G (2013) Apolipoprotein E and Alzheimer disease: risk, mechanisms and therapy. Nat Rev Neurol 9: 106-118.

46. Mahley RW (1988) Apolipoprotein E: cholesterol transport protein with expanding role in cell biology. Science 240: 622-630.

47. Weisgraber KH (1994) Apolipoprotein E: structure-function relationships. Adv Protein Chem 45: 249-302.

48. Pitas RE, Boyles JK, Lee SH, Foss D, Mahley RW (1987) Astrocytes synthesize apolipoprotein E and metabolize apolipoprotein E-containing lipoproteins. Biochim Biophys Acta 917: 148-161.

49. Grehan S, Tse E, Taylor JM (2001) Two distal downstream enhancers direct expression of the human apolipoprotein E gene to astrocytes in the brain. J Neurosci 21: 812-822.

50. Xu PT, Schmechel D, Qiu HL, Herbstreith M, Rothrock-Christian T, et al. (1999) Sialylated human apolipoprotein E (apoEs) is preferentially associated with neuron-enriched cultures from APOE transgenic mice. Neurobiol Dis 6: 63-75.

51. Xu Q, Bernardo A, Walker D, Kanegawa T, Mahley RW, et al. (2006) Profile and regulation of apolipoprotein E (ApoE) expression in the CNS in mice with targeting of green fluorescent protein gene to the ApoE locus. J Neurosci 26: 4985-4994.

52. Nickerson DA, Taylor SL, Fullerton SM, Weiss KM, Clark AG, et al. (2000) Sequence diversity and large-scale typing of SNPs in the human apolipoprotein E gene. Genome Res 10: 1532-1545.

53. Mahley RW, Rall SC, Jr. (2000) Apolipoprotein E: far more than a lipid transport protein. Annu Rev Genomics Hum Genet 1: 507-537.

54. Mahley RW, Huang Y, Rall SC, Jr. (1999) Pathogenesis of type III hyperlipoproteinemia (dysbetalipoproteinemia). Questions, quandaries, and paradoxes. J Lipid Res 40: 1933-1949.

55. Weisgraber KH (1990) Apolipoprotein E distribution among human plasma lipoproteins: role of the cysteine-arginine interchange at residue 112. J Lipid Res 31: 1503-1511.

56. Morrow JA, Hatters DM, Lu B, Hochtl P, Oberg KA, et al. (2002) Apolipoprotein E4 forms a molten globule. A potential basis for its association with disease. J Biol Chem 277: 50380-50385.

57. Mahley RW, Huang Y (1999) Apolipoprotein E: from atherosclerosis to Alzheimer's disease and beyond. Curr Opin Lipidol 10: 207-217.

58. Huang Y, Weisgraber KH, Mucke L, Mahley RW (2004) Apolipoprotein E: diversity of cellular origins, structural and biophysical properties, and effects in Alzheimer's disease. J Mol Neurosci 23: 189-204.

59. Buttini M, Orth M, Bellosta S, Akeefe H, Pitas RE, et al. (1999) Expression of human apolipoprotein E3 or E4 in the brains of Apoe-/- mice: isoform-specific effects on neurodegeneration. J Neurosci 19: 4867-4880.

60. Nathan BP, Bellosta S, Sanan DA, Weisgraber KH, Mahley RW, et al. (1994) Differential effects of apolipoproteins E3 and E4 on neuronal growth in vitro. Science 264: 850-852.

61. Nathan BP, Chang KC, Bellosta S, Brisch E, Ge N, et al. (1995) The inhibitory effect of apolipoprotein E4 on neurite outgrowth is associated with microtubule depolymerization. J Biol Chem 270: 19791-19799.

62. Holtzman DM, Pitas RE, Kilbridge J, Nathan B, Mahley RW, et al. (1995) Low density lipoprotein receptor-related protein mediates apolipoprotein E-dependent neurite outgrowth in a central nervous system-derived neuronal cell line. Proc Natl Acad Sci U S A 92: 9480-9484.

63. Reiman EM, Chen K, Liu X, Bandy D, Yu M, et al. (2009) Fibrillar amyloid-beta burden in cognitively normal people at 3 levels of genetic risk for Alzheimer's disease. Proc Natl Acad Sci U S A 106: 6820-6825.

64. Bales KR, Liu F, Wu S, Lin S, Koger D, et al. (2009) Human APOE isoform-dependent effects on brain beta-amyloid levels in PDAPP transgenic mice. J Neurosci 29: 6771-6779.

65. Castellano JM, Kim J, Stewart FR, Jiang H, DeMattos RB, et al. (2011) Human apoE isoforms differentially regulate brain amyloid-beta peptide clearance. Sci Transl Med 3: 89ra57.

66. Tai LM, Bilousova T, Jungbauer L, Roeske SK, Youmans KL, et al. (2013) Levels of soluble apolipoprotein E/amyloid-beta (Abeta) complex are reduced and oligomeric Abeta increased with APOE4 and Alzheimer disease in a transgenic mouse model and human samples. J Biol Chem 288: 5914-5926.

67. Ye S, Huang Y, Mullendorff K, Dong L, Giedt G, et al. (2005) Apolipoprotein (apo) E4 enhances amyloid beta peptide production in cultured neuronal cells: apoE structure as a potential therapeutic target. Proc Natl Acad Sci U S A 102: 18700-18705.

68. Sadowski MJ, Pankiewicz J, Scholtzova H, Mehta PD, Prelli F, et al. (2006) Blocking the apolipoprotein E/amyloid-beta interaction as a potential therapeutic approach for Alzheimer's disease. Proc Natl Acad Sci U S A 103: 18787-18792.

69. Jiang Q, Lee CY, Mandrekar S, Wilkinson B, Cramer P, et al. (2008) ApoE promotes the proteolytic degradation of Abeta. Neuron 58: 681-693.

70. Ji ZS, Mullendorff K, Cheng IH, Miranda RD, Huang Y, et al. (2006) Reactivity of apolipoprotein E4 and amyloid beta peptide: lysosomal stability and neurodegeneration. J Biol Chem 281: 2683-2692.

71. Brecht WJ, Harris FM, Chang S, Tesseur I, Yu GQ, et al. (2004) Neuron-specific apolipoprotein e4 proteolysis is associated with increased tau phosphorylation in brains of transgenic mice. J Neurosci 24: 2527-2534.

72. Tesseur I, Van Dorpe J, Spittaels K, Van den Haute C, Moechars D, et al. (2000) Expression of human apolipoprotein E4 in neurons causes hyperphosphorylation of protein tau in the brains of transgenic mice. Am J Pathol 156: 951-964.

73. Tesseur I, Van Dorpe J, Bruynseels K, Bronfman F, Sciot R, et al. (2000) Prominent axonopathy and disruption of axonal transport in transgenic mice expressing human apolipoprotein E4 in neurons of brain and spinal cord. Am J Pathol 157: 1495-1510.

74. Bennett RE, Esparza TJ, Lewis HA, Kim E, Mac Donald CL, et al. (2013) Human apolipoprotein E4 worsens acute axonal pathology but not amyloid-beta immunoreactivity after traumatic brain injury in 3xTG-AD mice. J Neuropathol Exp Neurol 72: 396-403.

75. Strittmatter WJ, Saunders AM, Goedert M, Weisgraber KH, Dong LM, et al. (1994) Isoform-specific interactions of apolipoprotein E with microtubule-associated protein tau: implications for Alzheimer disease. Proc Natl Acad Sci U S A 91: 11183-11186.

76. Kamino K, Nagasaka K, Imagawa M, Yamamoto H, Yoneda H, et al. (2000) Deficiency in mitochondrial aldehyde dehydrogenase increases the risk for late-onset Alzheimer's disease in the Japanese population. Biochem Biophys Res Commun 273: 192-196.

77. Gibson GE, Haroutunian V, Zhang H, Park LC, Shi Q, et al. (2000) Mitochondrial damage in Alzheimer's disease varies with apolipoprotein E genotype. Ann Neurol 48: 297-303.

78. Hirai K, Aliev G, Nunomura A, Fujioka H, Russell RL, et al. (2001) Mitochondrial abnormalities in Alzheimer's disease. J Neurosci 21: 3017-3023.

79. Mahley RW, Hui DY, Innerarity TL, Beisiegel U (1989) Chylomicron remnant metabolism. Role of hepatic lipoprotein receptors in mediating uptake. Arteriosclerosis 9: I14-18.

80. Chang S, ran Ma T, Miranda RD, Balestra ME, Mahley RW, et al. (2005) Lipid- and receptor-binding regions of apolipoprotein E4 fragments act in concert to cause mitochondrial dysfunction and neurotoxicity. Proc Natl Acad Sci U S A 102: 18694-18699.

81. Nakamura T, Watanabe A, Fujino T, Hosono T, Michikawa M (2009) Apolipoprotein E4 (1-272) fragment is associated with mitochondrial proteins and affects mitochondrial function in neuronal cells. Mol Neurodegener 4: 35.

82. Chen HK, Ji ZS, Dodson SE, Miranda RD, Rosenblum CI, et al. (2011) Apolipoprotein E4 domain interaction mediates detrimental effects on mitochondria and is a potential therapeutic target for Alzheimer disease. J Biol Chem 286: 5215-5221.

83. Valla J, Schneider L, Niedzielko T, Coon KD, Caselli R, et al. (2006) Impaired platelet mitochondrial activity in Alzheimer's disease and mild cognitive impairment. Mitochondrion 6: 323-330.

84. James R, Searcy JL, Le Bihan T, Martin SF, Gliddon CM, et al. (2012) Proteomic analysis of mitochondria in APOE transgenic mice and in response to an ischemic challenge. J Cereb Blood Flow Metab 32: 164-176.

85. Conejero-Goldberg C, Hyde TM, Chen S, Dreses-Werringloer U, Herman MM, et al. (2011) Molecular signatures in post-mortem brain tissue of younger individuals at high risk for Alzheimer's disease as based on APOE genotype. Mol Psychiatry 16: 836-847.

86. Miyata M, Smith JD (1996) Apolipoprotein E allele-specific antioxidant activity and effects on cytotoxicity by oxidative insults and beta-amyloid peptides. Nat Genet 14: 55-61.

87. Lin MT, Beal MF (2006) Mitochondrial dysfunction and oxidative stress in neurodegenerative diseases. Nature 443: 787-795.

88. Small GW, Mazziotta JC, Collins MT, Baxter LR, Phelps ME, et al. (1995) Apolipoprotein E type 4 allele and cerebral glucose metabolism in relatives at risk for familial Alzheimer disease. JAMA 273: 942-947.

89. Small GW, Ercoli LM, Silverman DH, Huang SC, Komo S, et al. (2000) Cerebral metabolic and cognitive decline in persons at genetic risk for Alzheimer's disease. Proc Natl Acad Sci U S A 97: 6037-6042.

90. Reiman EM, Caselli RJ, Chen K, Alexander GE, Bandy D, et al. (2001) Declining brain activity in cognitively normal apolipoprotein E epsilon 4 heterozygotes: A foundation for using positron emission tomography to efficiently test treatments to prevent Alzheimer's disease. Proc Natl Acad Sci U S A 98: 3334-3339.

91. Reiman EM, Chen K, Alexander GE, Caselli RJ, Bandy D, et al. (2004) Functional brain abnormalities in young adults at genetic risk for late-onset Alzheimer's dementia. Proc Natl Acad Sci U S A 101: 284-289.

92. Trimmer PA, Swerdlow RH, Parks JK, Keeney P, Bennett JP, Jr., et al. (2000) Abnormal mitochondrial morphology in sporadic Parkinson's and Alzheimer's disease cybrid cell lines. Exp Neurol 162: 37-50.

93. Wang X, Su B, Siedlak SL, Moreira PI, Fujioka H, et al. (2008) Amyloid-beta overproduction causes abnormal mitochondrial dynamics via differential modulation of mitochondrial fission/fusion proteins. Proc Natl Acad Sci U S A 105: 19318-19323.

94. Twig G, Elorza A, Molina AJ, Mohamed H, Wikstrom JD, et al. (2008) Fission and selective fusion govern mitochondrial segregation and elimination by autophagy. EMBO J 27: 433-446.

95. Chen H, Vermulst M, Wang YE, Chomyn A, Prolla TA, et al. (2010) Mitochondrial fusion is required for mtDNA stability in skeletal muscle and tolerance of mtDNA mutations. Cell 141: 280-289.

96. Chen H, Chomyn A, Chan DC (2005) Disruption of fusion results in mitochondrial heterogeneity and dysfunction. J Biol Chem 280: 26185-26192.

97. Chen H, McCaffery JM, Chan DC (2007) Mitochondrial fusion protects against neurodegeneration in the cerebellum. Cell 130: 548-562.

98. Chen Y, Liu Y, Dorn GW, 2nd (2011) Mitochondrial fusion is essential for organelle function and cardiac homeostasis. Circ Res 109: 1327-1331.

99. Smirnova E, Griparic L, Shurland DL, van der Bliek AM (2001) Dynamin-related protein Drp1 is required for mitochondrial division in mammalian cells. Mol Biol Cell 12: 2245-2256.

100. Frank S, Gaume B, Bergmann-Leitner ES, Leitner WW, Robert EG, et al. (2001) The role of dynamin-related protein 1, a mediator of mitochondrial fission, in apoptosis. Dev Cell 1: 515-525.

101. Pitts KR, McNiven MA, Yoon Y (2004) Mitochondria-specific function of the dynamin family protein DLP1 is mediated by its C-terminal domains. J Biol Chem 279: 50286-50294.

102. Lee YJ, Jeong SY, Karbowski M, Smith CL, Youle RJ (2004) Roles of the mammalian mitochondrial fission and fusion mediators Fis1, Drp1, and Opa1 in apoptosis. Mol Biol Cell 15: 5001-5011.

103. Gandre-Babbe S, van der Bliek AM (2008) The novel tail-anchored membrane protein Mff controls mitochondrial and peroxisomal fission in mammalian cells. Mol Biol Cell 19: 2402-2412.

104. Lu B (2009) Mitochondrial dynamics and neurodegeneration. Curr Neurol Neurosci Rep 9: 212-219.

105. Cho DH, Nakamura T, Lipton SA (2010) Mitochondrial dynamics in cell death and neurodegeneration. Cell Mol Life Sci 67: 3435-3447.

106. Wang X, Su B, Fujioka H, Zhu X (2008) Dynamin-like protein 1 reduction underlies mitochondrial morphology and distribution abnormalities in fibroblasts from sporadic Alzheimer's disease patients. Am J Pathol 173: 470-482.

107. Wang X, Su B, Lee HG, Li X, Perry G, et al. (2009) Impaired balance of mitochondrial fission and fusion in Alzheimer's disease. J Neurosci 29: 9090-9103.

108. Krieger M, Herz J (1994) Structures and functions of multiligand lipoprotein receptors: macrophage scavenger receptors and LDL receptor-related protein (LRP). Annu Rev Biochem 63: 601-637.

109. Nykjaer A, Willnow TE (2002) The low-density lipoprotein receptor gene family: a cellular Swiss army knife? Trends Cell Biol 12: 273-280.

110. Jeon H, Blacklow SC (2005) Structure and physiologic function of the low-density lipoprotein receptor. Annu Rev Biochem 74: 535-562.

111. Bu G (2009) Apolipoprotein E and its receptors in Alzheimer's disease: pathways, pathogenesis and therapy. Nat Rev Neurosci 10: 333-344.

112. Pinson KI, Brennan J, Monkley S, Avery BJ, Skarnes WC (2000) An LDL-receptor-related protein mediates Wnt signalling in mice. Nature 407: 535-538.

113. Tamai K, Semenov M, Kato Y, Spokony R, Liu C, et al. (2000) LDL-receptor-related proteins in Wnt signal transduction. Nature 407: 530-535.

114. Kelly OG, Pinson KI, Skarnes WC (2004) The Wnt co-receptors Lrp5 and Lrp6 are essential for gastrulation in mice. Development 131: 2803-2815.

115. van Amerongen R, Nusse R (2009) Towards an integrated view of Wnt signaling in development. Development 136: 3205-3214.

116. Nusse R, Varmus H (2012) Three decades of Wnts: a personal perspective on how a scientific field developed. EMBO J 31: 2670-2684.

117. Salinas PC, Zou Y (2008) Wnt signaling in neural circuit assembly. Annu Rev Neurosci 31: 339-358.

118. Inestrosa NC, Arenas E (2010) Emerging roles of Wnts in the adult nervous system. Nat Rev Neurosci 11: 77-86.

119. De Ferrari GV, Inestrosa NC (2000) Wnt signaling function in Alzheimer's disease. Brain Res Brain Res Rev 33: 1-12.

120. De Ferrari GV, Moon RT (2006) The ups and downs of Wnt signaling in prevalent neurological disorders. Oncogene 25: 7545-7553.

121. Chen RH, Ding WV, McCormick F (2000) Wnt signaling to beta-catenin involves two interactive components. Glycogen synthase kinase-3beta inhibition and activation of protein kinase C. J Biol Chem 275: 17894-17899.

122. Davidson G, Wu W, Shen J, Bilic J, Fenger U, et al. (2005) Casein kinase 1 gamma couples Wnt receptor activation to cytoplasmic signal transduction. Nature 438: 867-872.

123. van Noort M, Meeldijk J, van der Zee R, Destree O, Clevers H (2002) Wnt signaling controls the phosphorylation status of beta-catenin. J Biol Chem 277: 17901-17905.

124. Gordon MD, Nusse R (2006) Wnt signaling: multiple pathways, multiple receptors, and multiple transcription factors. J Biol Chem 281: 22429-22433.

125. Luo J, Chen J, Deng ZL, Luo X, Song WX, et al. (2007) Wnt signaling and human diseases: what are the therapeutic implications? Lab Invest 87: 97-103.

126. Dong Y, Lathrop W, Weaver D, Qiu Q, Cini J, et al. (1998) Molecular cloning and characterization of LR3, a novel LDL receptor family protein with mitogenic activity. Biochem Biophys Res Commun 251: 784-790.

127. Hey PJ, Twells RC, Phillips MS, Yusuke N, Brown SD, et al. (1998) Cloning of a novel member of the low-density lipoprotein receptor family. Gene 216: 103-111.

128. Houston DW, Wylie C (2002) Cloning and expression of Xenopus Lrp5 and Lrp6 genes. Mech Dev 117: 337-342.

129. Kato M, Patel MS, Levasseur R, Lobov I, Chang BH, et al. (2002) Cbfa1-independent decrease in osteoblast proliferation, osteopenia, and persistent embryonic eye vascularization in mice deficient in Lrp5, a Wnt coreceptor. J Cell Biol 157: 303-314.

130. Fujino T, Asaba H, Kang MJ, Ikeda Y, Sone H, et al. (2003) Low-density lipoprotein receptor-related protein 5 (LRP5) is essential for normal cholesterol metabolism and glucose-induced insulin secretion. Proc Natl Acad Sci U S A 100: 229-234.

131. Boonen RA, van Tijn P, Zivkovic D (2009) Wnt signaling in Alzheimer's disease: up or down, that is the question. Ageing Res Rev 8: 71-82.

132. Inestrosa NC, Montecinos-Oliva C, Fuenzalida M (2012) Wnt signaling: role in Alzheimer disease and schizophrenia. J Neuroimmune Pharmacol 7: 788-807.

133. Inestrosa NC, Varela-Nallar L (2014) Wnt signaling in the nervous system and in Alzheimer's disease. J Mol Cell Biol 6: 64-74.

134. Zhang Z, Hartmann H, Do VM, Abramowski D, Sturchler-Pierrat C, et al. (1998) Destabilization of beta-catenin by mutations in presenilin-1 potentiates neuronal apoptosis. Nature 395: 698-702.

135. Kawamura Y, Kikuchi A, Takada R, Takada S, Sudoh S, et al. (2001) Inhibitory effect of a presenilin 1 mutation on the Wnt signalling pathway by enhancement of beta-catenin phosphorylation. Eur J Biochem 268: 3036-3041.

136. Murayama M, Tanaka S, Palacino J, Murayama O, Honda T, et al. (1998) Direct association of presenilin-1 with beta-catenin. FEBS Lett 433: 73-77.

137. Caruso A, Motolese M, Iacovelli L, Caraci F, Copani A, et al. (2006) Inhibition of the canonical Wnt signaling pathway by apolipoprotein E4 in PC12 cells. J Neurochem 98: 364-371.

138. Pei JJ, Braak E, Braak H, Grundke-Iqbal I, Iqbal K, et al. (1999) Distribution of active glycogen synthase kinase 3beta (GSK-3beta) in brains staged for Alzheimer disease neurofibrillary changes. J Neuropathol Exp Neurol 58: 1010-1019.

139. Lucas JJ, Hernandez F, Gomez-Ramos P, Moran MA, Hen R, et al. (2001) Decreased nuclear beta-catenin, tau hyperphosphorylation and neurodegeneration in GSK-3beta conditional transgenic mice. EMBO J 20: 27-39.

140. De Ferrari GV, Papassotiropoulos A, Biechele T, Wavrant De-Vrieze F, Avila ME, et al. (2007) Common genetic variation within the low-density lipoprotein receptor-related protein 6 and late-onset Alzheimer's disease. Proc Natl Acad Sci U S A 104: 9434-9439.

141. Alarcon MA, Medina MA, Hu Q, Avila ME, Bustos BI, et al. (2013) A novel functional low-density lipoprotein receptor-related protein 6 gene alternative splice variant is associated with Alzheimer's disease. Neurobiol Aging 34: 1709 e1709-1718.

142. del Pino J, Ramos E, Aguilera OM, Marco-Contelles J, Romero A (2014) Wnt signaling pathway, a potential target for Alzheimer's disease treatment, is activated by a novel multitarget compound ASS234. CNS Neurosci Ther 20: 568-570.

143. Alvarez AR, Godoy JA, Mullendorff K, Olivares GH, Bronfman M, et al. (2004) Wnt-3a overcomes beta-amyloid toxicity in rat hippocampal neurons. Exp Cell Res 297: 186-196.

144. Quintanilla RA, Munoz FJ, Metcalfe MJ, Hitschfeld M, Olivares G, et al. (2005) Trolox and 17beta-estradiol protect against amyloid beta-peptide neurotoxicity by a mechanism that involves modulation of the Wnt signaling pathway. J Biol Chem 280: 11615-11625.

145. De Ferrari GV, Chacon MA, Barria MI, Garrido JL, Godoy JA, et al. (2003) Activation of Wnt signaling rescues neurodegeneration and behavioral impairments induced by beta-amyloid fibrils. Mol Psychiatry 8: 195-208.

146. Ishiguro K, Shiratsuchi A, Sato S, Omori A, Arioka M, et al. (1993) Glycogen synthase kinase 3 beta is identical to tau protein kinase I generating several epitopes of paired helical filaments. FEBS Lett 325: 167-172.

147. Takashima A, Honda T, Yasutake K, Michel G, Murayama O, et al. (1998) Activation of tau protein kinase I/glycogen synthase kinase-3beta by amyloid beta peptide (25-35) enhances phosphorylation of tau in hippocampal neurons. Neurosci Res 31: 317-323.

148. Mietelska-Porowska A, Wasik U, Goras M, Filipek A, Niewiadomska G (2014) Tau protein modifications and interactions: their role in function and dysfunction. Int J Mol Sci 15: 4671-4713.

149. He X, Semenov M, Tamai K, Zeng X (2004) LDL receptor-related proteins 5 and 6 in Wnt/beta-catenin signaling: arrows point the way. Development 131: 1663-1677.

150. MacDonald BT, Semenov MV, Huang H, He X (2011) Dissecting molecular differences between Wnt coreceptors LRP5 and LRP6. PLoS One 6: e23537.

151. Clevers H, Nusse R (2012) Wnt/beta-catenin signaling and disease. Cell 149: 1192-1205.

152. Alarcon MA, Medina MA, Hu Q, Avila ME, Bustos BI, et al. (2012) A novel functional low-density lipoprotein receptor-related protein 6 gene alternative splice variant is associated with Alzheimer's disease. Neurobiol Aging.

153. Hardy J, Selkoe DJ (2002) The amyloid hypothesis of Alzheimer's disease: progress and problems on the road to therapeutics. Science 297: 353-356.

154. Deshpande A, Mina E, Glabe C, Busciglio J (2006) Different conformations of amyloid beta induce neurotoxicity by distinct mechanisms in human cortical neurons. J Neurosci 26: 6011-6018.

155. Iversen LL, Mortishire-Smith RJ, Pollack SJ, Shearman MS (1995) The toxicity in vitro of beta-amyloid protein. Biochem J 311 (Pt 1): 1-16.

156. Nunomura A, Perry G, Aliev G, Hirai K, Takeda A, et al. (2001) Oxidative damage is the earliest event in Alzheimer disease. J Neuropathol Exp Neurol 60: 759-767.

157. Pappolla MA, Chyan YJ, Omar RA, Hsiao K, Perry G, et al. (1998) Evidence of oxidative stress and in vivo neurotoxicity of beta-amyloid in a transgenic mouse model of Alzheimer's disease: a chronic oxidative paradigm for testing antioxidant therapies in vivo. Am J Pathol 152: 871-877.

158. Galasko D, Montine TJ (2010) Biomarkers of oxidative damage and inflammation in Alzheimer's disease. Biomark Med 4: 27-36.

159. Padurariu M, Ciobica A, Hritcu L, Stoica B, Bild W, et al. (2010) Changes of some oxidative stress markers in the serum of patients with mild cognitive impairment and Alzheimer's disease. Neurosci Lett 469: 6-10.

160. Behl C, Davis JB, Lesley R, Schubert D (1994) Hydrogen peroxide mediates amyloid beta protein toxicity. Cell 77: 817-827.

161. Buee L, Bussiere T, Buee-Scherrer V, Delacourte A, Hof PR (2000) Tau protein isoforms, phosphorylation and role in neurodegenerative disorders. Brain Res Brain Res Rev 33: 95-130.

162. Augustinack JC, Schneider A, Mandelkow EM, Hyman BT (2002) Specific tau phosphorylation sites correlate with severity of neuronal cytopathology in Alzheimer's disease. Acta Neuropathol 103: 26-35.

163. Sundberg M, Savola S, Hienola A, Korhonen L, Lindholm D (2006) Glucocorticoid hormones decrease proliferation of embryonic neural stem cells through ubiquitin-mediated degradation of cyclin D1. J Neurosci 26: 5402-5410.

164. Luo Y, Shan G, Guo W, Smrt RD, Johnson EB, et al. (2010) Fragile x mental retardation protein regulates proliferation and differentiation of adult neural stem/progenitor cells. PLoS Genet 6: e1000898.

165. Misonou H, Morishima-Kawashima M, Ihara Y (2000) Oxidative stress induces intracellular accumulation of amyloid beta-protein (Abeta) in human neuroblastoma cells. Biochemistry 39: 6951-6959.

166. Butterfield DA, Perluigi M, Sultana R (2006) Oxidative stress in Alzheimer's disease brain: new insights from redox proteomics. Eur J Pharmacol 545: 39-50.

167. Shaykhalishahi H, Yazdanparast R, Ha HH, Chang YT (2009) Inhibition of H2O2-induced neuroblastoma cell cytotoxicity by a triazine derivative, AA3E2. Eur J Pharmacol 622: 1-6.

168. Engel T, Goni-Oliver P, Lucas JJ, Avila J, Hernandez F (2006) Chronic lithium administration to FTDP-17 tau and GSK-3beta overexpressing mice prevents tau hyperphosphorylation and neurofibrillary tangle formation, but pre-formed neurofibrillary tangles do not revert. J Neurochem 99: 1445-1455.

169. Beffert U, Arguin C, Poirier J (1999) The polymorphism in exon 3 of the low density lipoprotein receptor-related protein gene is weakly associated with Alzheimer's disease. Neurosci Lett 259: 29-32.

170. Kim DH, Inagaki Y, Suzuki T, Ioka RX, Yoshioka SZ, et al. (1998) A new low density lipoprotein receptor related protein, LRP5, is expressed in hepatocytes and adrenal cortex, and recognizes apolipoprotein E. J Biochem 124: 1072-1076.

171. Carmon KS, Loose DS (2010) Development of a bioassay for detection of Wnt-binding affinities for individual frizzled receptors. Anal Biochem 401: 288-294.

172. Fuentealba LC, Eivers E, Ikeda A, Hurtado C, Kuroda H, et al. (2007) Integrating patterning signals: Wnt/GSK3 regulates the duration of the BMP/Smad1 signal. Cell 131: 980-993.

173. Cedazo-Minguez A, Popescu BO, Blanco-Millan JM, Akterin S, Pei JJ, et al. (2003) Apolipoprotein E and beta-amyloid (1-42) regulation of glycogen synthase kinase-3beta. J Neurochem 87: 1152-1164.

174. Chan DC (2006) Mitochondria: dynamic organelles in disease, aging, and development. Cell 125: 1241-1252.

175. Liesa M, Palacin M, Zorzano A (2009) Mitochondrial dynamics in mammalian health and disease. Physiol Rev 89: 799-845.

176. Detmer SA, Chan DC (2007) Functions and dysfunctions of mitochondrial dynamics. Nat Rev Mol Cell Biol 8: 870-879.

177. Benard G, Bellance N, James D, Parrone P, Fernandez H, et al. (2007) Mitochondrial bioenergetics and structural network organization. J Cell Sci 120: 838-848.

178. Knott AB, Perkins G, Schwarzenbacher R, Bossy-Wetzel E (2008) Mitochondrial fragmentation in neurodegeneration. Nat Rev Neurosci 9: 505-518.

179. Karbowski M, Arnoult D, Chen H, Chan DC, Smith CL, et al. (2004) Quantitation of mitochondrial dynamics by photolabeling of individual organelles shows that mitochondrial fusion is blocked during the Bax activation phase of apoptosis. J Cell Biol 164: 493-499.

180. Rojo M, Legros F, Chateau D, Lombes A (2002) Membrane topology and mitochondrial targeting of mitofusins, ubiquitous mammalian homologs of the transmembrane GTPase Fzo. J Cell Sci 115: 1663-1674.

181. Santel A, Fuller MT (2001) Control of mitochondrial morphology by a human mitofusin. J Cell Sci 114: 867-874.

182. Chen H, Detmer SA, Ewald AJ, Griffin EE, Fraser SE, et al. (2003) Mitofusins Mfn1 and Mfn2 coordinately regulate mitochondrial fusion and are essential for embryonic development. J Cell Biol 160: 189-200.

183. Song Z, Ghochani M, McCaffery JM, Frey TG, Chan DC (2009) Mitofusins and OPA1 mediate sequential steps in mitochondrial membrane fusion. Mol Biol Cell 20: 3525-3532.

184. Zhang P, Hinshaw JE (2001) Three-dimensional reconstruction of dynamin in the constricted state. Nat Cell Biol 3: 922-926.

185. Zhu PP, Patterson A, Stadler J, Seeburg DP, Sheng M, et al. (2004) Intra- and intermolecular domain interactions of the C-terminal GTPase effector domain of the multimeric dynamin-like GTPase Drp1. J Biol Chem 279: 35967-35974.

186. Yoon Y, Pitts KR, McNiven MA (2001) Mammalian dynamin-like protein DLP1 tubulates membranes. Mol Biol Cell 12: 2894-2905.

187. Ingerman E, Perkins EM, Marino M, Mears JA, McCaffery JM, et al. (2005) Dnm1 forms spirals that are structurally tailored to fit mitochondria. J Cell Biol 170: 1021-1027.

188. Mears JA, Lackner LL, Fang S, Ingerman E, Nunnari J, et al. (2011) Conformational changes in Dnm1 support a contractile mechanism for mitochondrial fission. Nat Struct Mol Biol 18: 20-26.

189. DuBoff B, Feany M, Gotz J (2013) Why size matters - balancing mitochondrial dynamics in Alzheimer's disease. Trends Neurosci 36: 325-335.

190. Spinney L (2014) Alzheimer's disease: The forgetting gene. Nature 510: 26-28.

191. De Vos KJ, Allan VJ, Grierson AJ, Sheetz MP (2005) Mitochondrial function and actin regulate dynamin-related protein 1-dependent mitochondrial fission. Curr Biol 15: 678-683.

192. Trudeau K, Molina AJ, Roy S (2011) High glucose induces mitochondrial morphology and metabolic changes in retinal pericytes. Invest Ophthalmol Vis Sci 52: 8657-8664.

193. Tolar M, Marques MA, Harmony JA, Crutcher KA (1997) Neurotoxicity of the 22 kDa thrombin-cleavage fragment of apolipoprotein E and related synthetic peptides is receptor-mediated. J Neurosci 17: 5678-5686.

194. Tolar M, Keller JN, Chan S, Mattson MP, Marques MA, et al. (1999) Truncated apolipoprotein E (ApoE) causes increased intracellular calcium and may mediate ApoE neurotoxicity. J Neurosci 19: 7100-7110.

195. Harris FM, Brecht WJ, Xu Q, Tesseur I, Kekonius L, et al. (2003) Carboxyl-terminal-truncated apolipoprotein E4 causes Alzheimer's disease-like neurodegeneration and behavioral deficits in transgenic mice. Proc Natl Acad Sci U S A 100: 10966-10971.

196. Risner ME, Saunders AM, Altman JF, Ormandy GC, Craft S, et al. (2006) Efficacy of rosiglitazone in a genetically defined population with mild-to-moderate Alzheimer's disease. Pharmacogenomics J 6: 246-254.

197. Huang Y, Mahley RW (2006) Commentary on "Perspective on a pathogenesis and treatment of Alzheimer's disease." Apolipoprotein E and the mitochondrial metabolic hypothesis. Alzheimers Dement 2: 71-73.

198. Roses AD, Saunders AM (2006) Perspective on a pathogenesis and treatment of Alzheimer's disease. Alzheimers Dement 2: 59-70.

199. Zorn AM (2001) Wnt signalling: antagonistic Dickkopfs. Curr Biol 11: R592-595.

200. Brown SD, Twells RC, Hey PJ, Cox RD, Levy ER, et al. (1998) Isolation and characterization of LRP6, a novel member of the low density lipoprotein receptor gene family. Biochem Biophys Res Commun 248: 879-888.

201. Bourhis E, Tam C, Franke Y, Bazan JF, Ernst J, et al. (2010) Reconstitution of a frizzled8.Wnt3a.LRP6 signaling complex reveals multiple Wnt and Dkk1 binding sites on LRP6. J Biol Chem 285: 9172-9179.

202. Ahn VE, Chu ML, Choi HJ, Tran D, Abo A, et al. (2011) Structural basis of Wnt signaling inhibition by Dickkopf binding to LRP5/6. Dev Cell 21: 862-873.

203. Manczak M, Calkins MJ, Reddy PH (2011) Impaired mitochondrial dynamics and abnormal interaction of amyloid beta with mitochondrial protein Drp1 in neurons from patients with Alzheimer's disease: implications for neuronal damage. Hum Mol Genet 20: 2495-2509.

204. Vazquez-Higuera JL, Mateo I, Sanchez-Juan P, Rodriguez-Rodriguez E, Pozueta A, et al. (2009) Genetic interaction between tau and the apolipoprotein E receptor LRP1 Increases Alzheimer's disease risk. Dement Geriatr Cogn Disord 28: 116-120.

APPENDICES

Permission for the use of Figure 1-2

NATURE PUBLISHING GROUP LICENSE
TERMS AND CONDITIONS

Aug 12, 2014

This is a License Agreement between Luqi Zhang ("You") and Nature Publishing Group ("Nature Publishing Group") provided by Copyright Clearance Center ("CCC"). The license consists of your order details, the terms and conditions provided by Nature Publishing Group, and the payment terms and conditions.

All payments must be made in full to CCC. For payment instructions, please see information listed at the bottom of this form.

License Number	3446380079234
License date	Aug 12, 2014
Licensed content publisher	Nature Publishing Group
Licensed content publication	Nature Reviews Neurology
Licensed content title	Apolipoprotein E and Alzheimer disease: risk, mechanisms and therapy
Licensed content author	Chia-Chen Liu, Takahisa Kanekiyo, Huaxi Xu, Guojun Bu
Licensed content date	Mar 26, 2013
Volume number	9
Issue number	4
Type of Use	reuse in a dissertation / thesis
Requestor type	non-commercial (non-profit)
Format	print and electronic
Portion	figures/tables/illustrations
Number of figures/tables/illustrations	1
High-res required	no
Figures	The structure of apoE and the meta-analysis on the populations of people with apoE isoforms
Author of this NPG article	no
Your reference number	None
Title of your thesis / dissertation	FUNCTIONAL ROLE OF LOW DENSITY LIPOPROTEIN RECEPTOR-RELATED PROTEIN 5 AND 6 IN ALZHEIMER'S DISEASE
Expected completion date	Jan 2015
Estimated size (number of pages)	120
Total	0.00 USD

Permission for the use of Figure 1-3

NATURE PUBLISHING GROUP LICENSE
TERMS AND CONDITIONS

Aug 12, 2014

This is a License Agreement between Luqi Zhang ("You") and Nature Publishing Group ("Nature Publishing Group") provided by Copyright Clearance Center ("CCC"). The license consists of your order details, the terms and conditions provided by Nature Publishing Group, and the payment terms and conditions.

All payments must be made in full to CCC. For payment instructions, please see information listed at the bottom of this form.

License Number	3446810664192
License date	Aug 12, 2014
Licensed content publisher	Nature Publishing Group
Licensed content publication	Nature Reviews Neuroscience
Licensed content title	Apolipoprotein E and its receptors in Alzheimer's disease: pathways, pathogenesis and therapy
Licensed content author	Guojun Bu
Licensed content date	May 1, 2009
Volume number	10
Issue number	5
Type of Use	reuse in a dissertation / thesis
Requestor type	non-commercial (non-profit)
Format	print and electronic
Portion	figures/tables/illustrations
Number of figures/tables/illustrations	1
High-res required	no
Figures	The structure of LDL receptor family members
Author of this NPG article	no
Your reference number	None
Title of your thesis / dissertation	FUNCTIONAL ROLE OF LOW DENSITY LIPOPROTEIN RECEPTOR-RELATED PROTEIN 5 AND 6 IN ALZHEIMER'S DISEASE
Expected completion date	Jan 2015
Estimated size (number of pages)	120
Total	0.00 USD

Permission for the use of Figure 1-4

NATURE PUBLISHING GROUP LICENSE TERMS AND CONDITIONS

Oct 26, 2014

This is a License Agreement between Luqi Zhang ("You") and Nature Publishing Group ("Nature Publishing Group") provided by Copyright Clearance Center ("CCC"). The license consists of your order details, the terms and conditions provided by Nature Publishing Group, and the payment terms and conditions.

All payments must be made in full to CCC. For payment instructions, please see information listed at the bottom of this form.

License Number	3496820477224
License date	Oct 26, 2014
Licensed content publisher	Nature Publishing Group
Licensed content publication	Laboratory Investigation
Licensed content title	Wnt signaling and human diseases: what are the therapeutic implications?
Licensed content author	Jinyong Luo, Jin Chen, Zhong-Liang Deng, Xiaoji Luo, Wen-Xin Song et al.
Licensed content date	Jan 8, 2007
Volume number	87
Issue number	2
Type of Use	reuse in a dissertation / thesis
Requestor type	academic/educational
Format	print and electronic
Portion	figures/tables/illustrations
Number of figures/tables/illustrations	1
High-res required	no
Figures	Schematic representation of the canonical Wnt/β-catenin signaling pathway.
Author of this NPG article	no
Your reference number	None
Title of your thesis / dissertation	FUNCTIONAL ROLE OF LOW DENSITY LIPOPROTEIN RECEPTOR-RELATED PROTEIN 5 AND 6 IN ALZHEIMER'S DISEASE
Expected completion date	Jan 2015
Estimated size (number of pages)	120
Total	0.00 USD

Double-click to show white space

Permission for the use of Figure 5-1

ELSEVIER LICENSE
TERMS AND CONDITIONS

Oct 27, 2014

This is a License Agreement between Luqi Zhang ("You") and Elsevier ("Elsevier") provided by Copyright Clearance Center ("CCC"). The license consists of your order details, the terms and conditions provided by Elsevier, and the payment terms and conditions.

All payments must be made in full to CCC. For payment instructions, please see information listed at the bottom of this form.

Supplier	Elsevier Limited The Boulevard,Langford Lane Kidlington,Oxford,OX5 1GB,UK
Registered Company Number	1982084
Customer name	Luqi Zhang
Customer address	Department of Pharmacy Singapore, 117543
License number	3496860695336
License date	Oct 27, 2014
Licensed content publisher	Elsevier
Licensed content publication	Trends in Neurosciences
Licensed content title	Why size matters – balancing mitochondrial dynamics in Alzheimer's disease
Licensed content author	Brian DuBoff,Mel Feany,Jürgen Götz
Licensed content date	June 2013
Licensed content volume number	36
Licensed content issue number	6
Number of pages	11
Start Page	325
End Page	335
Type of Use	reuse in a thesis/dissertation
Intended publisher of new work	other
Portion	figures/tables/illustrations
Number of figures/tables/illustrations	1
Format	both print and electronic
Are you the author of this	No